

# POLITECNICO DI TORINO

**Master of science degree in Mechanical Engineering**



Master Thesis

**Frequency analysis of gait signals to assess gait  
symmetry**

**Supervisors:**

Prof.ssa Laura GASTALDI

Ing. Elisa PANERO

Ing. Dario ANASTASIO

**Candidate:** Margherita PEILA

A.A. 2021/2022

## Index

Abstract	4
1. Biomechanics of human gait	6
1.1 Basic concepts	6
1.2 Measurement and models of the BCoM trajectory	15
1.3 Laboratory methods for measurements of human gait parameters	18
Optoelectronic instruments	21
Not optical instruments	23
Dynamometric platforms	25
2. Gait symmetry and Body Center of Mass	26
2.1 Symmetry indexes	27
2.1.1 Discrete approaches	28
Ratio index	28
Robinson index	29
Symmetry angle	30
2.1.2 Statistically based approaches	30
2.1.3 Not-linear approaches	30
2.1.4 Complete gait cycle approaches	31
Cyclogram-based and symbol-based methods	31
Spectral analysis	31
2.2 Spectral analysis approach	31
Harmonic ratio	32
BCoM trajectory analysis and related symmetry indexes	33

3. The theory of Fourier series	35
3.1 The series and its coefficients	35
3.1.1 Mean value	37
3.1.2 Phase-angle form	37
3.2 Computational tool for the determination of the Fourier coefficients	38
3.2.1 Numerical example: sawtooth function	39
3.2.3 numerical example: gait cycle	41
3.2.2 Robustness tests	43
4. Studied BCoM trajectory symmetry indexes	48
4.1 The index proposed by Ochoa-Diaz & Padilha (2020)	48
4.2 The index proposed by Minetti et al. (2011)	54
5. Application of the studied symmetry indexes to experimental data	57
5.1 Available gait data	57
5.2 Results	60
5.2.1 Example of healthy subject gait cycle vs pathological one	60
5.2.2 Symmetry index of healthy subjects	66
Computed $SI_{O-P}$ index	67
Computed $SI_{Y-M}$ index	70
5.2.3 Symmetry indexes of pathological subjects	73
Computed $SI_{O-P}$ index	76
Computed $SI_{Y-M}$ index	78
5.2.4 Comparison of the results obtained with the $SI_{O-P}$ index and $SI_{Y-M}$ index	80
6. Conclusions and future developments	82
Bibliography	84
Annex 1:	89

## Abstract

Human gait is a complex cyclic spatio-temporally movement that requires human joints coordination and involves several biomechanical structures.

Some neurological and musculoskeletal pathologies might cause motion disorders and gait impairments, which play an important role for the quality of life and for the independence in performing daily activities. Several researches dealt with the objective assessment and biomechanical description of human gait characteristics, such as symmetry, variability and smoothness. Previous studies proposed different methods and approaches for the investigation of gait symmetry. Despite the several symmetry indexes validated in physiological gait, some challenges are still opened for the identification of robust and suitable methodology in pathological patterns. Recent analysis suggested the application of frequency analysis to biological signals to evaluate characteristics and components that cannot be detected in time domain.

This thesis focuses on the characterization of the human gait examining the Body Centre of Mass (BCoM) trajectory using the spectral analysis of the Fourier series. In the thesis, the study has been focused on the vertical displacement of the BCoM trajectory. Two literature symmetry indexes based on combinations of the Fourier series coefficients, developed respectively for the assessment of the gait symmetry of amputee and non-amputee subjects by Ochoa-Diaz & Padilha (2020) and the gait symmetry of healthy subjects at different speeds by Minetti et al. (2011), have been studied to verify their feasibility when applied to hemiparetic gait.

Preliminary analysis concentrated on the assessment of algorithm robustness through the investigation of synthetic data. Then, the algorithms have been applied to experimental data of the BCoM trajectory acquired in a previous study. These data refer to two groups of subjects (5 healthy young subjects and 14 pathological patients). Tests with healthy subjects were conducted in the POLITO BIOMed LAB of Politecnico di Torino, Italy. Tests with patients were performed in the specialized Movement Disorders Center of Unità Spinale Unipolare – Città della Salute e della Scienza, Italy.

In healthy subjects both indexes (Ochoa-Diaz & Padilha index:  $0.94 \pm 0.016$ , Minetti index:  $0.77 \pm 0.025$ ) provide values closed to 1, that is the value representing a symmetrical gait. These results are in good agreement with those obtained by the authors that proposed the indexes applied to healthy gait.

The pathological subjects were divided in two groups: under and over 65 years. When considering all the pathological subjects, the Ochoa-Diaz & Padilha index reported an average value of  $0.31 \pm 0.233$ , while the Minetti index provides an average value of  $0.39 \pm 0.125$ . These values are lower than those of healthy subjects and show that hemiparetic subjects have a walking alteration, as expected. Younger subjects have higher values (even if lower than the healthy ones) for both symmetry indexes.

In conclusion, these indexes have shown to be suitable to detect hemiparetic gait asymmetry and could be adopted in clinical analysis. Further development of the proposed methodology could be applied to different pathological conditions and the obtained results can be compared, taking into account the pathology and how it affects the gait. The same procedure of spectral analysis might be carried out considering different types of biomechanical signals.

# 1. Biomechanics of human gait

## 1.1 Basic concepts

Walking is the way men use to move on earth. Despite its apparent simplicity human gait is a cyclic spatio-temporally complex act: all people walk in a similar way (this applies also to running or skipping) but each human being has slight deviations from the common movement pattern. Furthermore, some pathological conditions can affect the gait and deviate it from the physiological pattern. Therefore, since walking induces the motion of all the body segments, an alteration of any one of these segments can induce adaptive movements across the whole body and therefore modify the gait. The description of the gait through objective parameters as spatiotemporal and cinematic ones, can be important for the identification of some alterations of the gait in subjects with diffused lesions of the central nervous system as hemiparesis or Parkinson disease.

In these last cases, in addition, it may be difficult to interpret all the numerous concurrent alterations and identify critical targets for clinical observation.

A complete quantitative assessment of locomotion it is necessary for:

- i) bio-mechanists mainly interested in the general features of gaits, such as the mechanical work needed to sustain locomotion and the energy saving strategies to contain the metabolic cost of the motion;
- ii) locomotion pathologists mainly interested to estimate forces and moments action on the body segments. Their goal is to compare the pathological and not pathological values since the success of a rehabilitative program should be ultimately evaluated on the basis of the restoration of a healthy and almost symmetrical path;
- iii) biomedical and automation engineers who are interested in the efficacy of locomotion and in the quantitative comparison of gaits of bipedal/quadrupedal robots and legged machines with the biological “vehicles” (Minetti et al., 2011).

The general principles of the physiology of walking in humans and, in general, in legged animals, have been extensively discussed in technical literature and the following references can be considered as base references: McMahon (1974), Gage

(1991), Alexander (2003) and Cavagna (2017).

Human gait can be defined as a cyclic and coordinate movement of various human body segments. The gait movement presents a periodic and repetitive pattern, and it requires two main requisites (Vaughan et al.; 1992):

- the periodic movement of each foot from one position of support to the next
- forces exchanged between the foot and the ground (ground reaction forces GFR)

Due to the cyclic characteristic, the human walk can be described by a single gait cycle. Figure 1.1 provides the basic definitions of the walk terminology.

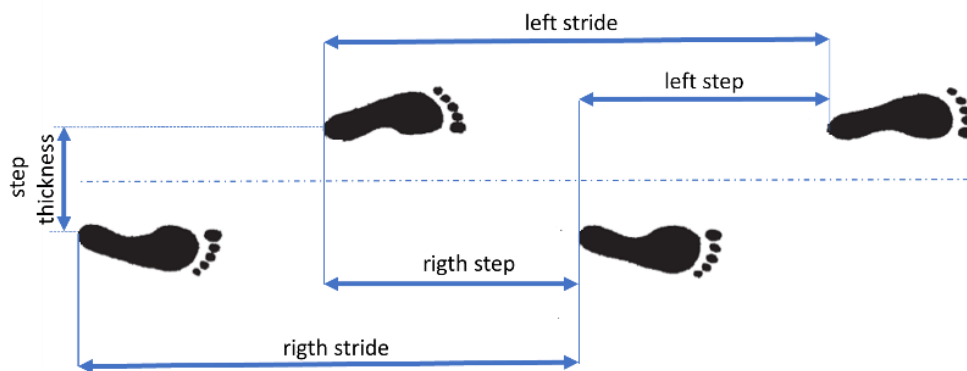


Figure 1.1 Graphical representation of the key terminologies in human gait.

A gait cycle can be divided in two main phases: the *stance phase* and the *swing phase*. During the stance phase the foot is in contact with the ground, while in the swing phase the same foot is no longer in contact with the ground and the leg is swinging through in preparation of the next foot strike.

In a normal gait the duration of the stance phase is about the 60% of the whole cycle while the swing phase is about the 40% of the cycle as reported in Figure 1.2

The swing phase can then be divided in three main parts: two parts with a double support, when both feet are in contact with the ground, and one single limb stance, when one foot is swinging through, and the other foot is on the ground.

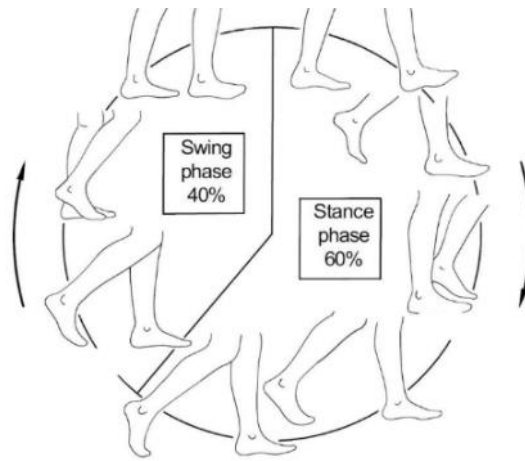


Figure 1.2. Schematic representation of the stance phase and the swing phase in the gait cycle (modified from Vaughan *et al.*, 1992).

Perry (1992) divided the gait cycle in eight elementary phases summarized Figure 1.3. This subdivision can be considered the most updated references of gait phases.

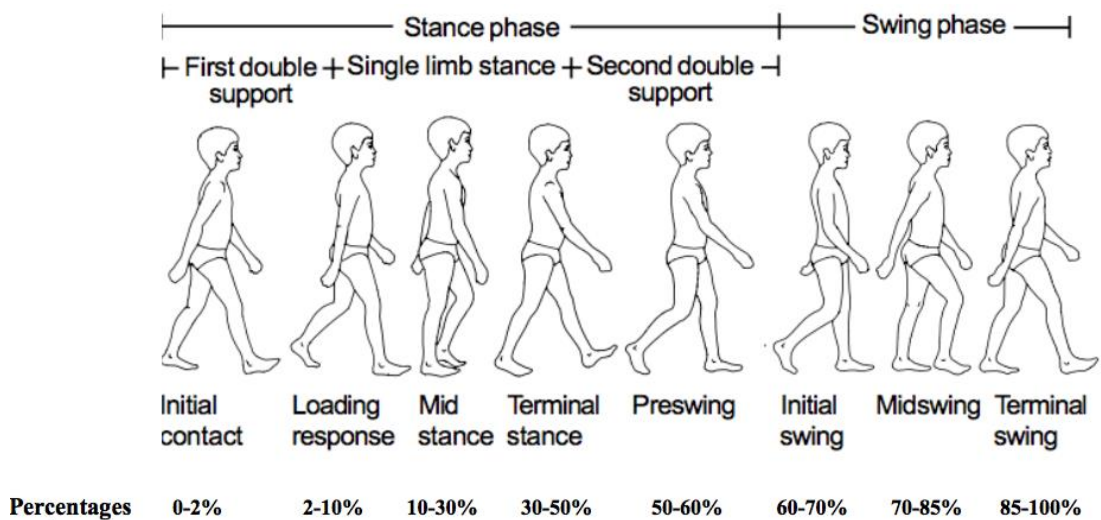


Figure 1.3 Cycle of human gait (Perry, 1992) with indication of the percentages of the cycle of each phase.

More in detail, based on the definition of Perry (1992), the stance phase includes the following five elementary subphases:

- *initial contact*: it is a very short phase only 2% of the gait cycle. During this phase the foot is moved forward, and the malleolus touches the ground. It is considered the starting point of the gait cycle;

- *loading response*: first period of double support: both feet are in contact with the ground;
- *mid stance*: it is a phase of single limb stance. It starts with the swinging of the contralateral foot and it ends when this foot completely touches the ground;
- *terminal stance*: is the final phase of the single limb stance. It starts with the lifting up of the malleolus till the other foot touches the ground. The body weight is transferred on the support foot due to the advancement of the body;
- *pre-swing*: is the final phase of the stance and the second period of double support. The weight of the body is transferred on the leg that is getting ready to be oscillated.

The swing phase includes the following three elementary phases:

- *initial swing*: it starts when the foot is lifted from the ground and the oscillating leg is parallel to the support foot;
- *mid swing*: it starts when the oscillating leg in opposite position of the support leg and ends when the support leg advances and its tibia is vertical;
- *terminal swing*: it starts when the tibia of the oscillating leg is vertical and ends when the foot touches the ground that ends the cycle.

The analysis of the percentage of stance time and swing time of both legs with reference to the whole gait cycle time, is important for clinicians that using these data can highlight the possible pathological conditions. An example is presented in Figure 1.4 that shows the gait cycle time subdivision of a not pathological subject and the gait cycle time subdivision of two patients with pathologies that affect the gait: one with a vascular necrosis in the left hip and the other with an osteoarthritis in the left hip. Based on this example it is possible to observe that when a patient has a pathological condition on one leg, he loses the symmetry of the cycles and the times of the stance and swing phases changes. The amount of this change depends on type of pathology since different muscles are working during the motion and they act in a different way from the not pathological condition.

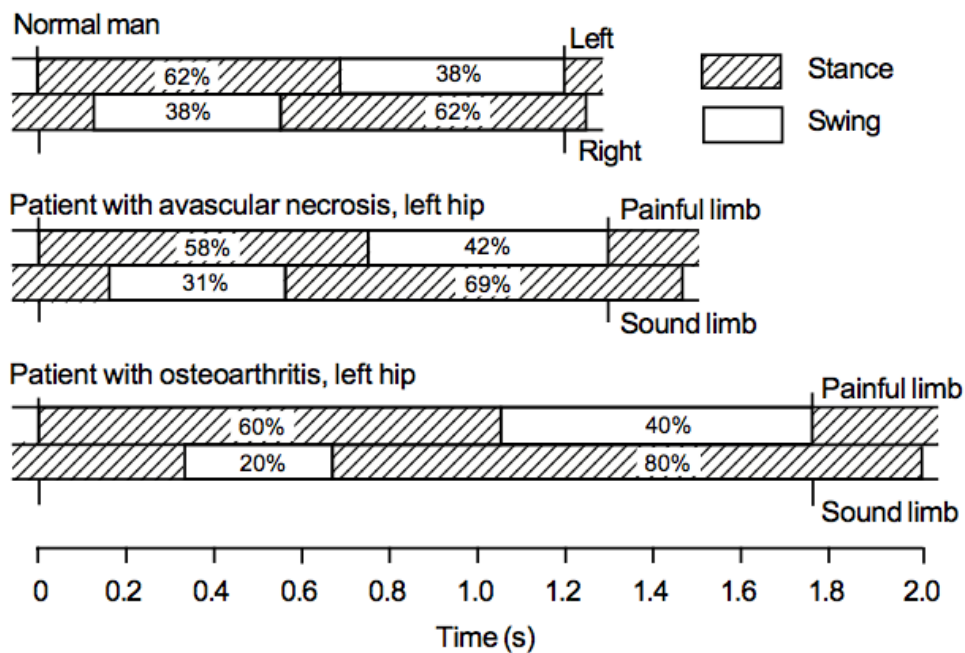


Figure 1.4 Measured time spend on each limb during the gait cycle of a not pathological subject (normal man) and of two patients with unilateral hip pain (Murrey and Gore; 1981 adapted by Vaughan et al., 1992)

The above concepts highlight the great importance of the study and understanding of the various parameters that describe the gait. This understanding provides information on both the type of disability and on how to treat it.

The two different most used approaches can be used to describe the human gait:

- the gait is represented as the sequence of cyclic rotations of the limbs and trunk and the body is modelled as a set of different segments moving and rotating during the motion. This approach can be called as “segmental approach” (Figure 1.5);
- the gait is studied as the translation of the body system as a whole and can be described by the trajectory of the motion of Body Center of Mass (BCoM) (Figure 1.6) and by its acceleration during the motion.

The goal of lower-limb movements (i.e. the gait) is the forward translation of the body system mainly in the sagittal plane of the body, in the anterior direction (Figures 1.5 and 1.6). The plantar flexors of the trailing limbs are the main engines of body propulsion. Walking is the results of synergic movements of skeleton around the joint and powered by several rhythmic muscles contraction. In the segmental approach, the human gait is analyzed by studying the relative motion of the various segments in which the body is subdivided and their relative position during the gait cycle. The

values of the relative angles between two nearby segments of the leg is an important information for the evaluation of gait disorders and pathological conditions. As an example, in Figure 1.5 (Cestari Soto, 2017) a clinical gait analysis pattern is presented highlighting the angular variation in the sagittal plane of the hip, knee and ankle joints of the leg are shown during the gait cycle.

On the other hand, the body, as a whole, is well represented, from a mechanical standpoint, by its BCoM. The BCoM of a distribution of mass (in this case the human body) is the unique point in space whose linear acceleration is determined only by the total external force acting on the system, without effects due to internal forces. When applied to the BCoM, such force causes a linear acceleration without angular acceleration. With reference to human body, one may also describe the BCoM as the unique point which invariably lies in planes dividing the body into two parts, sharing the same moment of inertia. The BCoM usually moves within the body when body segments are displaced with respect to each other.

In a quietly standing human body, based on anthropometric studies, the BCoM lies approximately a few centimeters in front of the lumbosacral joint.

Nowadays, numerous methods exist to observe and measure the BCoM motion during gait, that are better described in the following: the “sacral marker” simplification; the analysis of the ground reaction forces (the so-called “double integration”) and the kinematic analysis of the position of the various body segments (usually, through optoelectronic “capturing” of retroreflective skin markers) as for anthropometric modeling. All these methods provide reliable and very similar results with respect of the position of the BCoM during motion.

As a consequence, human gait can be well represented as the translation of the body system as a whole and it can be described by using the trajectory of the Body Center of Mass (BCoM) as stated by Carpentiers et al. (2017): “*The center of mass is a key descriptor in the understanding and the analysis of bipedal locomotion*”.

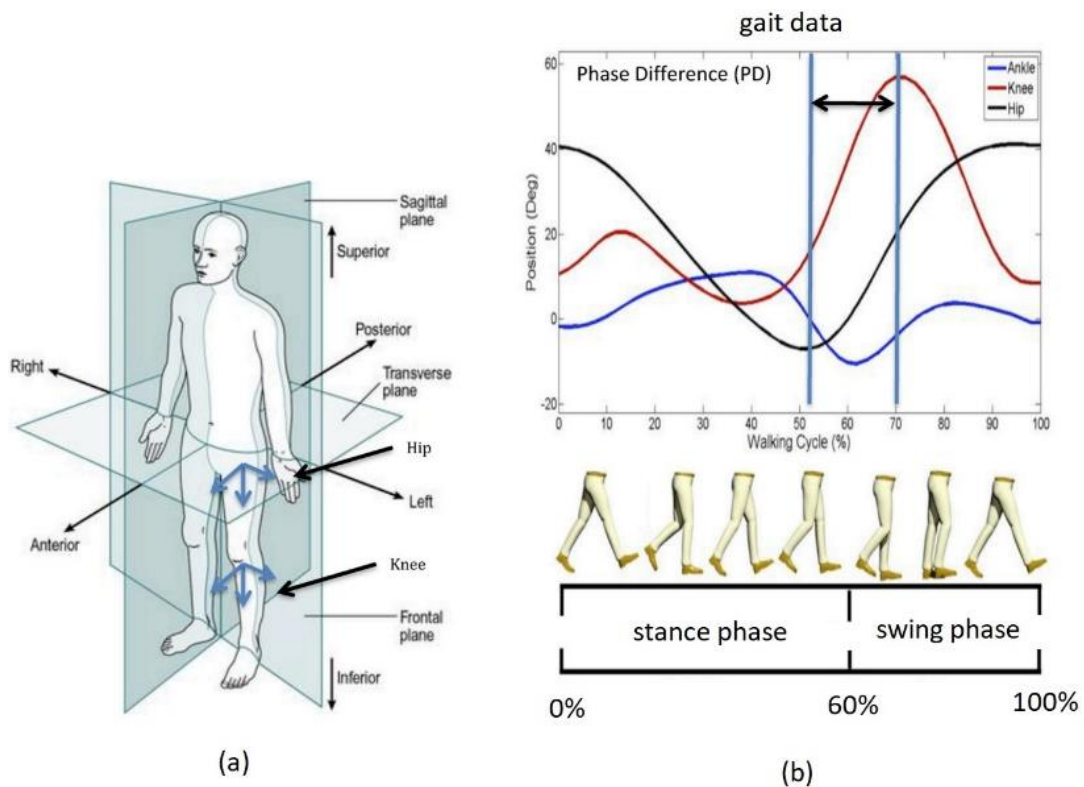


Figure 1.5 Example of the description of the gait using the segmental approach. (a) description of the hip and knee coordinate system that are referenced to the anatomical position in three reference planes; (b) description of the phase difference motion of the hip and knee in the sagittal plane (modified from Cestari Soto, 2017).

The BCoM motion was usually analyzed in the sagittal plane although, in principle, the same could be done to the frontal and horizontal planes. On the other hand, most of the work to move the body system and its segments, and its largest displacements, can be observed in the sagittal plane so that most of the conclusions on work production do not change remarkably when the other planes are also considered.

The lateral displacement of the BCoM, however, may be of crucial importance from a clinical standpoint, because lateral stability is challenged in many pathologic conditions that are caused by neurologic or orthopedic impairments. At each step, the BCoM oscillates laterally toward the supporting leg, then swings toward the opposite leg during the next step, producing an inverted pendulum-like mechanism in the frontal plane, too.

The composite motion of the sagittal and frontal pendulum during a stride follows a curved path around the line of progression. If advancement due to the average forward

velocity is subtracted (instantaneous velocity still undergoes periodic changes, of course) the BCoM path assumes a closed figure-eight shape, upwardly concave in the frontal plane, with an overall length of about 18 cm in healthy subjects (Tesio & Rota, 2019), as shown in Figure 1.6 b).

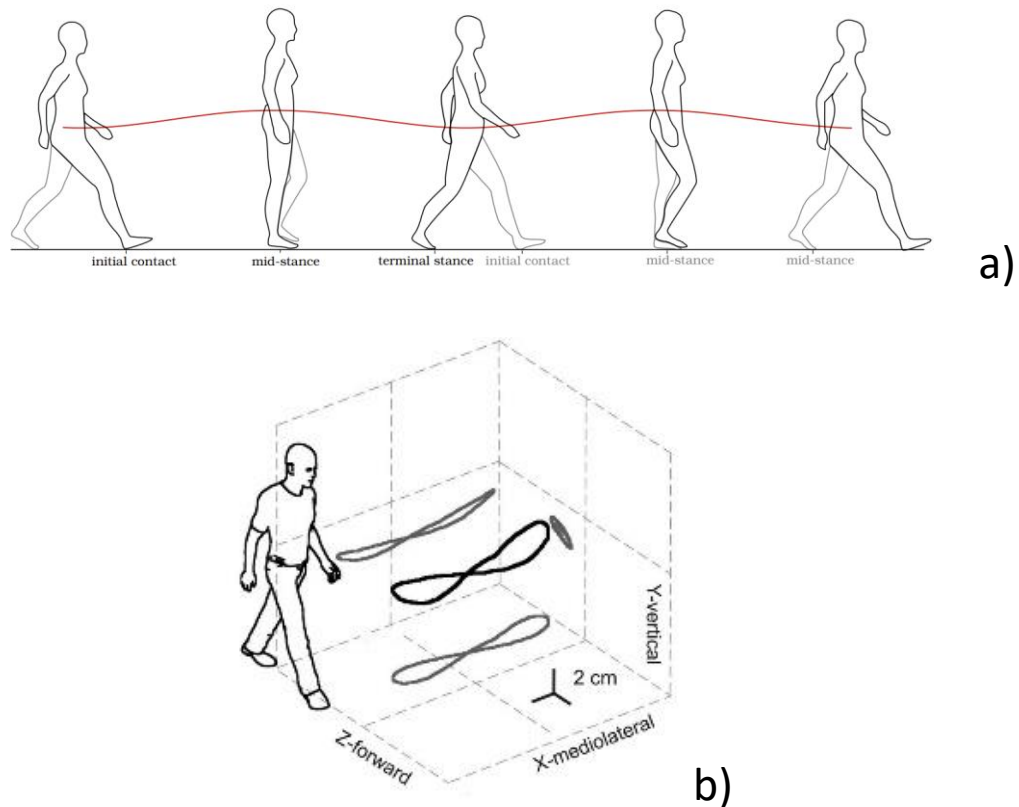


*Figure 1.6 Schematic example of the trajectory of the BCoM during human walking in vertical direction (a) and in a 3D geometry (b) (Tesio and Rota, 2019)*

Another important parameter linked with the gait and used to define the position of the BCoM in the “double integration” method is the force that the body exchanges with the floor in the support phase of the gait (i.e. when the foot touches the ground) usually called Ground Reaction Force (GRF) (Figure 1.7). The GRF vector is directed upward and induces external moments in the body joints that can be flexor or extensor if the vector of the external force passes in front or behind the considered joint of the body segment. Figure 1.8 shows the GRF changes in direction and modulus with reference to the leg position during the gait cycle while figure 1.9 shows the trend of a not pathological gait obtained through direct measurement using a dynamometric platform. It can be observed that the vertical component of the GRF during the gait is much higher than the other two components that are parallel to the ground. The peak

of the GRF occurs during the loading response phase and during the terminal swing and these two peaks are bigger than the body weight.

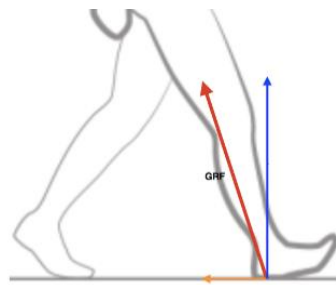


Figure 1.7 Schematic representation of the Ground Reaction Force in the plane of the motion

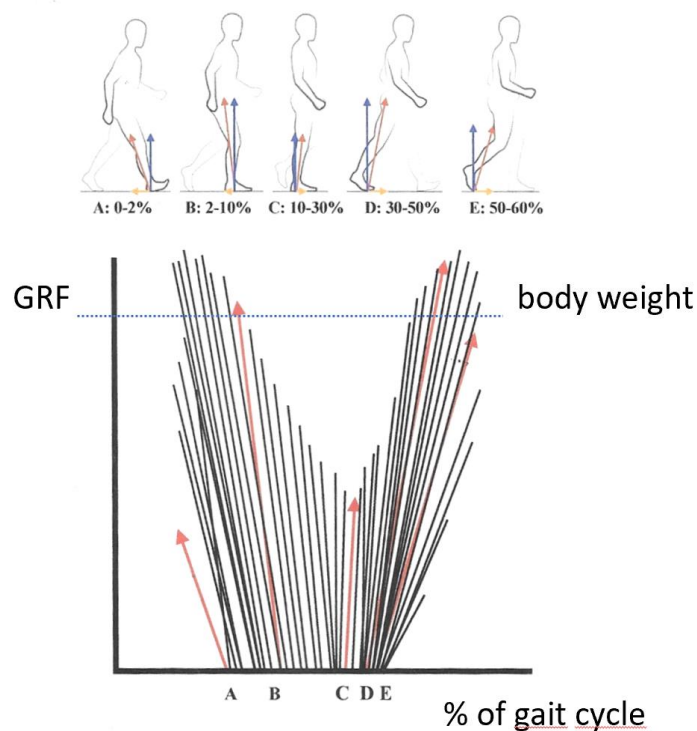


Figure 1.8 Example of measured Ground Reaction Force (Dimanico, 2018). In some of the gait phases, the GRF is bigger than the body weight due to dynamic effects. Key: A: initial contact, B: loading response, C: midstance, D: terminal swing, E: preswing.

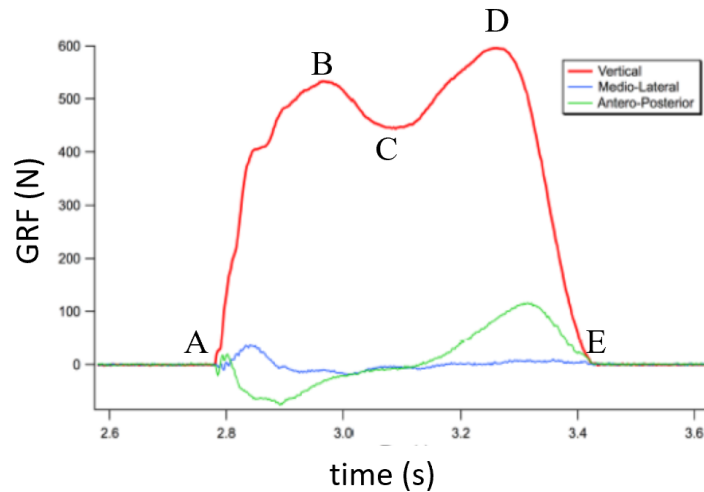


Figure 1.9 GRF components in the space during the cycle of a not pathological gait. Key: A: initial contact, B: loading response, C: midstance, D: terminal swing, E: preswing.

## 1.2 Measurement and models of the BCoM trajectory

The measurement of the motion parameters of the BCoM trajectory during walking has been a challenge for long time since the BCoM is a virtual point and it is not coincident with any anatomical landmark. The measurement of its position is not simple and requires assumptions/simplifications and/or indirect measurements and calculation as discussed by Carpentier et al. (2017).

The most frequently applied methods for the measurement of the BCoM motion are:

- the “*sacral marker*” simplification (sensors of various types are located in the sacral position of the body that is assumed to overlap with the position of the BCoM). Even if it is a simplification, the position of the sacrum is easy to be defined and the measurements are simple to be carried out;
- the “*double integration*” or Newtonian method (used for example by Cavagna, 1975, Tesio et al. 2010; Carpentier et al., 2017) that use the measurement of the ground reaction forces to determine the position of the BCoM;
- the kinematic method that uses the position of the body segments (usually, positioned using optoelectronic instruments) in the body anthropometric modeling (this method was used for example by Ploof et al., 2017). The application of this method implies several assumptions (e.g., that the BCoM is

stationary within the body) and approximations (e.g., a close matching between actual and modeled moments of inertia of the body segments).

The study of the BCoM trajectory provides valuable information on the gait type and characteristics and allows researchers and clinics to highlight the pathological aspects of the walk by comparing the “normal” trajectory i.e. that of a not pathological subject with that of a person affected by a disease or an amputation. Furthermore, since the BCoM trajectory is the motion of a single point, it is easier to be mathematically handled and this fact simplifies the interpretation also allowing the definition of global indexes as for example following the very old intuition that the BCoM moves up and down and accelerates or decelerates during each step like an inverted pendulum (Figure 1.10 and 1.11).



*Figure 1.10 Illustration of the inverted pendulum model of the human walk. Some of the sagittal, frontal and horizontal rotations of the joints are seen as major determinants of gait as long as they smooth the trajectory of the BCoM (Saunders et al., 1953; Tesio and Rota, 2019). Saunders et al. (1953) suggested that smoothing the BCoM oscillations is the aim of some of the segmental motions of the lower limbs, such as pelvic tilt and knee flexion, named the six “major determinants” of the gait. These authors suggested that these six determinants are fundamental in clinical observation of the gait.*

Today, the research has mainly focused on the complete measurement of the position of the BCoM point in the 3D space, as done by Tesio et al. (2011) and by Minetti et al. (2011) and the measurement of its acceleration (as done for example by Panero et al., 2021).

As already discussed, after adjusting for displacement due to the average forward speed, the trajectory assumes a figure-eight shape (dubbed the “bow-tie”). It is important to focus that the lateral size of this figure decreases increasing the walking velocity, thus ensuring dynamic stability (Figure 1.12). Lateral redirection appears as a critical phase of the step, requiring precise muscle sequencing, therefore its measurements is interesting for clinical observations. The shape and size of the “bow-tie” as functions of dynamically equivalent velocities do not change from child to adulthood, despite anatomical growth (Minetti et al., 2011). The trajectory of the BCoM thus appears to be a promising tool to provide summary indexes of balance of walking useful in clinical applications.

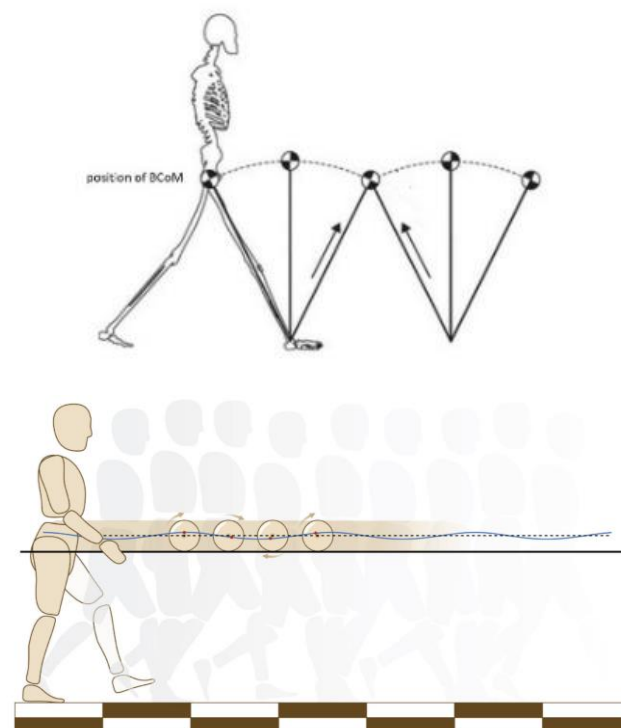


*Figure 1.11 Scheme of the simplified double inverted pendulum model created by the hip-leg relationship during the gait cycle (on the left). On the right there is an upgrade of this model proposed by Carpentier et al. (2017): the BCoM trajectory has a cycloidal pattern i.e. can be described by a point on a wheel rolling at a constant velocity on a flat surface.*

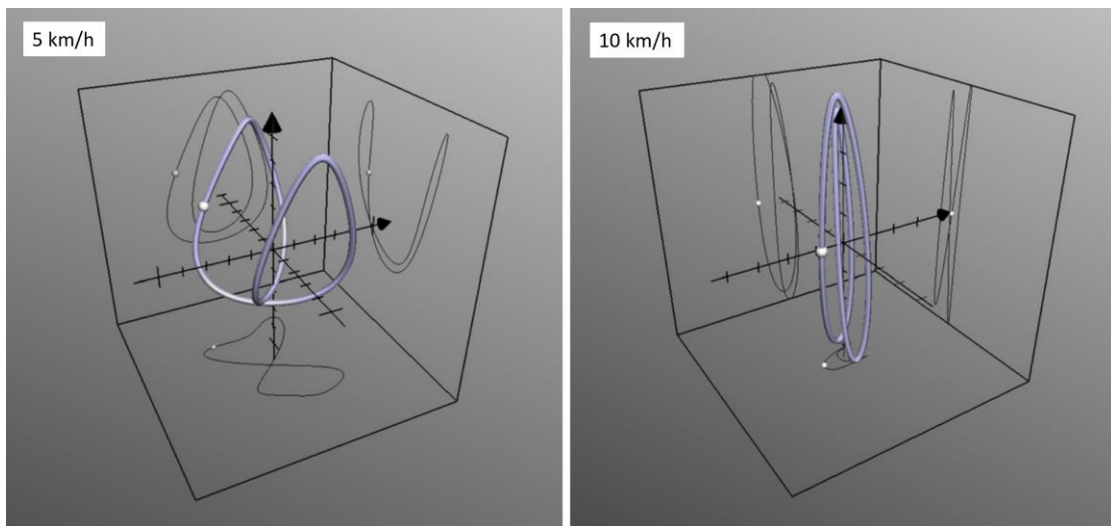


Figure 1.12 Example of the BCoM trajectory during walking at 5 km/h and 10 km/h presented by Minetti et al. (2011) using the Lissajous curve. Pointed arrows refer to the vertical ( $y$ ) and the progression ( $x$ ) axes. On each plane of the box, whose side is 60 mm long, the projection of the 3D contour is shown.

### 1.3 Laboratory methods for measurements of human gait parameters

The measurement of anatomical and biomechanical parameters is of great importance to provide the data to describe the characteristic of the gait of a specific subject. In the past, the study of the gait was based on the simple analyses of video frames, but the quality of the obtained data strongly depends on the operator's experience (Figure 1.13).

Today, more precise laboratory devices allow to get the exact position in space of the various elements of the body during the gait, to measure the force that the body exchanges with the ground and the acceleration of the body. These data can be combined, in clinical analysis, with the electrical signals provided by the muscles during their activation.

The direct measurement of the geometrical aspects of the moving body (specific point and segments) and the applied force exchanged with the ground, allow to precisely describe the motion and its quality. The usually measured data are:

- kinematic (i.e. position, displacements, angles, velocity, and accelerations of the various points of the human body during the gait cycle)
- dynamic (i.e. forces that the body exchanges with the ground through the feet during the gait cycle)

- biological i.e. muscles activations usually measuring the muscle electrical activity using the electromyography technology. This method is mainly a clinical tool and its application is behind the scope of the present work.

To get the kinematic data the following instrumentations are usually used:

- optoelectronic systems marker-based;
- optoelectronic systems markerless;
- not optical systems
  - o accelerometers
  - o dynamometric platforms.

The advantages and disadvantages of the various instruments are shortly summarized in Table 1.1 (Viteckova et al., 2019)

Hardware		Advantages	Disadvantages
<b>Optoelectronic systems</b>	General	Accurate measures the absolute position of a point (for example the BCoM) and the body in the three-dimensional space. Requires a model of the body segments.	Free line of sight between the markers and the cameras is needed. Measurement requires a defined space without obstacles for visibility.
	With passive markers	Light weight markers	Scene requires proper lighting
	With active markers	Does not require additional lightning	Ambient light may adversely affect optical system performance Markers have a certain weight
	Without markers	Cheap	Difficult processing Imprecision of the obtained data
<b>Not-Optical systems: Accelerometers &amp; gyroscopes</b>		Measure the immediate acceleration and orientation of the device. Movements are not limited to a specific space.	Difficult reconstruction of the motion trajectory Complex to define the proper the position of the sensor that can affect the quality of the data interpretation Need of a power supply for the sensors Higher weight when compared with the optical markers
<b>Not-Optical systems: dynamometric platforms</b>		Accurate measurement	Movement is limited to a specific space Requires the physical contact with the body

*Table 1.1 Vantages and disadvantages of the various data acquisition systems (modified from Viteckova et al., 2018).*

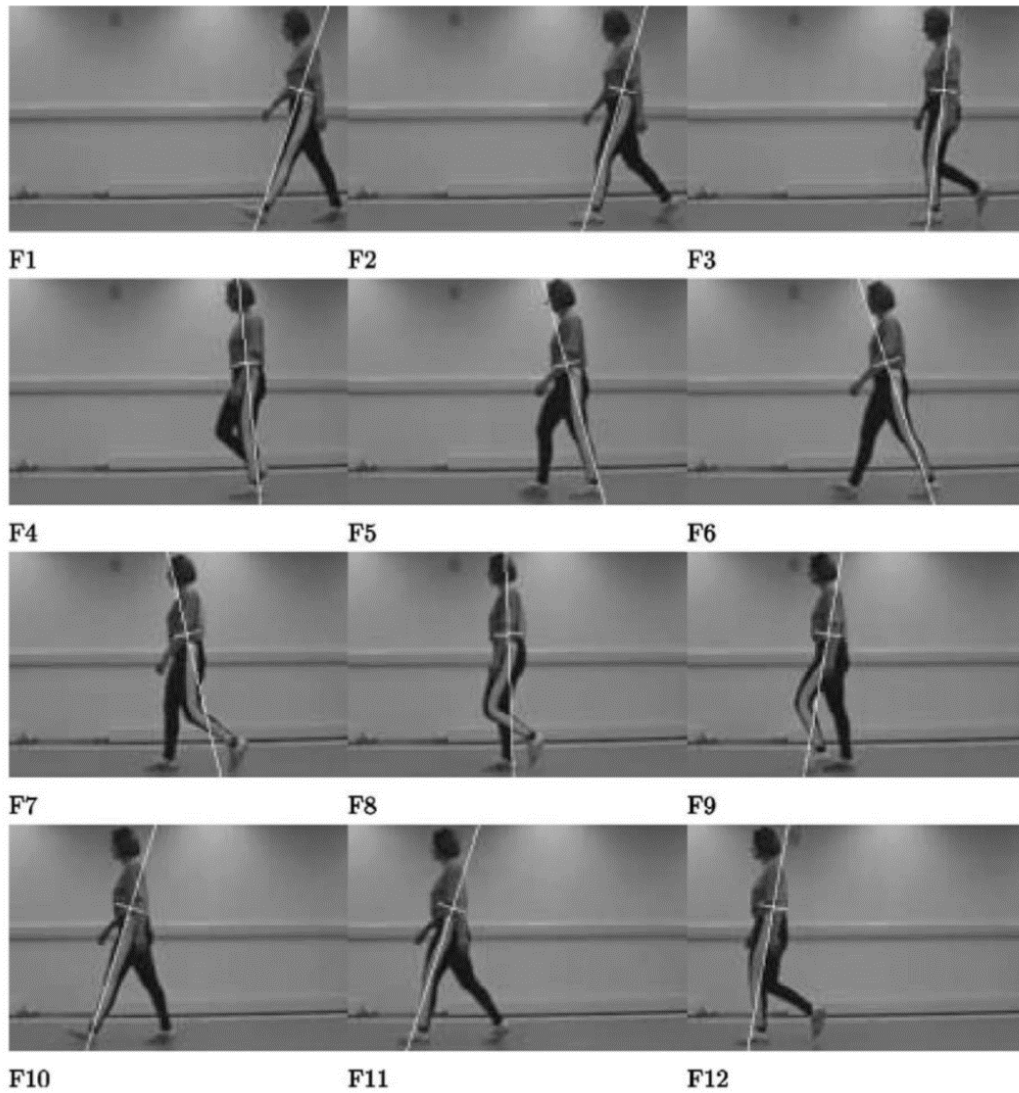


*Figure 1.13 Example of a simplified gait model from obtained from a VHT images (Cunado et al., 2003).*

#### *Optoelectronic instruments*

The optoelectronic instruments are based on the stereo-photogrammetry to reconstruct the human body motion during time. They are based on video recording of a moving body on which some markers have been installed (Cappozzo et al., 2005).

In general, the stereo-photogrammetry allows to reconstruct the trajectory of the point during its motion in a 3D space, using a sequence of images taken from two or more cameras with a constant frequency of acquisition and properly calibrated and synchronized (1.14). The number of the cameras to be used, depends from the type of

the movement to be studied and of the complexity of the biomechanical model to be applied for the interpretation: 2 to 4 cameras are used to study the body movement in a specific direction, 6 cameras are used to have a complete picture of the movement of small bodies while 10 or more cameras are used for the complete movement of large volumes and complete bodies, particularly when sport movements are analyzed. The images recording can be carried out using the visible light spectrum or the infrared light. Spherical markers must be positioned on anatomical landmarks of the human body to allow the reconstruction of multibody model starting from the 3D markers position. To improve the precision of the identification of the geometrical elements of the body markers are usually attached to the skin. The markers (Figures 1.15 and 1.16) can be divided in passive (made of a plastic support covered by a reflector surface) and active (made of small leds that generate a light signal).

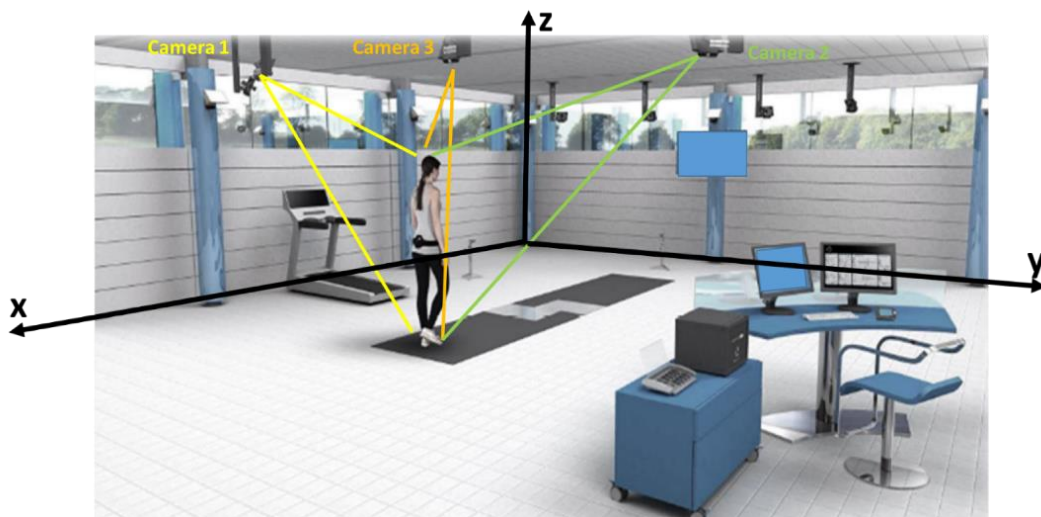


*Figure 1.14 Schematic overview of a laboratory equipped with video recording of a human walking on a dynamometric platform*

The active markers do not need the use of an illumination system, but it is necessary to connect each marker with a power alimentation. The synchronization is done by the cable linking and it is not necessary the pre-elaboration of the signal. One limit of this type of markers is that their emission angle is limited and this aspect could induce some problems in the camera setup.



*Figure 1.15 Examples of active (left) and passive (right) markers*

The correct positioning of the markers is very important for a complete description of the motion of the body and they should be correctly positioned on the body and different protocols of marker positioning have been developed during years by various researchers (Frigo et al., 1998; Gage, 1991; Cappozzo et al., 1995; Rabuffetti and Crenna, 2004; Leardini et al., 2007).



*Figure 1.16 Example of the passive marker located on the legs and on a walking body (<https://www.ouh.nhs.uk/gait-lab/research/oxford-foot-model.aspx>)*

For the transformation of the coordinates of the markers located on the body to the coordinate (and therefore the position vs time) of the anatomical reference points it is necessary to have a reference biometrical model based on the orientation of the considered body segments as shown in Figure 1.17 that presents the example of the anatomical reference system of a lower limb and the positioning of the anatomical landmarks.

#### *Not optical instruments*

The not optical devices most frequently used are accelerometers and gyroscopes to measure the acceleration and angular velocity of specific points of the body.

They are frequently used to measure the acceleration of the Body Center of Mass during its motion in the gait (Smidt et al., 1971). For example, Panero et al. (2021) used the acceleration signal acquired by a magnetic inertial measurement placed on the trunk of the patient, to study the effect of the deep brain stimulation for the treatment of the motion symptoms typical of Parkinson's disease and Simonetti et al.

(2021) used a wearable inertial sensor network to measure the Body Center of Mass acceleration and instantaneous velocity, to study a case history of a transfemoral amputee gait.

Since trunk, thighs, shanks and feet are the major contributors to 3D BCoM acceleration for people with transfemoral amputation in Simonetti et al. (2021) experiments seven wearable inertial sensors were mounted on these segments and manually aligned with their respective longitudinal axes. The BCoM acceleration and velocity was obtained from different combinations of sensor measurements and by considering the mass of each segment. Alternatively, the “sacral marker” simplification can be used by positioning the sensor in the sacral position of the body (Figure 1.18).

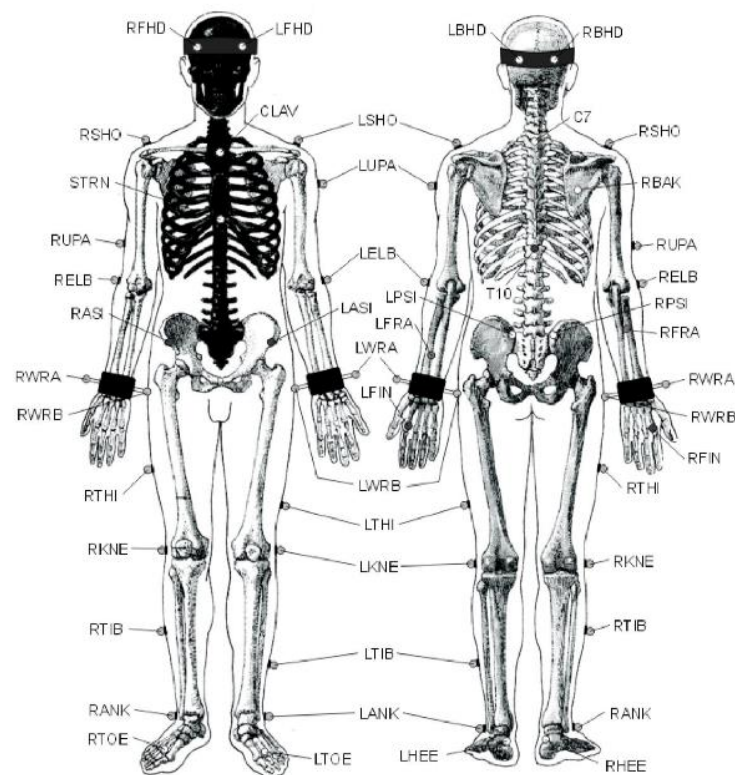


Figure 1.17 Example of the marker position used in the Plug in Gait protocol (<http://www.idmil.org/mocap/Plug-in-Gait+Marker+Placement.pdf>).



*Figure 1.18 Example of the experimental set-up of a subject walking on a treadmill walking machine equipped with accelerometers on the sacrum and the shank (Sabatini et al. 2015).*

#### *Dynamometric platforms*

To measure the Ground Reaction Force, dynamometric platforms are usually used (Figure 1.19) normally combined with optical instruments. With this force sensors it is possible to measure the vertical and the horizontal components of the Ground Reaction Force (in intensity, direction and point of application) and obtain the position of the center of pressure. For example, a device using a force measurement equipped treadmill has been used by Tesio et al. (2010) to determine the 3D path of the Body Center of Mass during walking at different walking speed while Carpentier et al. (2017) combined these measured with optical measurements for the reconstruction of the contact force distribution and the instantaneous position of the BCoM.

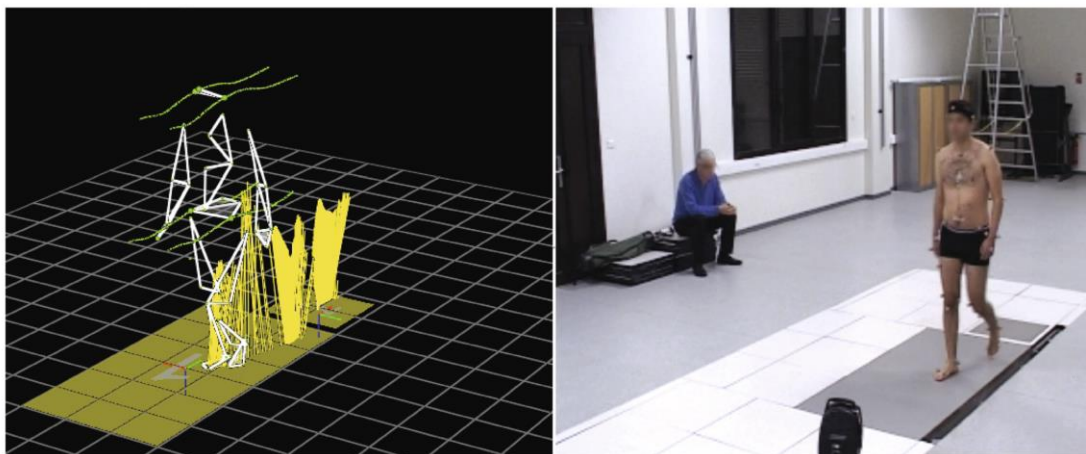


*Figure 1.19 Example of the experiment room used by Carpentier et al. (2017). A man walked barefoot in straight line at his comfort walking speed on force platforms and the position of the body segments were measured using an optical device. On the left there is the reconstruction of the GRF diagram.*

## 2. Gait symmetry and Body Center of Mass

Gait in a healthy person is symmetrical with minor deviations: able-bodied people show minimal laterality with only subtle differences between the dominant and non-dominant leg.

Asymmetry, or lack of symmetry, appears to be a relevant aspect for differentiating between a not pathological and pathological gait. The inter-limb deviations are the basis for the understanding of the overall quality gait. Alteration of the motion of any one segment of the body induces adaptive movements across the whole body inducing a loss of symmetry of the gait. A single local malfunctioning can therefore be responsible for the alteration of the general symmetry of the motion, for example in amputee subjects, even if in subjects that present balance deficits or paresis due to diffused lesions of the central nervous system it may be difficult to interpret the numerous concurrent alterations and therefore identify critical targets for clinical observation (Tesio & Rota, 2019). Asymmetric gait is not efficient as it increases oxygen consumption and energy cost of locomotion, it may lead to loss of bone mass density and osteoporosis of the affected leg, a higher dynamic load on the contralateral limb and joints and an increased risk of osteoarthritis and musculoskeletal injury (Block & Shakoor, 2010). In asymmetric gaits, the affected lower limb avoids muscle work by pivoting almost passively, but extra work is required from the unaffected side during the next step, in order to keep the body system in motion. This condition was clearly observed in the analysis of the data available for this thesis' work.

For the above-mentioned reasons, for clinical reasons it is essential to quantify if symmetry/asymmetry exists and to measure the asymmetry level as clearly stated by Viteckova et al. (2018) "*Gait symmetry is important in measuring gait pattern alterations for establishing the level of functional limitation due to pathology*". Numerous researches have highlighted that gait symmetry is sensitive to the differences between healthy individuals and those with gait impairments and several studies have focused on gait symmetry to distinguish at what stage a patient is with reference to a specific disease (frequently early stages of the disease are manifested by a low level of asymmetry while later stages of the disease are manifested by higher asymmetry), while other researchers investigated the positive effects of rehabilitation vs. symmetry (Tesio et al., 2011; Zverev, 2015; Wafaiet al. 2015; Tesio & Rota, 2019; Panero et al., 2021). In fact, alterations in BCoM motion could reveal motor

impairments that are not always detectable by clinical observation and symmetry/asymmetry is important tool.

Various global indexes have been used to describe gait asymmetry and they are shortly presented in the following paragraph. Among them, the spectral analysis using the Fourier series, recently applied, provides a valuable tool for solving the assessment of the symmetry of the gait.

## 2.1 Symmetry indexes

Sadeghi et al. (2000) and Viteckova et al. (2018) published extensive reviews of the symmetry indexes. That are summarized in Figure 2.1.

In the past, *discrete methods* and *statistical-based methods* were the only two classes of symmetry quantifiers used (Herzog et al., 1989; Gutierrez-Farewik et al. 2006). Currently, the most common approach used to assess symmetry is by finding a single or more discrete value and by describing symmetry/asymmetry for space-temporal, kinetic and kinematics parameters between the right and left sides or affected and unaffected limbs, using the data obtained by the observation of a complete gait cycle.

According to data sources, time-series are often used to quantify the symmetry of parameters of human gait and methods based on the use of Fourier time series (*spectral analysis*) have been developed mainly based on the measured trajectory of the BCoM.

In the following, a concise overview of the most frequently applied quantitative indexes for the gait symmetry assessment is reported.

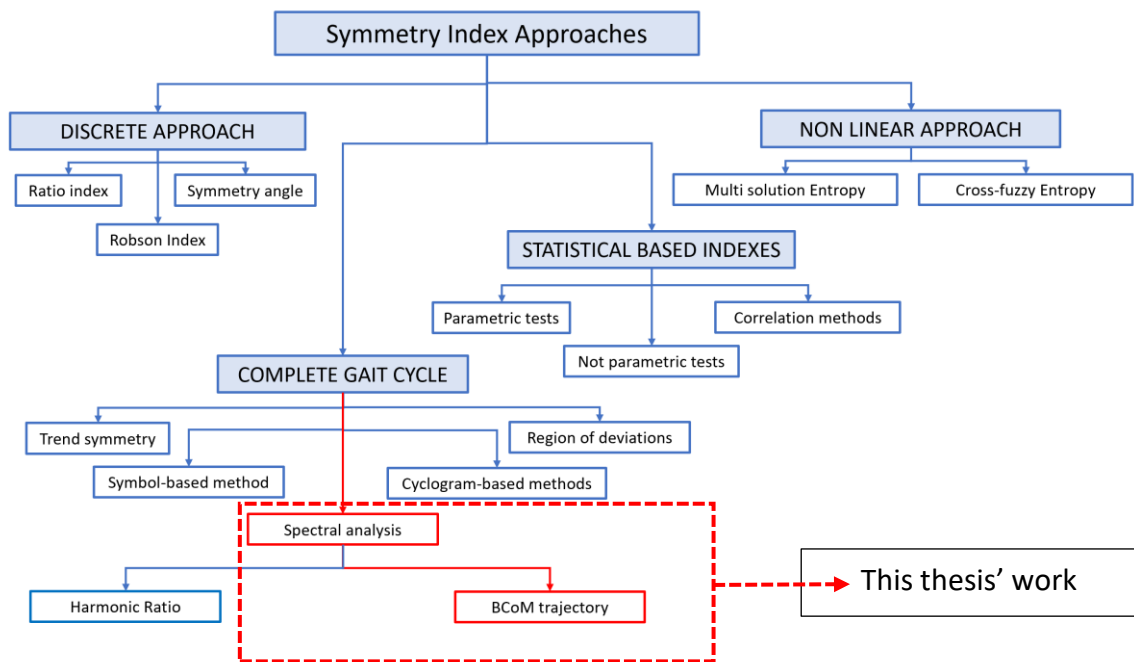


Figure 2.1. Global overview of the used symmetry indexes (modified from Viteckova et al., 2018). The spectral analysis has been recently applied for this task and it has been studied in this thesis to the analysis of symmetry of the BCoM trajectory.

### 2.1.1 Discrete approaches

Discrete methods use equations to calculate and evaluate gait symmetry from spatio-temporal parameters of the gait. These methods differ with reference to the equation chosen to calculate the symmetry index, which gait feature is used in the equations and which comparison between gait variable values is performed (e.g. a variable from the left and right side of the body).

The most commonly used equations for assessing gate symmetry are: Ratio Index, Robinson index and Symmetry Angle Index.

#### *Ratio index*

The gait symmetry/asymmetry is represented by the ratio between the value of a gait parameter measured for one limb and the value of the same gait parameter determined for contralateral limb. This ratio is called Ratio Index or Symmetry Ratio Index.

The basic formula of the Ratio Index (RI) is:

$$RI = X_1/X_2 \quad (2.1)$$

where  $X_1$  is the parameter value of one limb and  $X_2$  is the parameter value of the contralateral limb (the gait used parameters that can be found in technical literature

are: step length, single support phase duration and swing duration).

Perfect theoretical symmetry for a given variable is achieved when the value of the RI=1 while lower or higher values indicates asymmetry in the gait pattern. For example, with reference to the literature data reported in Figure 1.4 of the duration of the swing time: the computed values of RI are: RI for the normal subject = 1; RI for the subject with avascular necrosis, left hip = 0.73 and RI for the subject with osteoarthritis, left hip = 0.5.

#### *Robinson index*

Robinson et al. (1987) developed an index to quantify the symmetry of the Ground Reaction Force in the gait of patients with chronic unilateral sacroiliac dyskinesia. The basic formula of the Robinson Index also called Symmetry Index (SI) is:

$$SI = 200 \frac{(X_u - X_a)}{(X_u + X_a)} \quad (2.2)$$

where  $X_u$  is the parameter's value of the unaffected leg and  $X_a$  is the parameter's value of affected leg (the used parameters in technical literature are: gait phases duration, step length, step width, step height, arm swing magnitude, range of arm swing angle, arm swing duration, lower limb angular rate, Ground Reaction Force max value, muscle strength, muscle force, EMG).

When the value of the proposed index equals zero, it is considered a symmetrical gait, divergence from zero means asymmetry. This index is the most commonly used to describe gait symmetry. For example, with reference to the literature data reported in Figure 1.4 of the duration of the swing time: the computed values of SI are: SI for the normal subject = 0; SI for the subject with avascular necrosis, left hip = -30 and RI for the subject with osteoarthritis, left hip = -66.

The main disadvantages of this index are the following: it is variable dependent i.e. it is not possible to use one single criterion value to assess gait asymmetry for all the several gait variables and it needs to be normalized to a reference value.

### *Symmetry angle*

To overcome the disadvantages of the Robinson index and its modifications, such as the need a required reference value, Zifchock et al. (2008) proposed to use the Symmetry Angle index (SA). The basic formula of the Symmetry Angle (SA) is:

$$SA = \left(\frac{100}{90}\right) \arctan\left(\frac{X_a}{X_u}\right) \quad (2.3)$$

where  $X_u$  is the parameter's value of the unaffected leg and  $X_a$  is the parameter's value of affected leg (the used parameters in technical literature are: stride duration, standard deviation of arm angular acceleration, wrist displacement, maximum trunk angular rotation, Ground Reaction Force max).

#### 2.1.2 Statistically based approaches

Statistical approaches can be used with discrete values as well as with continuous signals. In the case of continuous signals, the cross-correlation, autocorrelation, PCA, and root-mean-square difference were used (Hoerzer et al. 2015).

The detailed description of these methods is outside the scope of the present work and an overview of them and the key literature references can be found in Viteckova et al. (2018).

#### 2.1.3 Not-linear approaches

Similar to discrete methods, nonlinear methods employ discrete variables extracted from a continuous signal to symmetry assessment. These methods evaluate the evolution of a discrete variable (mainly the entropy) over a set of consecutive gait cycles.

The detailed description of these methods is outside the scope of the present work and an overview of them and the key literature references can be found in Viteckova et al. (2018).

#### 2.1.4 Complete gait cycle approaches

An important limit of the use of discrete symmetry indexes in the analysis of the gait is that they neglect the temporal information of gait waveforms and that their extraction is often subjective and potentially difficult in atypical waveforms.

Discrete symmetry indices provide valuable information about discrete time events but do not describe the complete curves i.e. development of the gait vs time (e.g. two curves may have similar peak values but different waveforms).

For this reason, the research has addressed toward the development of indexes able to take the complete signal of the gait cycle into account.

##### *Cyclogram-based and symbol-based methods*

In this family of methods study the gait cycle as a whole and they are the trend symmetry method, the cyclogram-based method, the region-of-deviation method, and symbol-based method.

The detailed description of these methods is outside the scope of the present work and an overview of them and the key literature references can be found in Viteckova et al. (2018).

##### *Spectral analysis*

The development of the spectral analysis has become more and more popular in recent times, since it allows a mathematical description of the cyclic signal of the gait thanks to the use of the Fourier series. The method has been mainly applied to the study of the acceleration of the BCoM (with the development of the Harmonic Ratio) or the BCoM trajectory indexes.

#### 2.2 Spectral analysis approach

As already said the spectral analysis is applied to study the symmetry of the gait taking the complete signal of the gait cycle into account. Frequently it is applied to study the BCoM trajectory in the three-dimensional space.

When the BCoM acceleration is studied the proposed index is the Harmonic Ratio while when studying the trajectory of the BCoM during the gait cycle, the researchers

have focused on two different approaches: the study of the complete trajectory with the implementation of the Lissajous curves as done, for example, by Tesio & Rota (2019) and by Minetti et al (2021) and the implementation of symmetry indexes that based on the Fourier coefficient are able to describe the symmetry of the motion. This last approach has been studied and applied in this thesis work.

#### *Harmonic ratio*

The Harmonic Ratio (HR) is a measure of the gait symmetry, smoothness and variability (Gage, 1964; Menz et al., 2003a and 2003b; Yack and Berger, 1993; Bellanca et al., 2013; Esser et al. 2013; Panero et al., 2021). It is commonly extracted from trunk acceleration measures. The higher is the HR the greater is the walking symmetry and smoothness.

The Harmonic Ratio is obtained from the combination of the Fourier series coefficient of the signal of the acceleration of selected human body segments during gait (Figure 2.5).

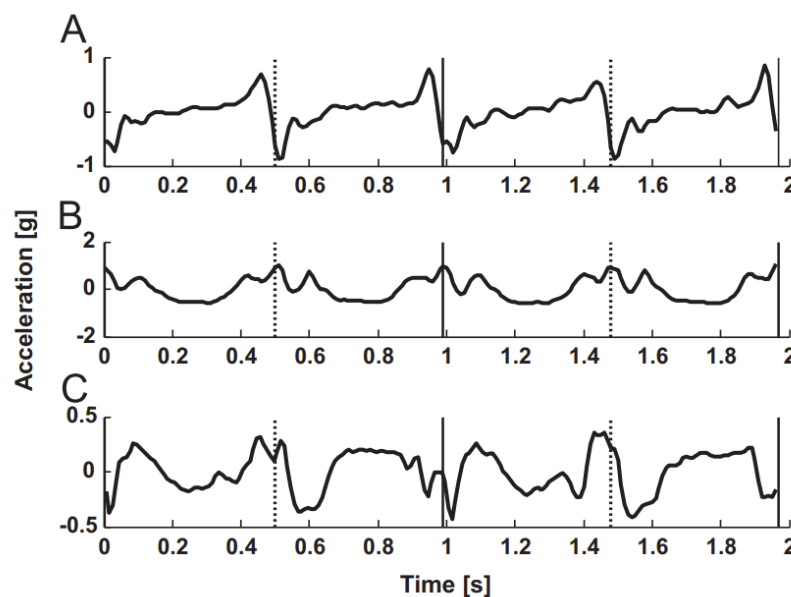


*Figure 2.5 Example of the acceleration signal for (A) Anteroposterior, (B) vertical and (C) mediolateral direction with the right (vertical line solid) and left (vertical line dotted) heel contacts. Note: the gravitational component has been removed. (Bellanca et al., 2013).*

This index is defined as the ratio of the sum of the amplitudes of the even harmonics to the sum of the amplitudes of the odd harmonics of the acceleration signal:

$$HR = \frac{\sum_i a_i}{\sum_k a_k} \quad i = 2,4,6, \dots \text{ and } k = 1,3,5, \dots \quad (2.4)$$

Usually, the first 20 harmonic coefficients are used. This choice is justified by the standard walking cadences. The majority of the power occurs below 10 Hz and the normal stride frequency generally ranges from 0.8 Hz for older adults walking slowly, to 1.1 Hz for young adults walking quickly (100–135 steps/min respectively). Slower cadences (60 steps/min or slower i.e 0.5 Hz stride frequency) may be problematic, since the first 20 harmonics only encompasses frequencies up to 10 Hz.

The advantage of the method is that the spectrum should be inspected to ensure that enough coefficients are incorporated in the definition of the index allowing a proper description of the signal. Therefore, the number of coefficients can be increased as needed.

This index has been recently applied to discriminate between individuals with different pathologies and to monitor the impact of rehabilitation protocols (Sabatini et al., 2015; Panero et al., 2021).

#### *BCoM trajectory analysis and related symmetry indexes*

This approach is based on the observation that despite the asymmetric condition of amputee and other anomalous gait due to pathological reasons, the trajectory of the BCoM preserves a base periodicity between strides (i.e. the trajectory has a fundamental period that coincides to the step duration). This fact addressed the researches to study the BCoM motion with the tools offered by the Fourier series. With this mathematical technique it is possible to reduce the complexity of the BCoM 3D trajectory into a manageable entity and therefore to provide a quantitative description of the gait.

The application of the spectral analysis and Fourier series to the evaluation of the symmetry of the BCoM trajectory is a relatively recent but has already shown to be a valuable tool and it has allowed some authors to develop robust symmetry indexes based on the Fourier coefficient.

The advantage of the indexes computed using this approach is that the trajectory of BCoM exhibits the effects of compensatory mechanisms in amputee gait is the body Center of Mass and that as an anatomical point that reflects the entire body mechanics, the trajectory of the BCoM has an asymmetric behavior between consecutive steps when certain compensations take place. As an example, as highlighted by Ochoa-Diaz & Padilha (2020) the vertical BCoM from amputees showed an amplitude four times greater than the normal values from able-bodied subjects, besides a different shape from the observed sine-wave shape in the non-amputee case.

Among the others the indexes proposed by Minetti et al. (2011) and by Ochoa-Diaz & Padilha (2020) are discussed more in detail in Chapter 4 since they were found to be the most interesting to be applied for the study of the gait of subjects affected by hemiparesis even is these indexes were not originally developed for this purpose.

### 3. The theory of Fourier series

The Fourier series is a standard tool for the analysis and the study of periodic functions and experimental signals. It was originally developed by Joseph Fourier (1768-1830) and it was applied for the series representation of the solution of the second-order heat equation. The series is based on the expansion of a periodic function in terms of an infinite sum of trigonometric functions (sine and cosine). As a consequence, the coefficients of the trigonometric functions determine the characteristics of the periodic function that is expanded.

For our purposes the Fourier series appears to be an adequate and efficient mathematical tool to characterize the periodic experimental data, since, as already explained above, the BCoM trajectory preserves periodicity between strides.

In the following the basic theory of the Fourier series and the algorithm developed to obtain the coefficients are shortly described (Butkov, 1968).

#### 3.1 The series and its coefficients

Let us assume that  $f(x)$  is a periodic function of period  $T$ . The independent variable  $x$  can be rescaled using the transformation  $x = (2\pi/T)t$ , leading to a periodic function  $f(t)$  that is periodic with a period  $2\pi$ . This function is represented by means of a linear combination of basic sinusoidal functions (harmonic functions) characterized by the same periodicity, as:

$$f(t) = a_0 + \sum_{i=1}^{\infty} [a_i \sin(i\omega_0 t) + b_i \cos(i\omega_0 t)]. \quad (3.1)$$

The function is thus expressed as a superposition of trigonometric function characterized by increasing frequencies as  $i$  increases (harmonic representation).

The terms  $a_0$ ,  $a_i$  and  $b_i$  (where  $i = 1, 2, \dots$ ) are named the Fourier coefficients and, of course, they depend on the function  $f$  itself. They fully characterize the given function, and the set of their values is often referred to as the “Fourier spectrum” of the function.

The coefficients can be determined through a straightforward integration operation over one period of both sides of Eq. (3.1). One should notice that:

$$\int_0^{2\pi} \sin(i\omega_0 t) dt = \int_0^{2\pi} \cos(i\omega_0 t) dt = 0, \quad (3.2)$$

For all values of  $i > 0$ . Consequently, if the left-hand side of Eq. (3.1) is integrated, all terms in the sum disappear, except the first one, of order 0. One can thus find the coefficient  $a_0$  as:

$$a_0 = \frac{1}{2\pi} \int_0^{2\pi} f(t) dt = \frac{I_0}{2\pi}. \quad (3.3)$$

The trigonometric functions satisfy the following properties:

$$\int_0^{2\pi} \sin(i\omega_0 t) \sin(m\omega_0 t) dt = 0, \quad (3.4)$$

$$\int_0^{2\pi} \sin(i\omega_0 t) \cos(m\omega_0 t) dt = 0, \quad (3.5)$$

$$\int_0^{2\pi} \cos(i\omega_0 t) \cos(m\omega_0 t) dt = 0, \quad (3.6)$$

for all values of integers  $i > 1$  and  $i \neq m$ . This property is known as “orthogonality property” for the trigonometric functions, as it appears as a natural generalization to functions of the orthogonality property of vectors.

Furthermore, it can be easily proved that:

$$\int_0^{2\pi} [\sin(m\omega_0 t)]^2 dt = \pi, \quad (3.7)$$

and:

$$\int_0^{2\pi} [\cos(m\omega_0 t)]^2 dt = \pi. \quad (3.8)$$

If one multiplies both sides of Eq. (3.1) by  $\sin(mt)$  ( $m \neq 0$ ) and integrates over a period, all terms will disappear using the orthogonality properties, except the one for  $i = m$ , and therefore:

$$\int_0^{2\pi} f(t) \sin(m\omega_0 t) dt = a_m \int_0^{2\pi} [\sin(m\omega_0 t)]^2 dt. \quad (3.9)$$

The coefficients  $a_m$  are thus determined by:

$$a_m = \frac{1}{\pi} \int_0^{2\pi} f(t) \sin(m\omega_0 t) dt = \frac{I_m}{\pi}. \quad (3.10)$$

Similarly, if both sides of Eq. (3.1) are multiplied by  $\cos(mt)$  ( $m \neq 0$ ) and integrated over a period, it is possible to determine the coefficients  $b_m$  as:

$$b_m = \frac{1}{\pi} \int_0^{2\pi} f(t) \cos(m\omega_0 t) dt = \frac{H_m}{\pi}. \quad (3.11)$$

### 3.1.1 Mean value

The mean value  $\bar{f}$  of a function  $f$  over a given interval is defined as the ratio between the integral of the function itself on the chosen interval and the amplitude of the interval, namely for interval  $[a, b]$ :

$$\bar{f} = \frac{1}{b-a} \int_a^b f(x) dx. \quad (3.12)$$

Noticing that the mean values of the trigonometric functions over a period or multiples of the period vanish (see Eqs. (3.2)), one can immediately observe that the mean value of a periodic function is given by its Fourier coefficient  $a_0$ , expressed by equation (3.3).

In the analysis carried out in this thesis the coefficient  $a_0$  has not been considered since it represents a static contribution.

### 3.1.2 Phase-angle form

Another way to express the Fourier series is the so called “phase-angle form”, which, unlike the expression in Equation (3.1), contains functions of only one species, either sine or cosine. In the following, sine functions are adopted. It is well known that one can set

$$a_i \sin(i\omega_0 t) + b_i \cos(i\omega_0 t) = c_i \sin(i\omega_0 t + \phi_i). \quad (3.13)$$

Using the sum formula for the sine function, one easily finds that the above equality holds only if:

$$\begin{aligned}c_i \sin(\phi_i) &= a_i, \\c_i \cos(\phi_i) &= b_i.\end{aligned}\tag{3.14}$$

By squaring and summing, the new coefficient  $c_i$  is determined:

$$c_i = \sqrt{a_i^2 + b_i^2}.\tag{3.15}$$

Taking the ratio of the two relationships, one finds:

$$\phi_i = \frac{\pi}{2} \operatorname{sgn}(b_i) - \tan^{-1}\left(\frac{b_i}{a_i}\right).\tag{3.16}$$

In conclusion, an alternative formulation of the Fourier series is given by the following expression:

$$f(t) = a_0 + \sum_{i=1}^{\infty} c_i \sin(i\omega_0 t + \phi_i).\tag{3.17}$$

The coefficients  $c_i$  are usually denoted as the “amplitudes” of each harmonic, while the angles  $\phi_i$  are referred to as the corresponding “phases”.

The harmonic function having the lowest frequency ( $i = 1$ ) is usually denoted as the “fundamental” (or “dominant”) harmonic, where the meaning appears clear as one thinks of the series representation, whence it is expected that the contributions of the terms decrease with increasing order.

### 3.2 Computational tool for the determination of the Fourier coefficients

For the calculation of the coefficients of the Fourier series a specific Matlab code has been developed. The code is able to calculate the Fourier coefficients for a generic periodic function.

For the application to the analysis of the data in the specific problem of interest for this thesis work, the code takes the input data from the matrix obtained from direct experimental observation of the coordinates  $x(t)$ ,  $y(t)$  and  $z(t)$  of the BCoM trajectory vs test time for each subject. The coefficients are computed using a discrete integration formula.

### 3.2.1 Numerical example: sawtooth function

The algorithm has been implemented using the Matlab software.

The code has been verified using some elementary analytical test function: the accuracy of the Fourier representation is verified comparing the results with those obtained by a direct analytical approach.

This preliminary phase is important to confirm the reliability of the developed code.

The periodic sawtooth function  $f(t) = t$  for  $t \in [0, 2\pi]$  is assumed (see Figure 3.1).

All the harmonics give a contribution to the series, although the amplitudes decrease with increasing order, as expected, and this confirms the feasibility of the code.

The computed Fourier spectrum for the first 10 harmonics is shown in Figure 3.2.

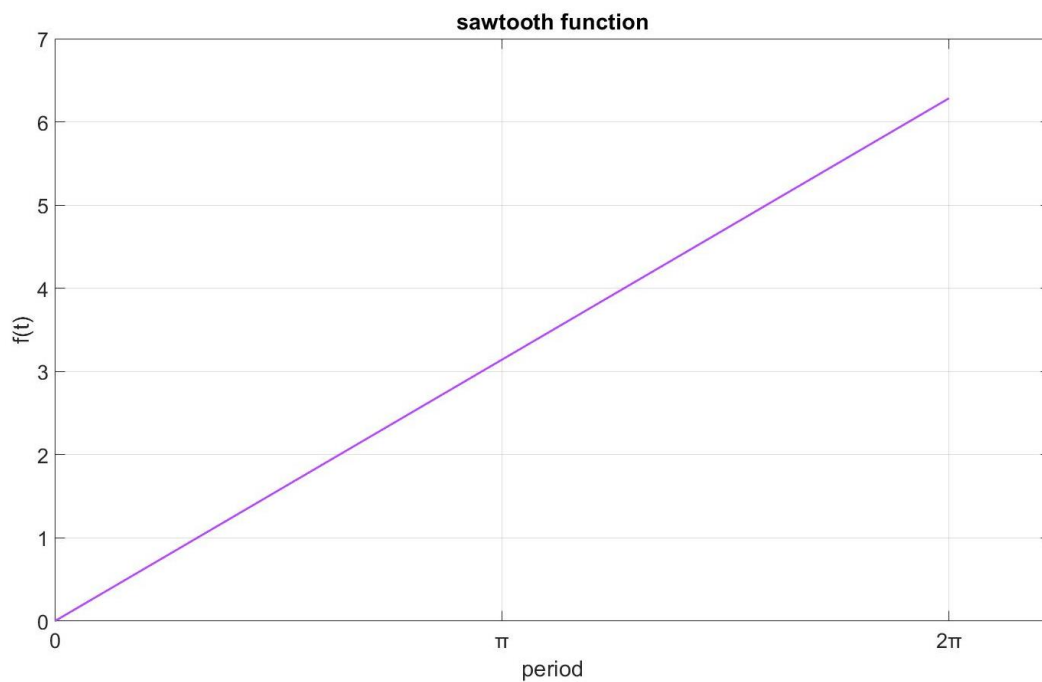


*Figure 3.1. Sawtooth function in the first period  $t \in [0, 2\pi]$ .*

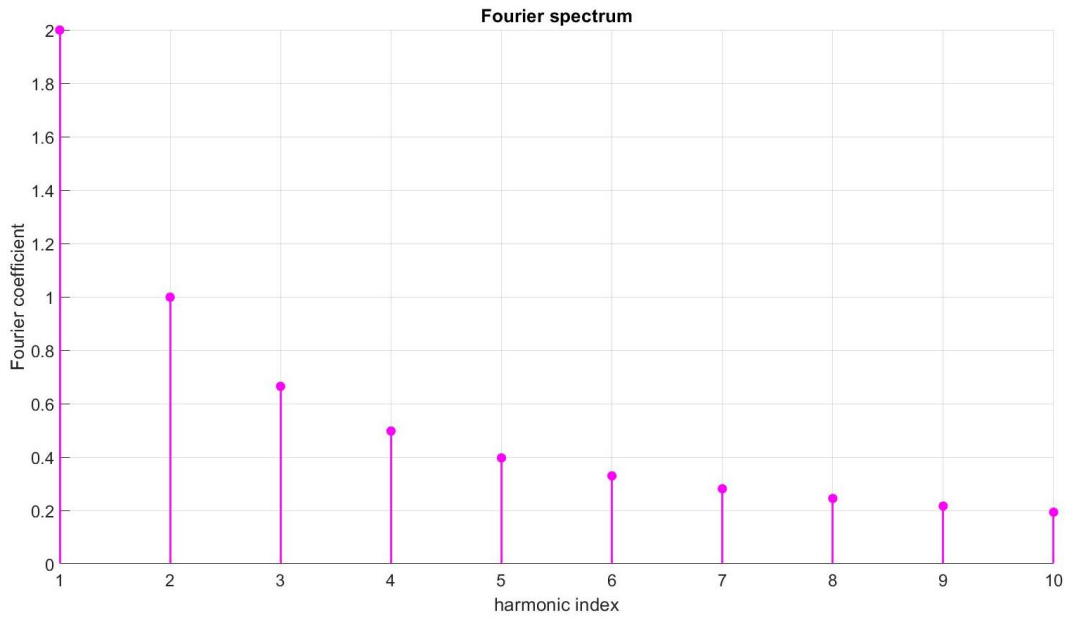


Figure 3.2. Fourier spectrum up to tenth order.

The representation of a sawtooth signal using the Fourier series is shown in Figure 3.3 considering different points of integration.

The choice of proper number of harmonics is limited by the frequency of sampling of the experimental signal.

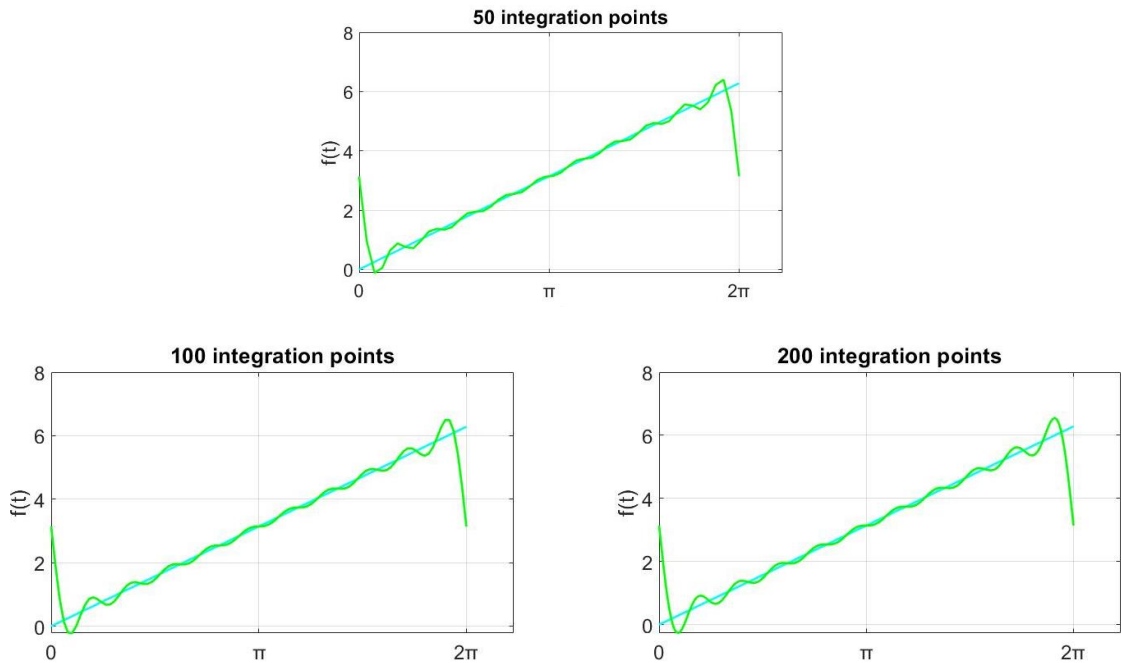


Figure 3.3. representation of the sawtooth function using 10 harmonics and a different number of integration meshes (green=reference function blue=representation function).

### 3.2.3 numerical example: gait cycle

The accuracy of the code has been verified also using the data taken from the supplementary material of Minetti et al. (2011).

Starting from the experimental measurements, the data reported in table 3.1 represents a typical gait cycle of a healthy subject reconstructed using the Fourier series in the phase angle form truncated to the 6th harmonic:

$$\begin{aligned}
 x = & (1,6 \sin(t - 2,42) \\
 & + 10,7 \sin(2t - 1,41) \\
 & + 0,7 \sin(3t - 0,16) \\
 & + 1 \sin(4t + 0,15) + 0,2 \sin(5t + 2,81) + 0,5 \sin(6t - 0,02)
 \end{aligned}$$

harmonics	Vertical direction											
	<b>1</b>		<b>2</b>		<b>3</b>		<b>4</b>		<b>5</b>		<b>6</b>	
coefficient and phase	c	$\phi$	c	$\phi$	c	$\phi$	c	$\phi$	c	$\phi$	c	$\phi$
values	<b>1,6</b>	-2,42	<b>10,7</b>	-1,41	<b>0,7</b>	-0,16	<b>1</b>	0,15	<b>0,2</b>	2,81	<b>0,5</b>	-0,02

*Table 3.1. data from supplementary material of Minetti et al. (2011)*

The figure 3.4 represents the trajectory of the BCoM in the vertical direction in a stride of a healthy subject analysed by Minetti et al. in their work.

The figure 3.5 reports the Fourier spectrum of the experimental signal. It highlights the expected values of the harmonic contribution expressed with the Fourier coefficients reported in table 3.1. This result confirms the feasibility of the code.

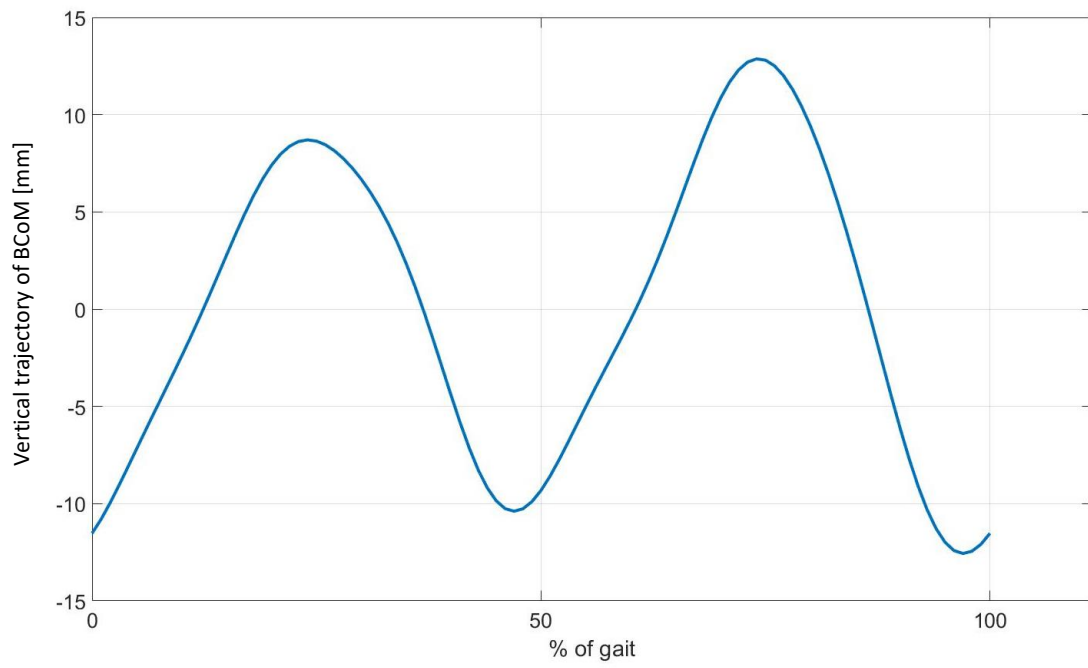


Figure 3.4. Gait signal

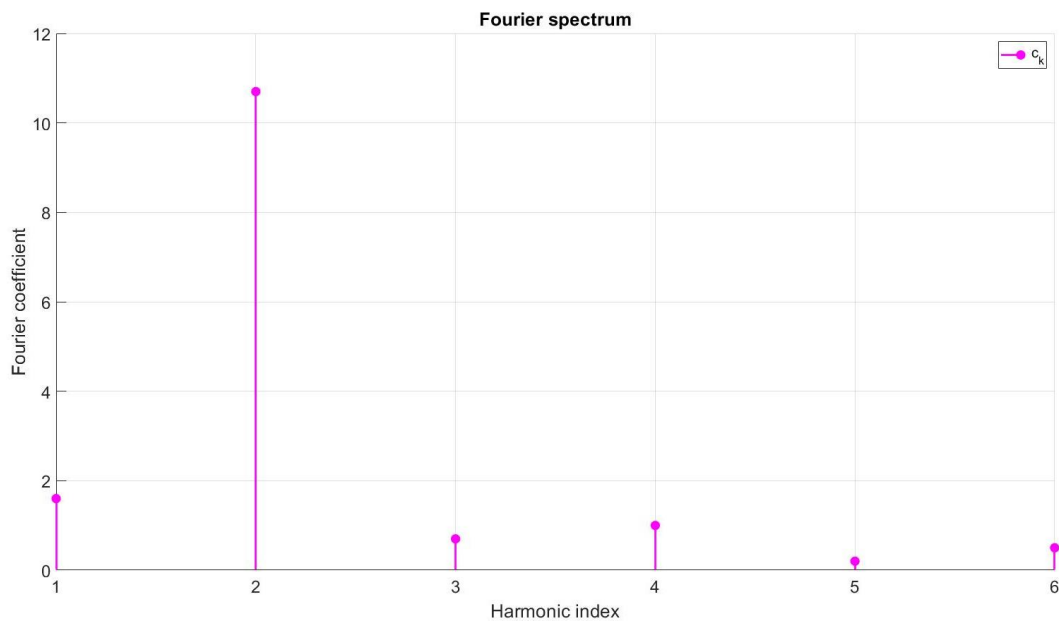


Figure 3.5. Fourier spectrum up to sixth order.

### 3.2.2 Robustness tests

The robustness of the code has been verified applying a white noise to the signal of the gait cycle previously analyzed, to simulate the variability of a real signal and evaluate the respective relative error between the theoretical values of the Fourier coefficients of the function and the real ones.

A white noise is characterized by a constant amplitude on all its frequency spectrum. For the test 3 different values of constant amplitude of the noise are chosen, defined as a percentage of the signal standard deviation. Calling  $x(t)$  the noiseless signal,  $p$  the noise percentage and  $\xi(t)$  a unit white noise, the signal affected by noise can be defined as:

$$x_{noise}(t) = x(t) + \frac{p}{100} \sigma(x) \xi(t) \quad (3.18)$$

In particular, 1%, 5% and 10% noise amplitude are considered in the following.

The Figures 3.6-3.8 report the graphs of the function adopted and its representation with a different percentage of noise and their respectively Fourier spectrum.

The deviation between true and estimated Fourier coefficients is computed as the percentage RMS error  $\epsilon$  for each level of noise, defined as

$$\epsilon = 100 \frac{RMS[vec(c_{th}) - vec(c_{est})]}{RMS[vec(c_{th})]} \quad (3.19)$$

Where  $c_{th}$  are the theoretical coefficients and  $c_{est}$  are the estimated ones. The results are listed in table 3.2 for the different levels of noise.

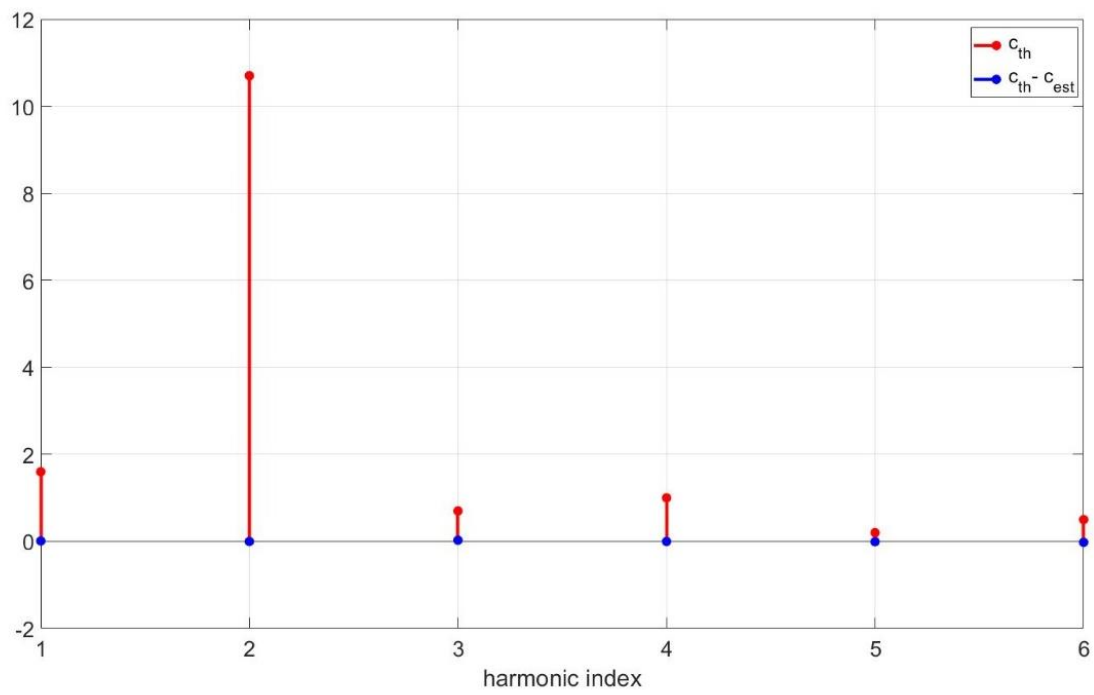
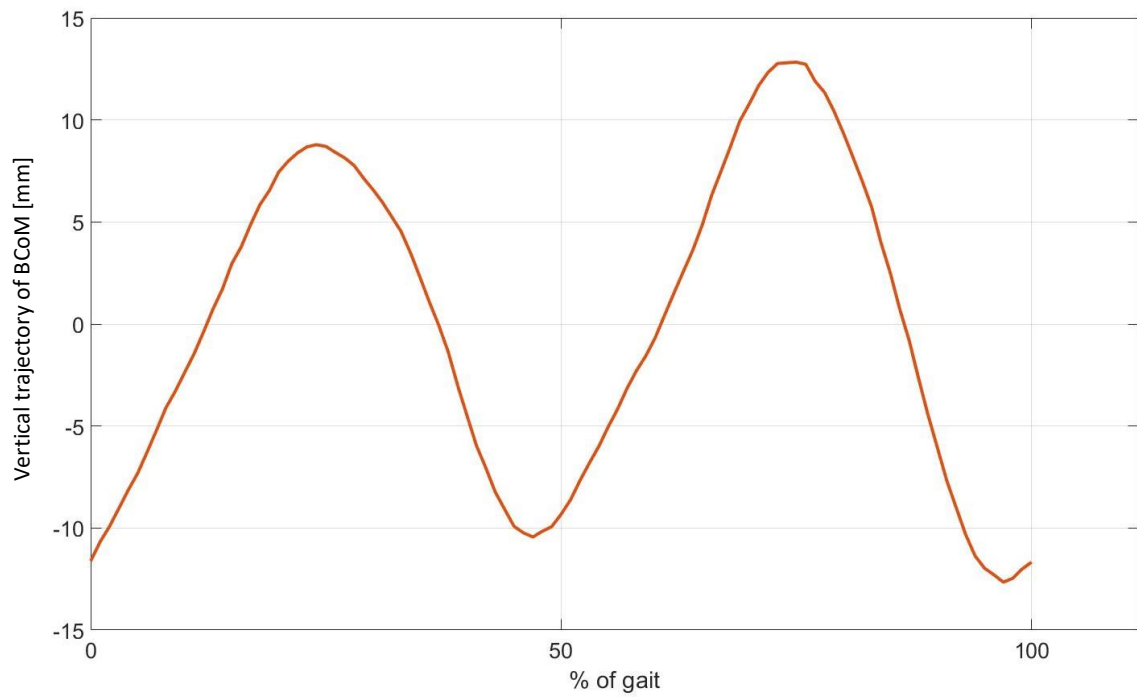


Figure 3.6. representation of the function adopted with 1% of noise and its Fourier spectrum. (red= $c_{th}$ , light blue= $c_{th} - c_{est}$ )

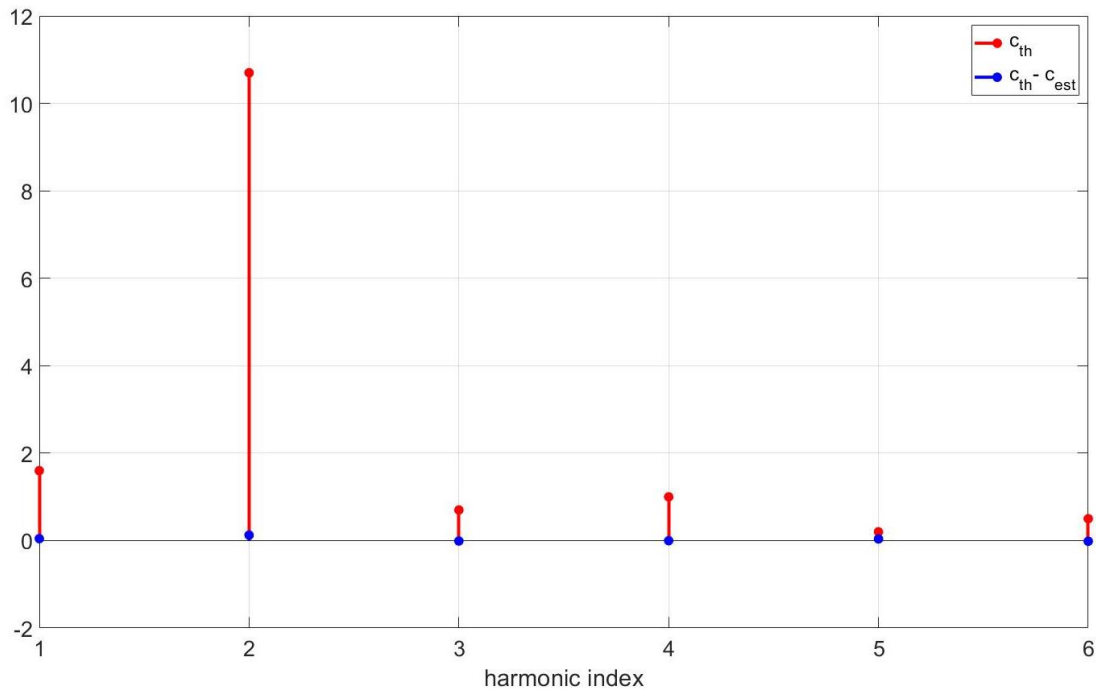
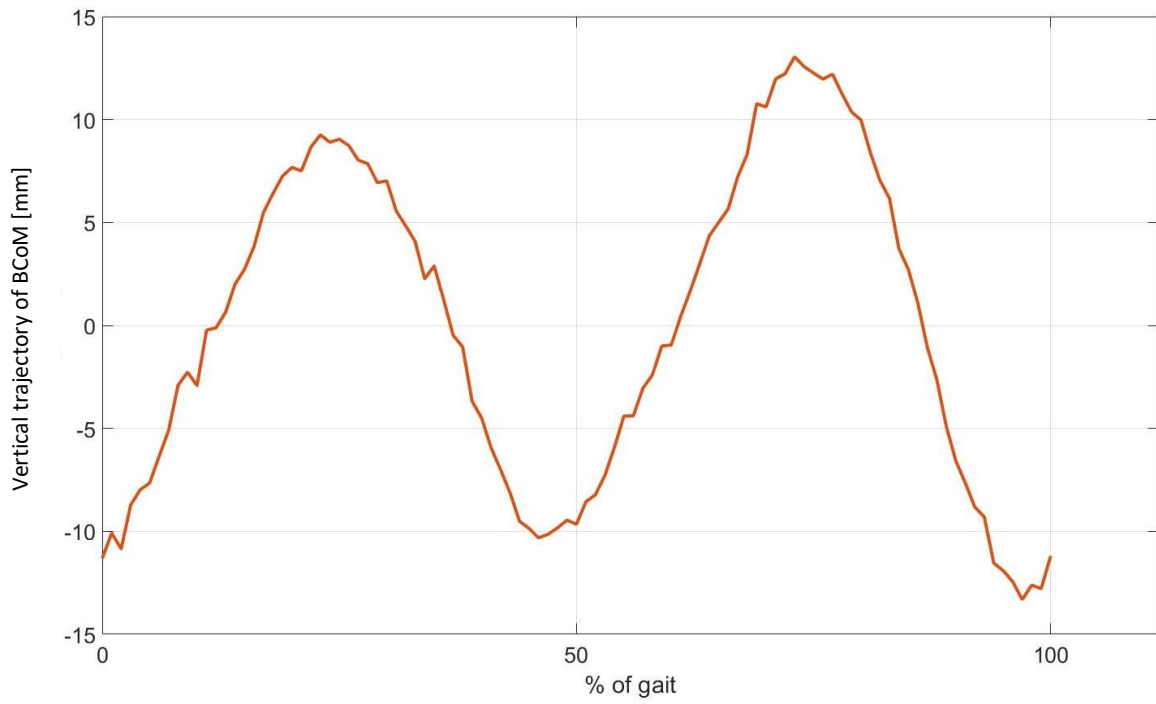


Figure 3.7. representation of the function adopted with 5% of noise and its Fourier spectrum. (red= $c_{th}$ , light blue= $c_{th} - c_{est}$ )

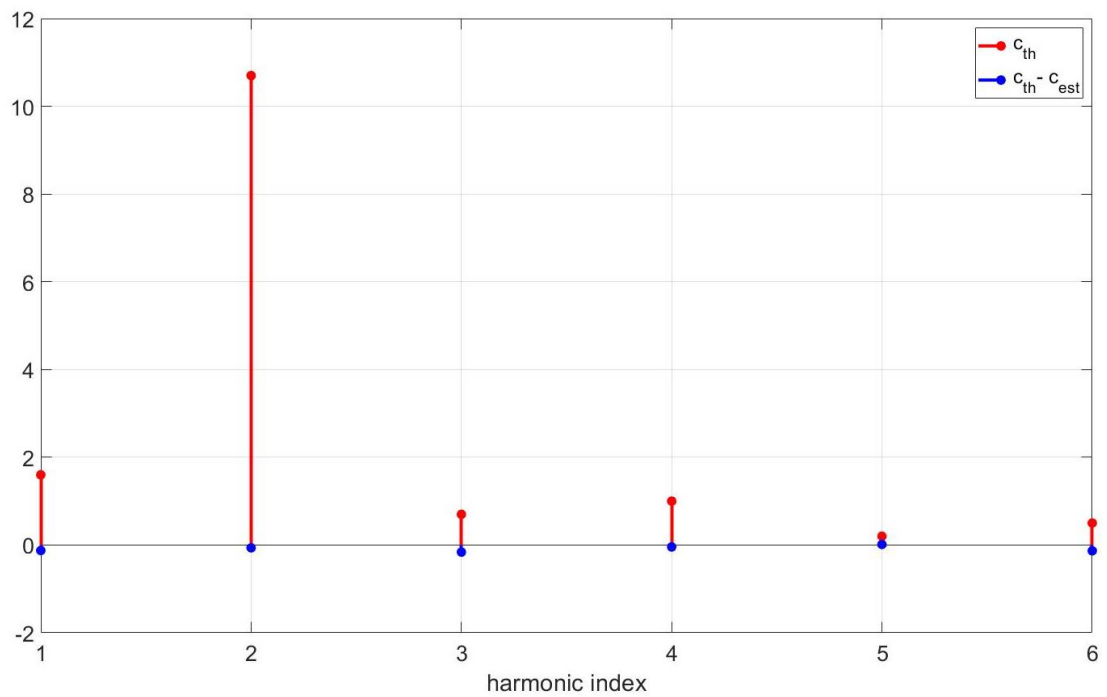
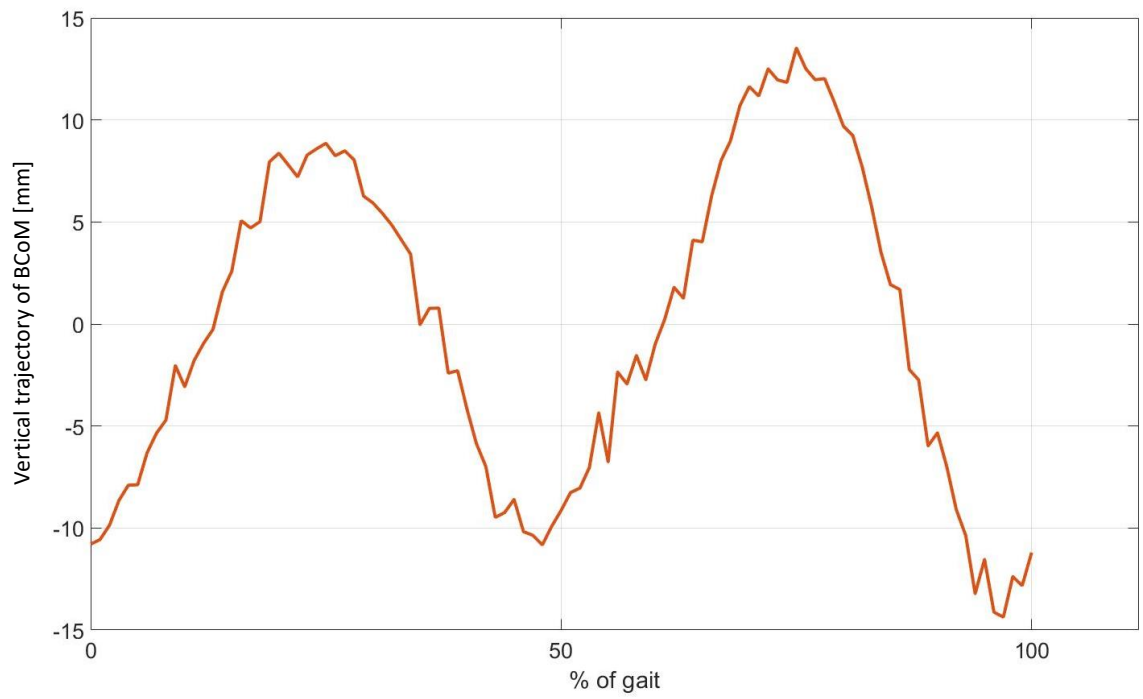


Figure 3.8. representation of the function adopted with 10% of noise and its Fourier spectrum. (red= $c_{th}$ , light blue= $c_{th} - c_{est}$ )

<b>% noise</b>	<b>Percentage RMS error (<math>\epsilon</math>)</b>
1%	0.3
5%	1.5
10%	2.5

*Table 3.2 computed values of percentage RMS error vs noise*

The analysis of the data reported in table 3.2 shows that increasing the noise the percentage RMS error increases but the error remains always within the reasonable limits of acceptability. This result confirms the robustness of the used algorithm

## 4. Studied BCoM trajectory symmetry indexes

The basis of this work is the evaluation of the symmetry of the BCoM trajectory because the BCoM, as already said, represents the whole-body motion. For this reason, BCoM trajectory is considered to represent well the movement of the whole body and therefore the symmetry of the gait.

Since the gait is a cyclic motion, the Fourier series coefficients is a valuable tool for the definition of robust symmetry indexes. The gait signal in the motion direction can be described using cyclic functions even or odd (mediolateral direction odd functions, progression and vertical displacement even functions)

Some previous researches have used this approach and in the thesis two of these indexes have been studied and applied to verify their feasibility when applied to hemiparetic gait.

The two literature symmetry indexes, used in this work and based on combinations of the Fourier series coefficients, were developed respectively for the assessment of the gait symmetry of amputee and non-amputee subjects by Ochoa-Diaz & Padilha (2020) and the gait symmetry of healthy subjects at different speeds by Minetti et al. (2011). These indexes are among the few that use the Fourier series coefficients to analyze the symmetry of the gait considering the BCoM trajectory.

In the following the formulation of these indexes and the results obtained by these authors are shortly presented and discussed.

### 4.1 The index proposed by Ochoa-Diaz & Padilha (2020)

The authors observed that for the case of walking at normal speed for a non-amputee subject, the BCoM trajectory (i.e. waveform) behaves like an even function with respect to the vertical axis at a time equals to the step time. This observation allows to say that the fundamental period of the gait trajectory coincides to the step duration and that in the context of the Fourier analysis, a symmetric pattern of the vertical BCoM will contain only even coefficients.

Ochoa-Diaz & Padilla (2020) in order to assess and quantify the symmetry of the vertical BCoM trajectory (and therefore of the gait) proposed to use an index in terms of the ratio between the energy from the even components and the total signal energy.

Considering that the even components make equal contribution to each vertical oscillation (one per step) of the BCoM during a gait cycle, the presence of odd components will represent the asymmetries.

The symmetry index proposed by these authors (in the following named  $SI_{O-P}$ ) takes 20 harmonics

into account and is expressed by the following formulation:

$$SI_{O-P} = \frac{\sum_{i \text{ even}}^{20} |c_i|^2}{\sum_{k=1}^{20} |c_k|^2}. \quad (4.1)$$

A value of the  $SI_{O-P}$  equal to 1 represent perfect symmetry of the gait that is to say that the vertical BCoM motion during the first step is equal to the one during the next step while divergences from the value of 1 represent an index of the asymmetrical behavior of the gait of the studied subject.

The authors applied the proposed index to quantitatively assess the symmetry level of amputee gait compared to a non-amputee subject.

The amputee group was of three male subjects with unilateral transfemoral amputation caused by trauma or malignancy and all of them used the same knee and foot prosthesis model for the last five years before the experiment.

The control group of not-amputee subjects was of five male subjects with the same fitness level (obtained with three weekly sessions of aerobic exercise and with none previous or current diagnosed of movement disorder, with no joint pain or injury). The mean height and body mass were of 1.75m ( $\pm 0.02$ m) and of 74.8kg ( $\pm 8.3$  kg) for the non-amputee subjects and 1.78m ( $\pm 0.06$  m) and 78.17 ( $\pm 5.48$  kg) for the amputee volunteers. The mean age was 29.38 ( $\pm 2.26$  years) for all subjects.

The participants of the study walked at their normal walking speed over a walkway with a length of 3m instrumented force platforms while a motion capture system recorded the trajectory of 31 passive markers, including one marker placed specifically on the second sacral vertebrae that was considered the closest anatomical point to the location of the BCoM (Figure 4.1).



(a)



*Figure 4.1 Experimental set-up used by Ochoa-Diaz & Padilla (2020) (a) the walkway with the cameras and the force platforms and the used position of the marker set.*

The other markers were placed across the lower limbs and the pelvis of the subjects based on the Helen Hayes protocol (Zuk & Trzeiak, 2017; <http://www.idmil.org/mocap/Plug-in-Gait+Marker+Placement.pdf>). The frequency rate of the motion capture picture system and the force platforms were both set to 250 Hz. A total of ten trials per subject was recorded.

The BCoM vertical trajectories obtained for the non-amputee group obtained by Ochoa-Diaz & Padilla (2020) are summarized in Figure 4.2.

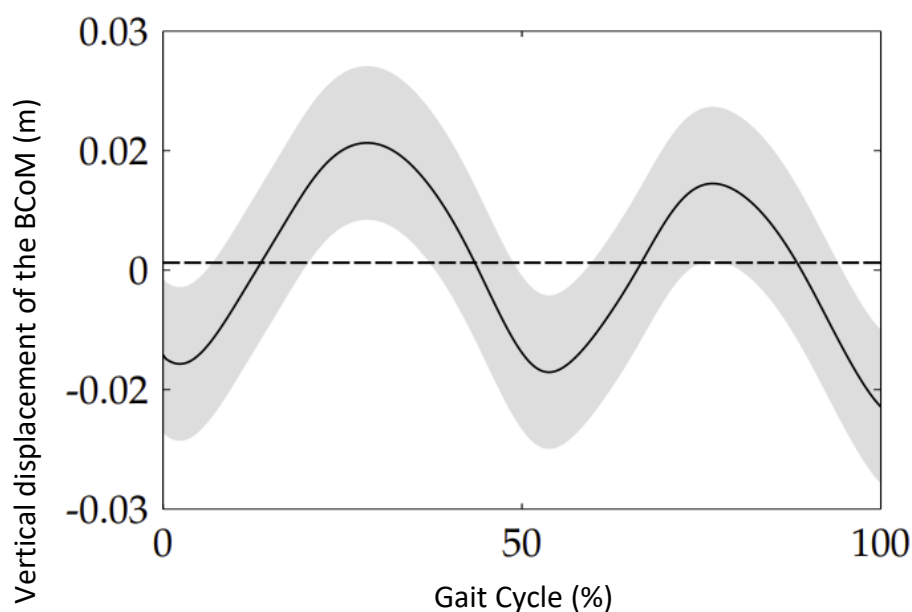


*Figure 4.2 The BCoM vertical displacement of the non-amputee subjects studied by Ochoa-Diaz & Padilla (2020). The grey area represents the area of the measured values while the continuous line represents the average value of all the subjects.*

The continuous line of the trajectory, reported in Figure 4.2, is the curve of a single gait cycle for each trial of the entire control group (5 subjects), where the initial contacts (at the moment of the heel strike event) of the same limb were taken as the initial and the final point of the stride. As expected for the not pathological subjects the shape of the gait shows a periodic signal with two periods corresponding to each step. The highest value occurs at midstance of the trailing leg, and it is repeated at the same instant in the contralateral limb. The lowest points coincide with the feet contacts at each new step. The patterns of the BCoM trajectory that were obtained for each amputee subject, as shown in Figure 4.3 differs from each other and from the normal gait of the control group of not amputee subjects.

For the specific cases of amputee patients B and D, the BCoM displaces downwards from its initial position at first double support with a different shape from the ascendant behavior in non-amputee subject A that was used as a reference. During the final double support the BCoM height from the amputee group is not the same as the one at the initial contact and the vertical position of BCoM goes to a lower position for the case of subjects C and D and an upper position for subject B. The comparison of the index  $SI_{O-P}$  for the various subjects allow to observe that for the not-amputee subject

A) the index has a value of 0.959. This means that a good symmetry of the gait. For the amputee subjects the index is more distant to unity: for subject B) the  $SI_{O-P}$  is of 0.804; for subject C) the  $SI_{O-P}$  is of 0.421 and for subject D) the  $SI_{O-P}$  is of 0.788. These results clearly indicate a divergence from unity that highlight the asymmetry of the gait of the three amputee subjects. Looking at figure 4.3 it is clear that the most irregular path, the one of patient C), has also the lowest value of the Symmetry index.

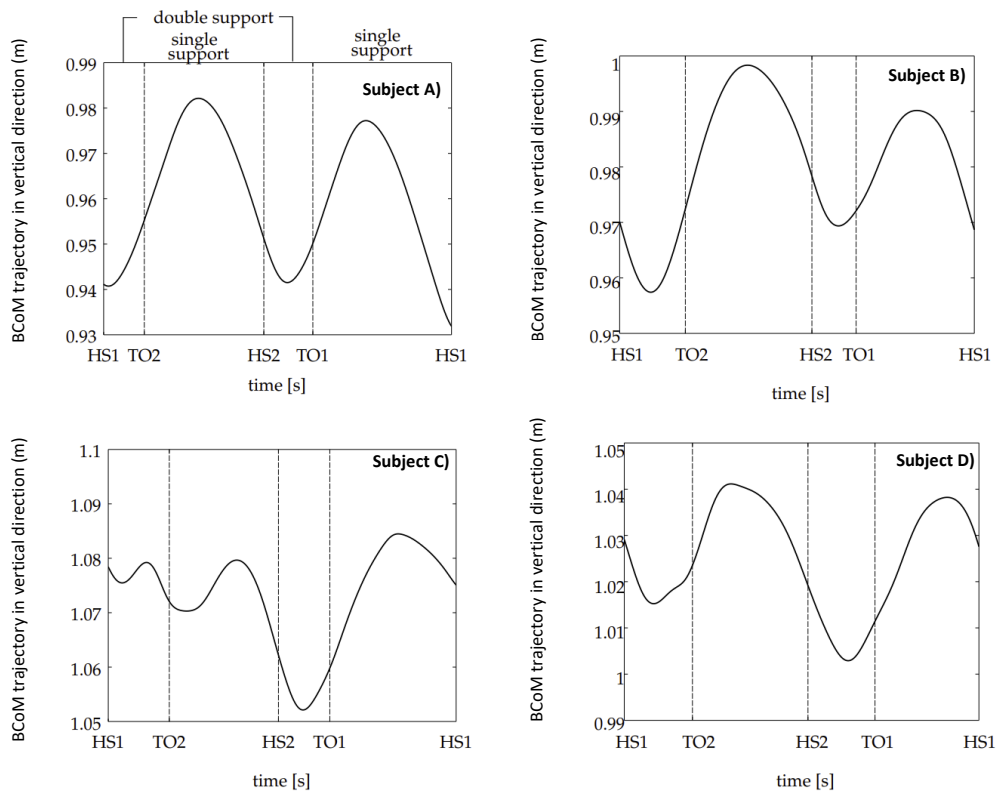


Figure 4.3. The vertical displacement of the BCoM for a non-amputee subject selected in the control group (subject A) and three amputee subjects (subjects B, C and D). The illustrated trajectories correspond to a single recorded trial for each subject. HS1 and HS2 represent the heel strike moments of the trailing and leading leg, respectively while TO1 and TO2 are the toe-off moment for the same legs (Ochoa-Diaz & Padilla, 2020).

The analysis of the Fourier series spectrum of the BCoM vertical displacement of the subjects A, B, C and D (Figure 4.4) allows some very interesting observations.

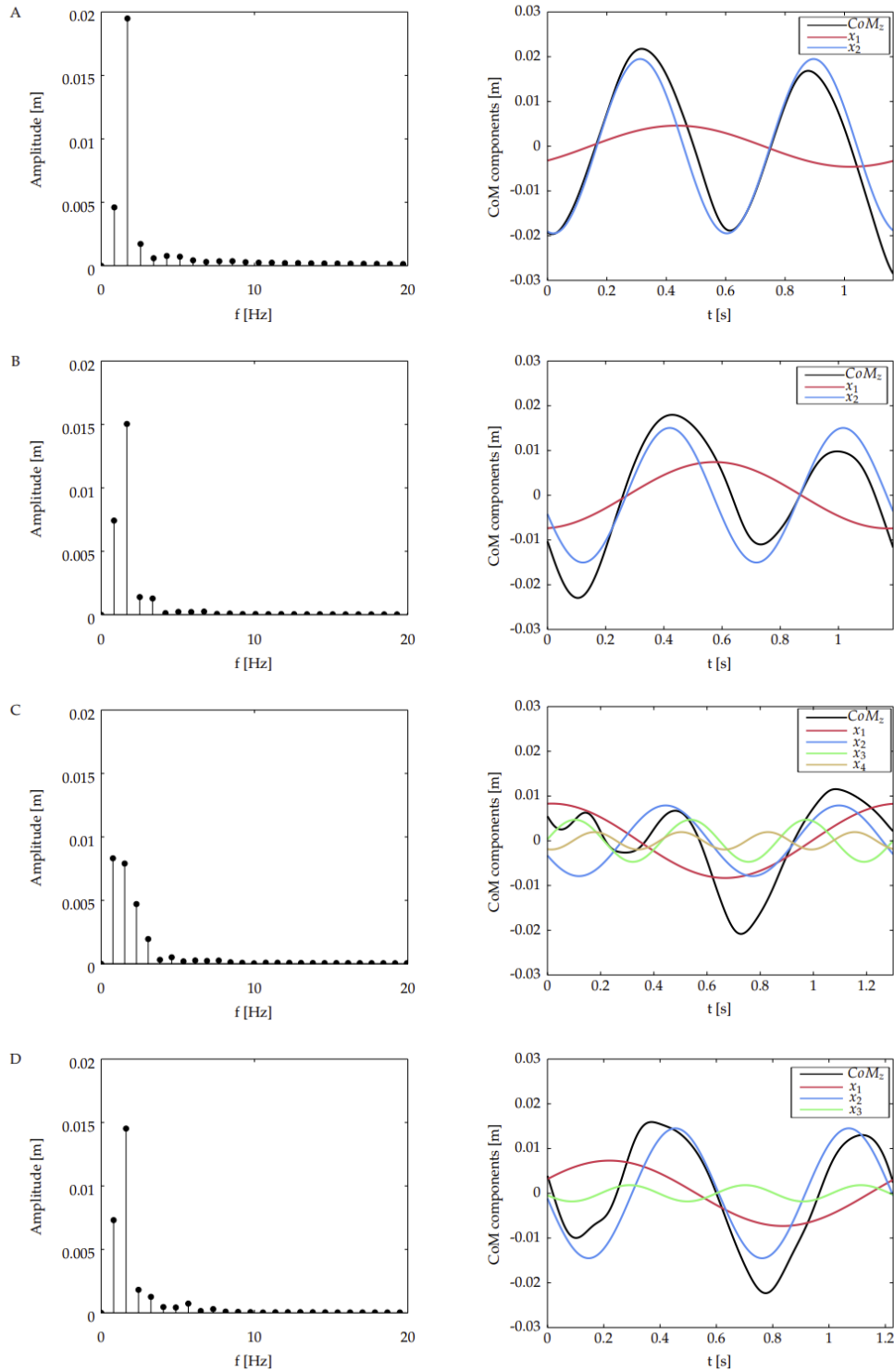


Figure 4.4 Amplitude of the spectrum coefficient of the Fourier series of the vertical BCoM trajectory (CoM) and decomposition into its main harmonics. The black curve corresponds to the measured trajectory (Ochoa-Diaz & Padilla, 2020) for the subjects A, B, C and D.

The not-amputee subject A) shows two oscillations with almost the same duration. The analysis of the spectrum reveals that the two main coefficients are the first and the second harmonics are strongly prevalent, and the other coefficients are much less significant. The first harmonic is approximately the 5% of the total considered signal, while the second harmonic has 94% of the considered signal. This last harmonic oscillates at a frequency very close to the inverse of the step period of this subject ( $t_{\text{step}} = 0.58\text{s}$ ).

From the amputee group, subjects B) and D) have a similar behavior and the energy signal is concentrated in the first two harmonics, which have approximately 20% and 79% of the total signal energy, respectively. The second harmonic oscillates at a frequency very close to the inverse of the step period of the not amputee subject.

A much different behavior can be observed in subject C) where the energy signal is spread out into the first four harmonics and with the first two have, almost, the same contribution in terms of energy.

Analyzing the decomposition of the signal into its base harmonic, it is evident how the subject C has a very different gait cycle and that much more harmonics are needed to describe its gait in a complete way.

These results are close to the ones obtained by comparing the proposed symmetry indexes.

#### 4.2 The index proposed by Minetti et al. (2011)

Minetti et al. (2011) studied the shape and the symmetry of the BCoM in different subjects walking in a treadmill at different speeds. These authors proposed different symmetry indexes in the three directions of the motion, based on the Fourier series coefficient.

The 3D position of the BCoM was obtained by the combination of the position of the coordinate of 12 segments of the body measured at 100 Hz on a treadmill using an optoelectronic device and anthropometric tables considering the fractional mass of the various segments of the body and their relative position.

The research has been carried out on 11 male subjects with a mean age of 27.77 years, with a mean height of 1.81m and a mean body mass of 80.47kg.

The subjects walked at 5 different speeds from 3km/h to 7 km/h (step 1 km/h) and ran

at 9 speeds from 7 km/h to 15 km/h (step 1 km/h). The body segment positions were sampled for about 30s to measure a consistent number of consecutive strides. Individual strides were then extracted by searching the maxima in the vertical coordinates of BCoM and choosing the begin/end frame in the time corresponding to every other value of the maxima (due to the double periodicity within a stride). A number of 1120 strides has been analyzed.

The proposed procedure and experimental setup allowed to represent the BCoM trajectory as relative to its forward translation, resulting in a compact 3D loop, where locomotion characteristics (speed changes, asymmetries, etc.) are more easily identifiable than when using an “absolute” trajectory in the space as done by Ochoa-Diaz & Padilla (2020).

Minetti et al. (2021) highlight that differently from describing the gait as three independent time trajectories of the BCoM trajectory, the use of the closed 3D loop contains information about the functional interaction among them and can easily allow to extract quantitative information about the effects of speed on the symmetry of the gait.

Based on the observation that the motion of BCoM exhibits a perfect right–left symmetry (i.e. contains just even harmonics) in the x (progression) and y (vertical) directions and just odd in the z (lateral) direction, these authors proposed three symmetry indexes based on the Fourier series coefficients developed up to 6 harmonics. The symmetry indexes proposed by these authors (in the following named  $SI_{X,Y,Z-M}$ ) are expressed by the following formulation:

$$SI_{x-M} = \frac{c_2^x + c_4^x + c_6^x}{\sum_{i=1}^6 c_i^x}, \quad (4.2)$$

$$SI_{y-M} = \frac{c_2^y + c_4^y + c_6^y}{\sum_{i=1}^6 c_i^y}, \quad (4.3)$$

$$SI_{z-M} = \frac{c_1^z + c_3^z + c_5^z}{\sum_{i=1}^6 c_i^z}. \quad (4.4)$$

A value of the  $SI_{X,Y,Z-M}$  equal to 1 represent perfect symmetry of the gait that is to say that the vertical BCoM motion during the first step is equal to the one during the next step while divergences from the value of 1 represent an index of the asymmetrical

behavior of the gait of the studied subject.

Based in their results, Minetti et al. (2011) proposed the diagram of Figure 4.5 where it can be observed that since perfect symmetry correspond to indexes of 1, also for not-pathological subjects the indexes values are usually lower than 1. The lower is the speed the higher is the distance from symmetrical path.

It should be observed that these authors did not made any analysis on pathological subjects as was done in the present thesis work.

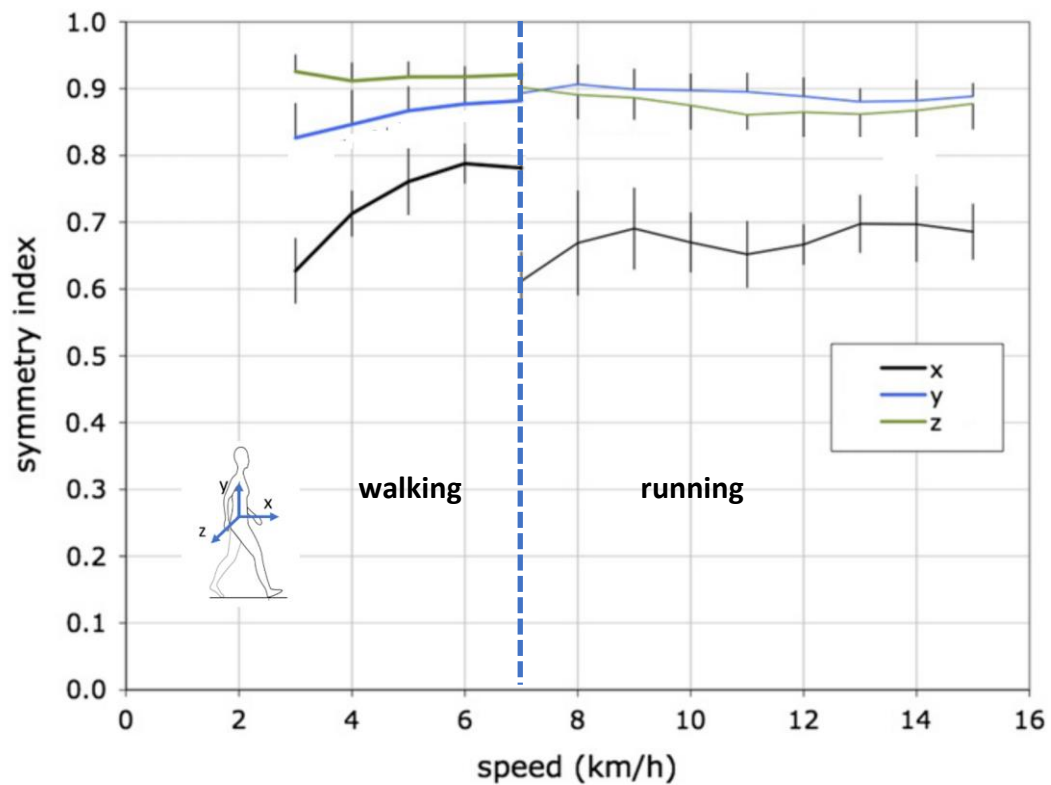


Figure 4.5 Values of the symmetry indexes proposed by Minetti et al. (2011) for different walking and running speeds (modified from Minetti et al. 2011).

## 5. Application of the studied symmetry indexes to experimental data

The two symmetry indexes based on combination of the Fourier series coefficients developed by Ochoa-Diaz & Padilha (2020) ( $SI_{O-P}$ ) and by Minetti et al. (2011) ( $SI_{Y-M}$ ) have been applied to the study of hemiparetic gait of pathological subjects, with the goal to verify their feasibility to study this pathological condition and compared with the values obtained by a control group of healthy subjects.

In the following, the obtained results are presented and discussed.

### 5.1 Available gait data

The used data were obtained from previous researches.

The tests with healthy subjects were previously conducted in the POLITO BIOMed LAB of Politecnico di Torino and the tests with pathological subjects were performed in the specialized Movement Disorders Center of Unità Spinale Unipolare – Città della Salute e della Scienza, Italy.

Experimental tasks were performed in a laboratory environment and a stereophotogrammetric system was used for the data acquisition and elaboration. Two instruments setting were adopted based on the subjects' categories:

- 2 cameras Vicon VUE for video recording (1080p, 50 Hz) and 8 infrared-cameras Vicon Bonita 10 for infrared capture (1024x1024 resolution, 100 Hz) for the pathological subjects;
- 3 cameras Vicon VUE for video recording (1080p, 50 Hz) and 12 infrared-cameras Vicon Vero v2.2 for infrared capture (2048x2048 resolution, 100 Hz) for the healthy subjects;

The data refers to the measurements of the gait of 5 healthy subjects (control group) and 14 pathological subjects affected by hemiparesis. They were obtained from the direct measurement of the trajectory of the pelvis (on which a marker was positioned), that in this experiment was considered coincident with the BCoM position.

Due to the type and quality of available data only the symmetry indexes in the vertical direction were analyzed.

In these tests, each subject developed 4 trial walks. Each subject was asked to walk at their comfortable speed. Two force platforms were located along the path. During the trial the spatial three-dimensional position of the pelvis (i.e. BCoM position) was measured, using a VICON system, with an acquisition frequency of 100 Hz.

For the healthy subjects the walking speed ranged between 2 and 2.5 km/h while for the pathological subject the walking speed was more variable, depending on the ability and age of the subject (the 8 subjects with an age  $\geq 65$  years walked at a mean speed of  $1.4 \pm 0,61$  [km/h] while the 6 subjects with an age  $< 65$  years walked at a mean speed of  $1.0 \pm 0,51$  [km/h]).

The 5 healthy subjects were all males, with an age ranging from 27-30 years (mean value:  $28.6 \pm 0.89$  years), a mean height of 174.6 cm ( $\pm 3.5$  cm) and a mean weight of 69.6 kg ( $\pm 4.4$  kg) (Table 5.1).

The 14 pathological subjects (10 males and 4 females) have an age ranging between 40 to 76 years old with 6 subjects with an age ranging between 40 to 64 years (mean value of  $53.16 \pm 7.84$  years) and 8 subjects with an age  $\geq 65$  years (mean value of  $72.75 \pm 3.34$  years) (Table 5.2). The pathological subjects with an age ranging between 40-64 years have a mean height of 166.3cm ( $\pm 2.1$ cm) and a mean weight of 66.6kg ( $\pm 6.5$  kg) while the pathological subjects with an age  $\geq 65$  years have a mean height of 173.2 cm ( $\pm 7.6$ cm) and a mean weight of 71.1 kg ( $\pm 7.6$  kg).

Six subjects have left side hemiparesis and eight have right side hemiparesis. Some of the patients needed to use an auxilium device to walk.

subject #	gender	age (years)	weight (kg)	height (m)	BMI
1	male	28	67	1.74	22.1
2	male	28	63	1.80	19.4
3	male	30	70	1.75	22.8
4	male	29	72	1.69	25.2
5	male	28	76	1.75	24.8

*Table 5.1 Summary of the general data of the healthy subjects*

<b>subject #</b>	<b>gender</b>	<b>age (years)</b>	<b>weight (kg)</b>	<b>height (m)</b>	<b>BMI</b>	<b>hemiparesis side</b>	<b>auxilium device</b>
1	male	62	75	1.70	25.9	Right	
2	male	75	82	1.80	25.3	Left	stick
3	male	76	80	1.88	22.6	Right	stick
4	female	42	58	1.65	21.3	Right	stick
5	male	73	68	1.70	23.5	Right	
6	male	60	72	1.68	25.5	Right	quadripode
7	male	73	77	1.75	25.1	Right	stick
8	male	56	70	1.69	24.5	Left	
10	male	76	72	1.62	27.4	Left	
12	female	73	58	1.70	20.0	Right	
14	male	65	67	1.78	21.1	Right	stick
15	female	71	65	1.67	23.3	Right	stick
16	male	56	65	1.65	23.9	Left	
17	female	43	58	1.62	22.1	Left	

*Table 5.2 Summary of the general data of the pathological subjects. The reference number of the subject is the one used as reference number in the experiment.*

## 5.2 Results

### 5.2.1 Example of healthy subject gait cycle vs pathological one

As an example of the operational procedure, in the following, the comparison of the Fourier spectrum of a healthy and a pathological subject is presented.

Knowing that in the sagittal plane there is a double frequency of the step (2 steps in a stride) is possible to say that the signal of the vertical trajectory of the BCoM is roughly an even function so is expected to have only the even harmonic contributions in the Fourier spectrum (Minetti et al.,2011)

In Figure 5.1 the trend of the trajectory of the BCoM of a healthy subject (subject 1) and its spectrum are reported. The spectrum highlights that the second harmonic gives the largest contribution in the definition of the subject's gait, as expected for the nature of the signal in a symmetric gait that is the standard in a healthy subject as shown in Figure 5.4. This observation is confirmed in all the five healthy subjects considered in this thesis, furthermore the second harmonic values are very close for all of them.

In figures 5.2 and 5.3 the trend of the trajectory of the BCoM of a pathological subject (subject 5) and its spectrum are reported. The spectrums highlighted that the first two harmonics are the most important for the description of the gait. Since the trajectory of the BCoM of a pathological subject has a more complex shape than that of a healthy one the signal is no more an even signal. The harmonic contributions are shared on more harmonics (odd and even) as shown in Figure 5.5 and this fact is observed in all the 14 pathological subjects. Furthermore, the trend of the vertical trajectory of the BCoM of the homolateral side highlights that the first peak is flat. This behavior is due to a physical limitation of hemiparetic subject. Indeed, during the stance on the affected side, the hemiparetic subject presents a deficit in loading acceptance with a limitation in the lifting of pelvis and in the swing of the contralateral limb.

Considering the Fourier spectrum of the trajectory of the BCoM of one healthy subject and a pathological one it's possible to underline the differences between the two behaviours of the gait. This comparison shows that the use of the Fourier spectrum coefficient can be used as a good tool for the clinical analysis of the gait.

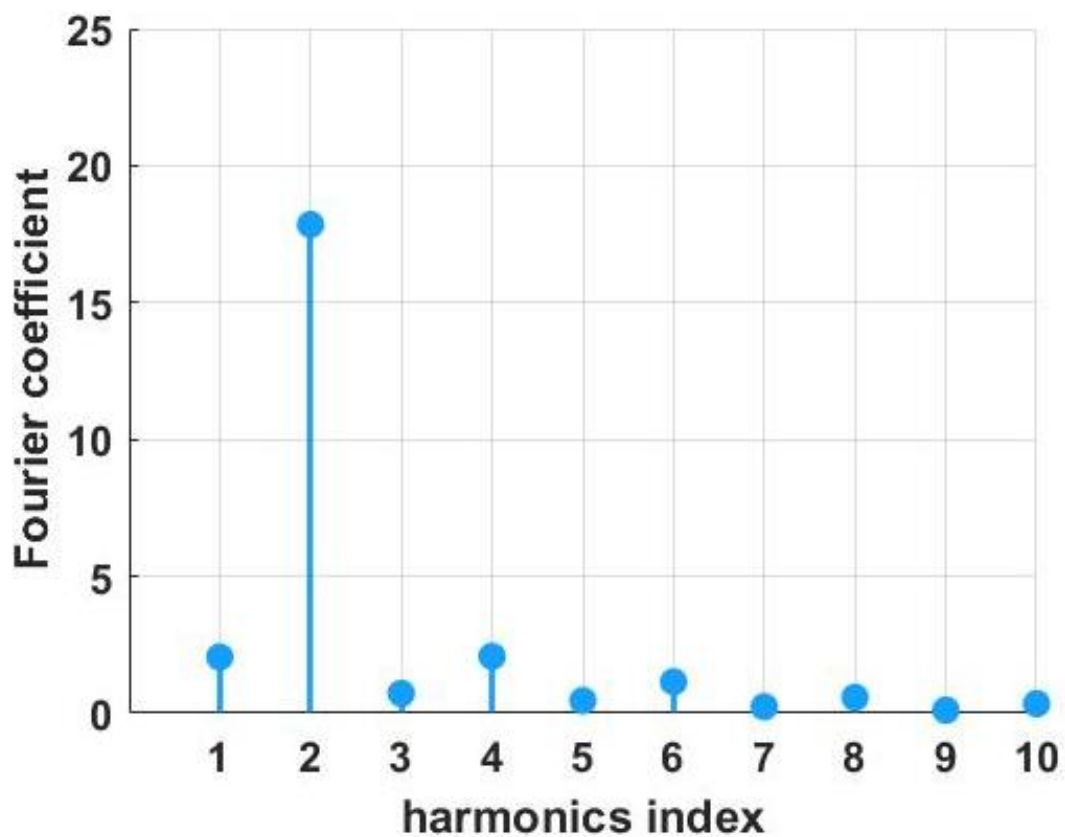
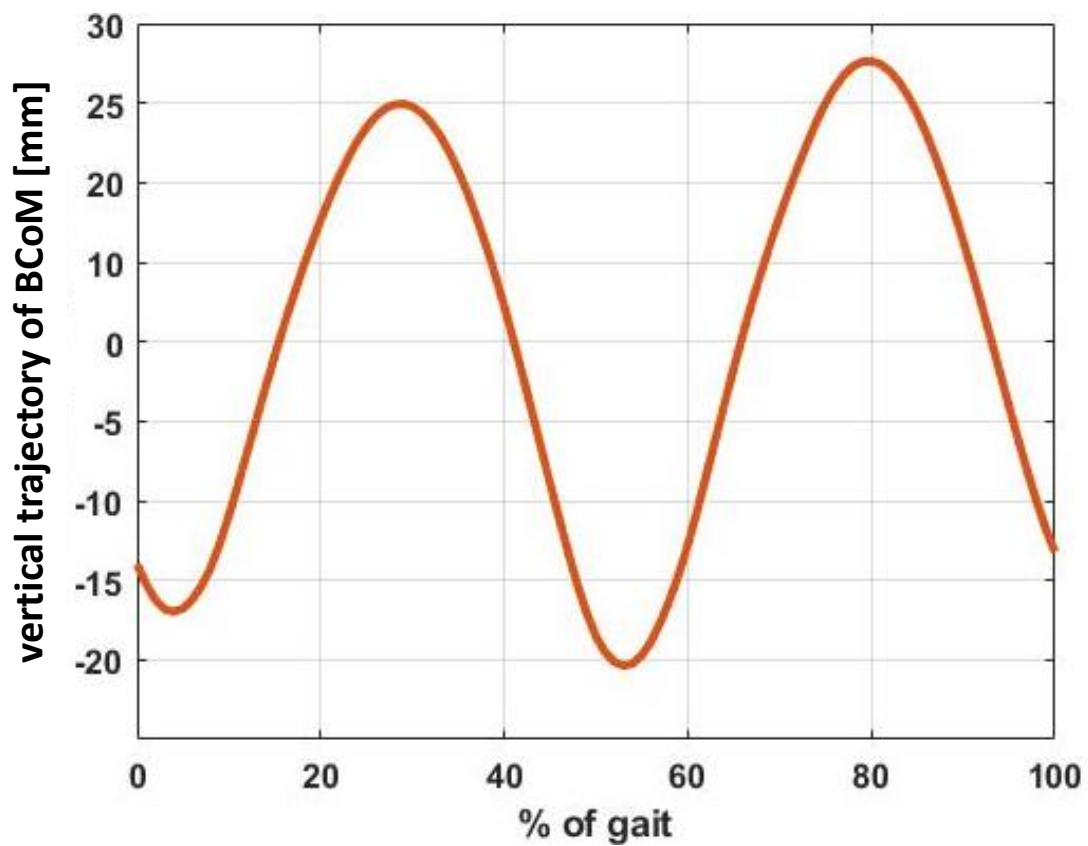


Figure 5.1 Vertical displacement of the BCoM trajectory (mm) normalized on the gait and Fourier spectrum of the first 10 harmonics of the BCoM vertical trajectory for healthy subjects 1

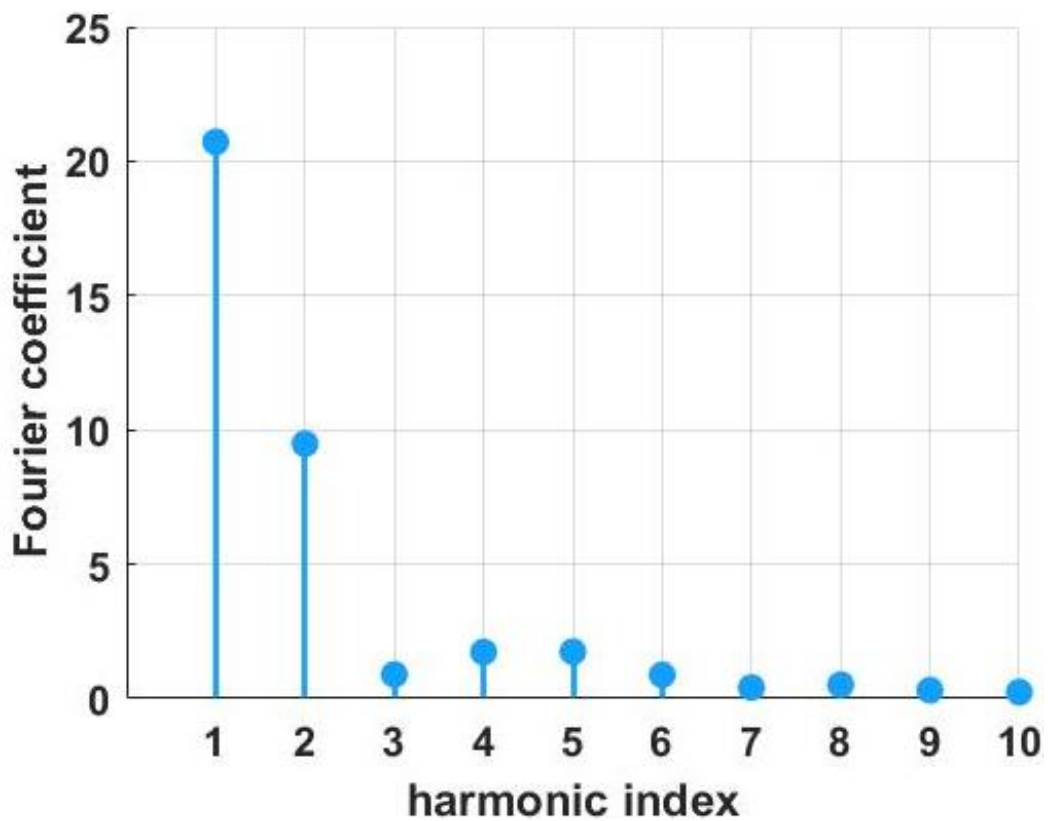
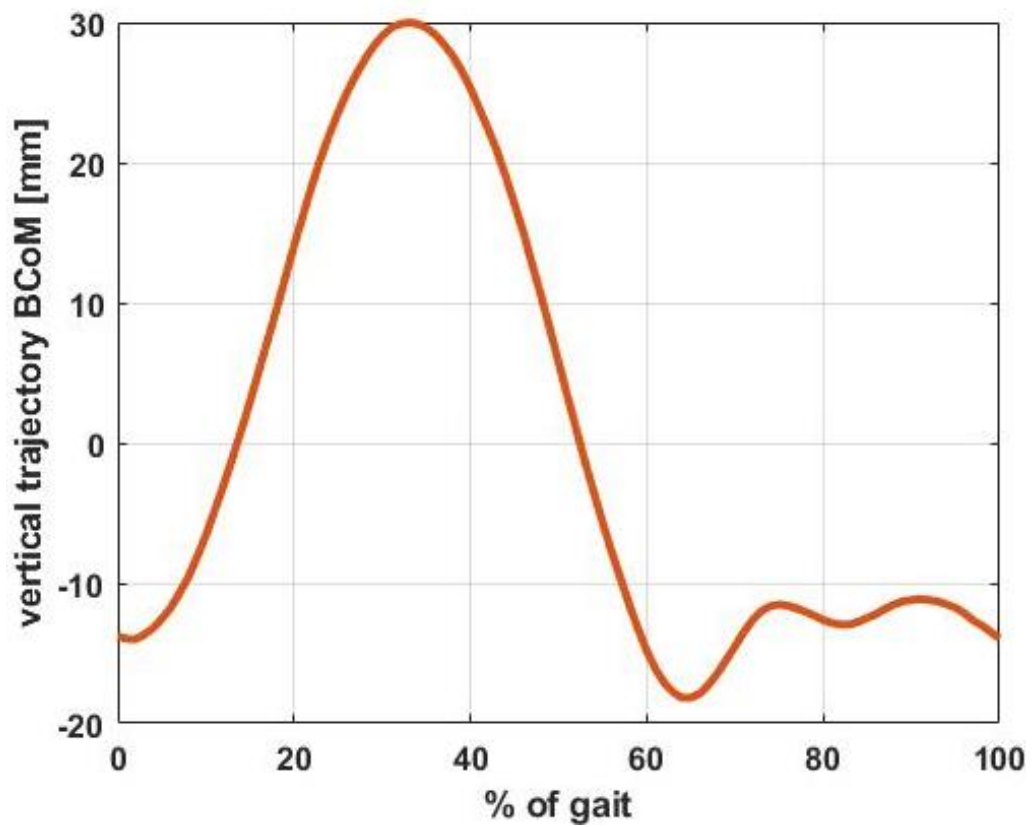


Figure 5.2 Vertical displacement of the BCoM trajectory (mm) normalized on the gait and Fourier spectrum of the first 10 harmonics of the BCoM vertical trajectory for pathological subjects 5 (contralateral side)

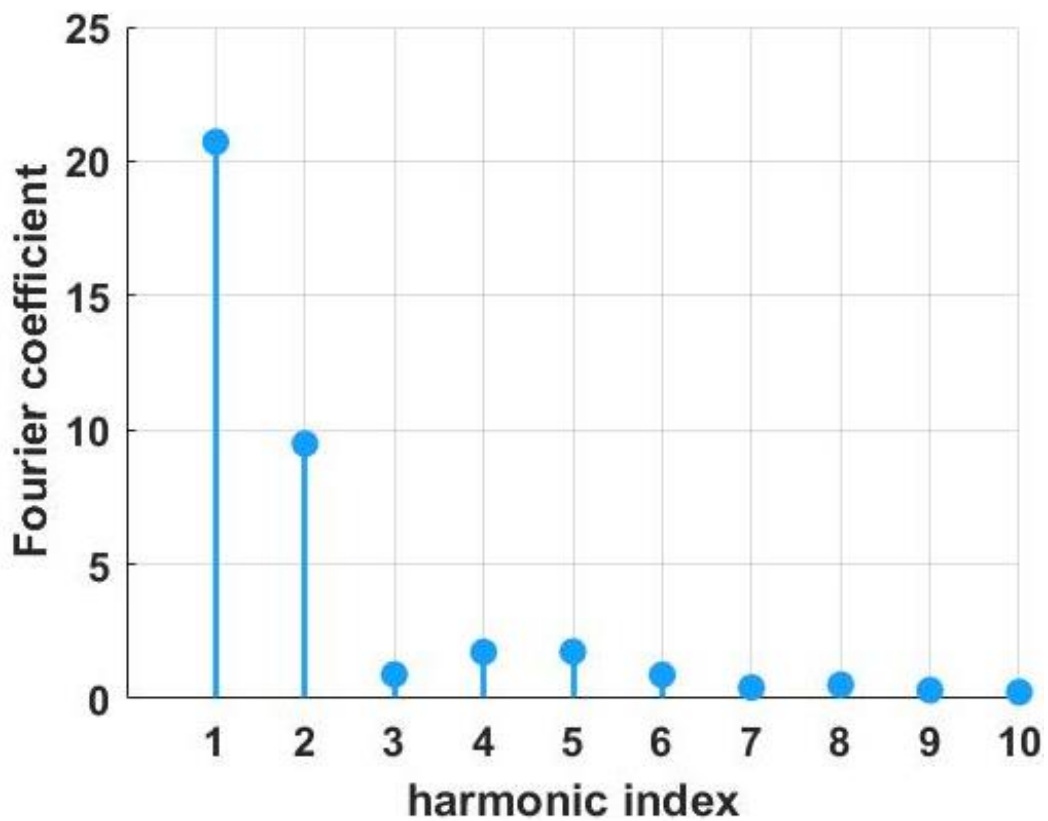
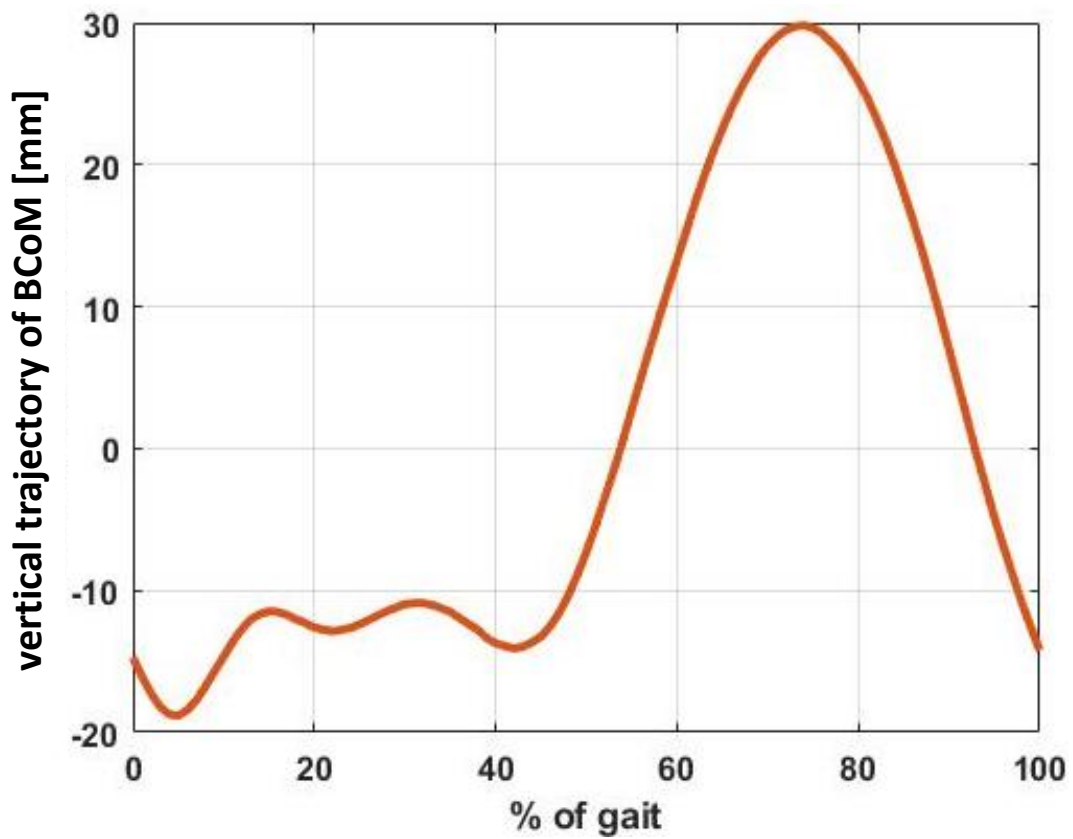


Figure 5.3 Vertical displacement of the BCoM trajectory (mm) normalized on the gait and Fourier spectrum of the first 10 harmonics of the BCoM vertical trajectory for pathological subjects 5 (homolateral side)

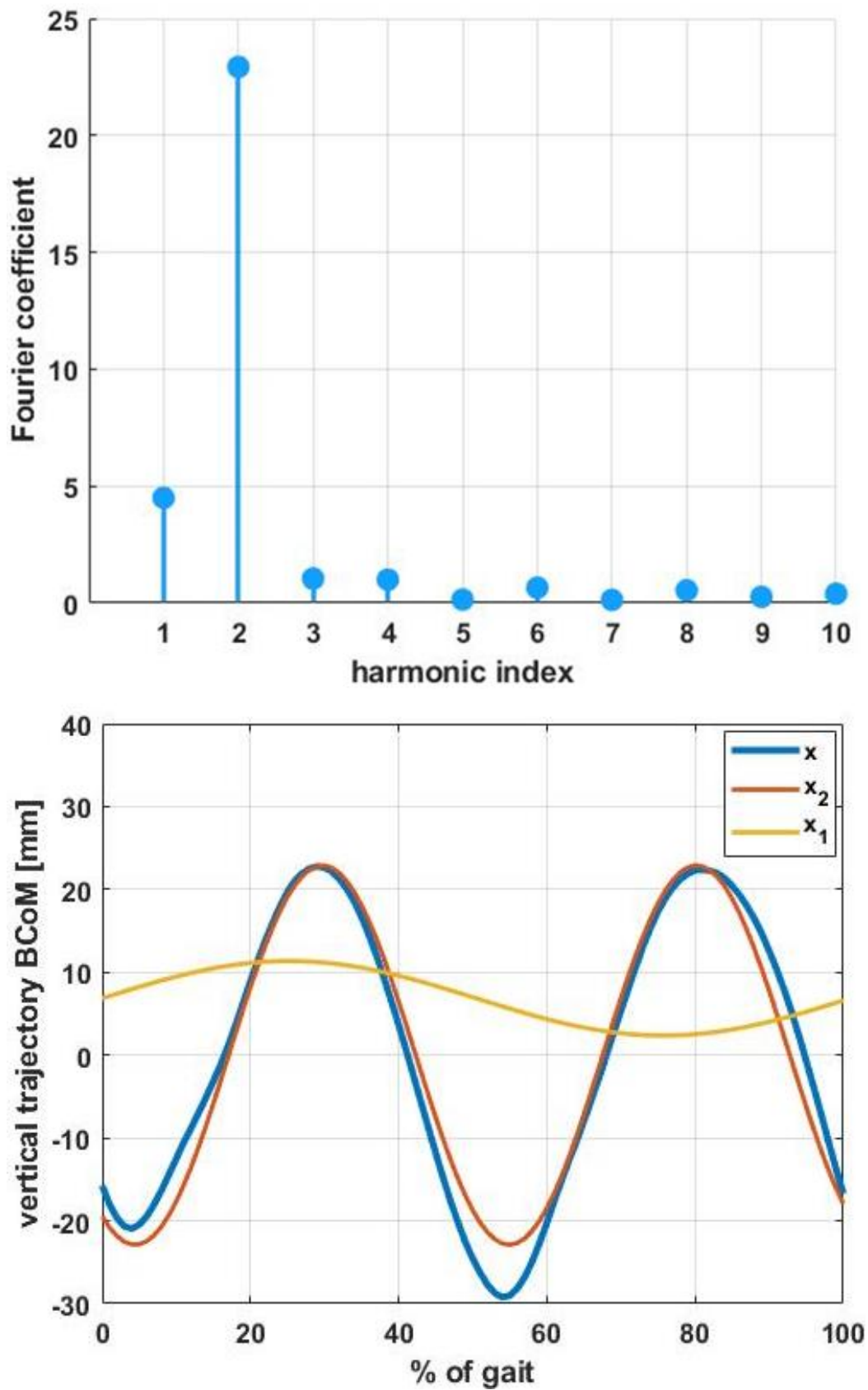


Figure 5.4 Amplitude of the spectrum coefficient of the Fourier series of the vertical BCoM trajectory and decomposition into its main harmonics for the healthy subject.

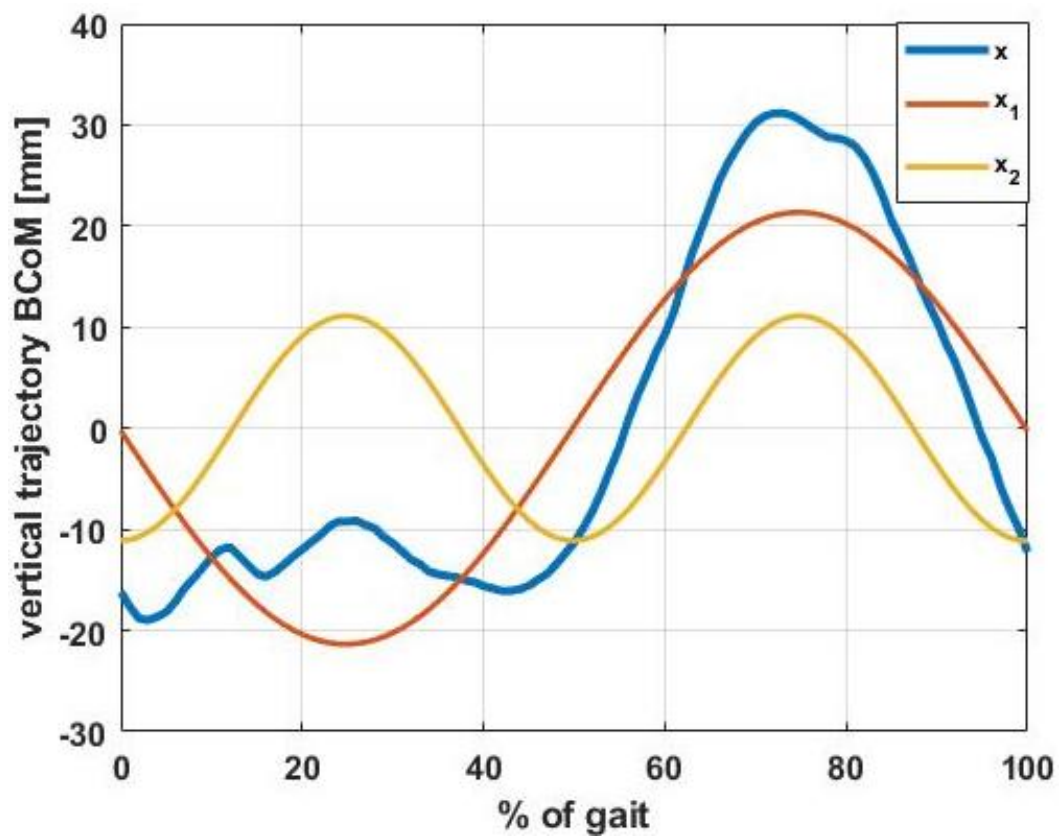
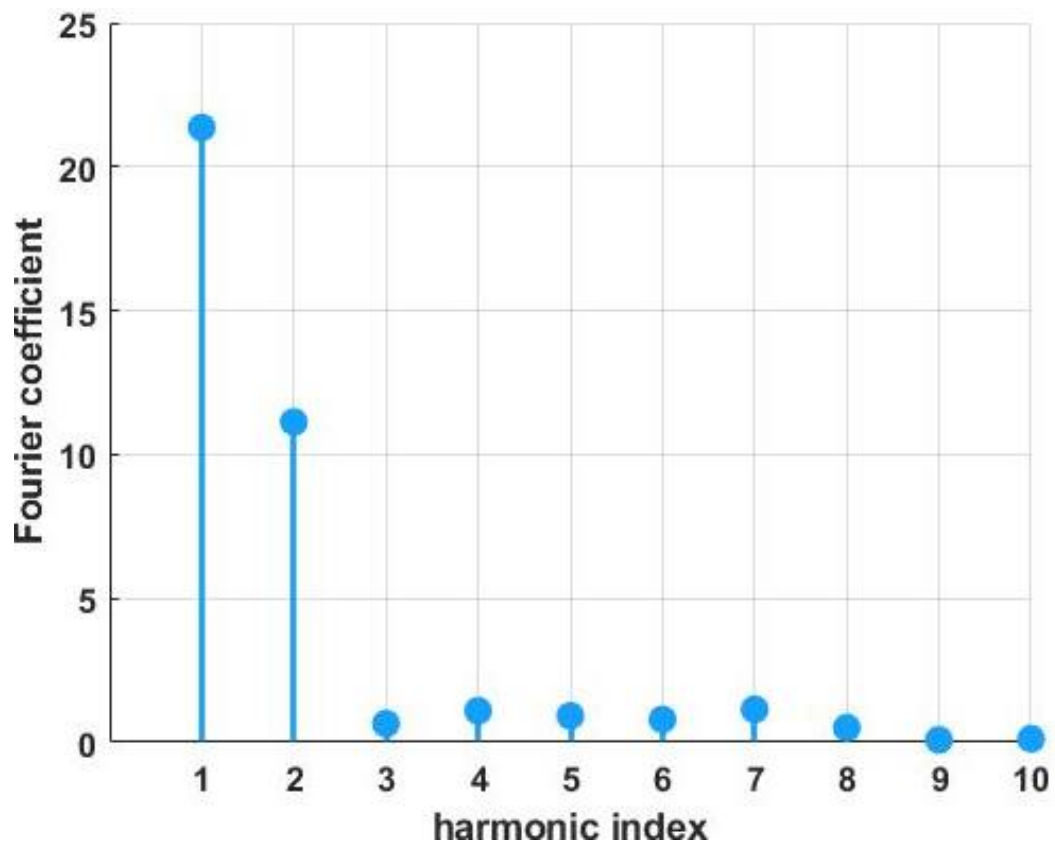


Figure 5.5 Amplitude of the spectrum coefficient of the Fourier series of the vertical BCoM trajectory and decomposition into its main harmonics for the pathological subject.

### 5.2.2 Symmetry index of healthy subjects

The healthy subjects carried out a variable number of strides per trial ranging from 11 to 18, globally 136 strides were analyzed.

The diagrams of the vertical trajectory of the BCoM, computed as the average of all the strides for each subject is reported in Figures 5.6

It is possible to see that the shape of the trajectories is very close to each other. The measured gates are within standard ranges already reported in technical literature. The periodical shape of the BCoM trajectory depends to the alternance of single support phases and double support phases, as well represented in Figure 1.2. In Figure 5.6 it is possible to see that, for all the studied subjects, the double support phases are located between 0% and 10% and between 45% and 60% of the gait cycle while the single support phases occur around the 30% and 80% of the gait cycle.

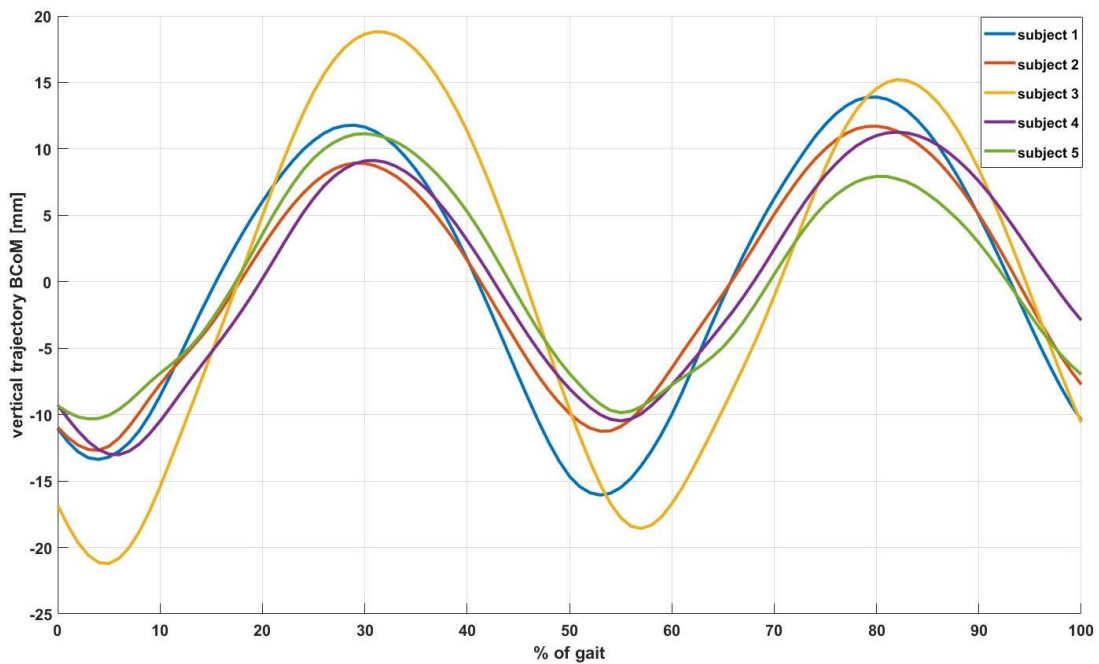


*Figure 5.6 Vertical displacement of the BCoM trajectory (mm) normalized on the gait and mean values of the first 10 harmonics of the BCoM vertical trajectory for the 5 healthy subjects*

*Computed  $SI_{O-P}$  index*

The computed value of the  $SI_{O-P}$  index for the available strides of all the 5 healthy subjects are reported in Tables 5.3-5.7. It is possible to see that each stride of a subject has a little different level of symmetry index value from the others.

The mean values of all the trails are always above the value of  $SI_{O-P} = 0.91$ , with the exclusion of the trial number 4 of the subject 5. This trail is also different from the other trials of the same subject.

As expected, no relevant differences can be observed when considering the right and left strides for the healthy subjects. The mean values of the  $SI_{O-P}$  index for all the trials and all the healthy subjects are reported in Table 5.8. The mean reference value of all  $SI_{O-P}$  index considering all the trials of all the healthy subjects is  $0.94 (\pm 0.02)$ .

This value is in good agreement with the results presented by Ochoa-Diaz & Padilha (2020) who indicated a mean value for healthy subjects of 0.95.

Subject 1					
trial	RIGHT STRIDE				mean
1	0,98	0,95	0,99		0,97
2	0,95	0,95	0,93	0,99	0,95
3	0,97	0,95	0,87		0,93
4	0,94	0,99	0,97	0,98	0,97
trial	LEFT STRIDE				mean
1	0,93	0,95	0,96		0,94
2	0,97	0,92	0,98	0,98	0,96
3	0,96	0,93			0,94
4	0,97	0,88	1,00	0,94	0,94

*Table 5.3 Summary of the computed  $SI_{O-P}$  for all the strides of healthy subject 1.*

Subject 2				
trial	RIGHT STRIDE			mean
1	0,98	0,99	0,89	0,95
2	0,94	0,96	0,86	0,92
3	0,98	0,99	0,98	0,98
4	0,90	0,87	0,78	0,85
trial	LEFT STRIDE			mean
1	0,96	0,85		0,91
2	0,98	0,96		0,97
3	0,97	0,90		0,94
4	0,97	0,80	0,93	0,90

*Table 5.4 Summary of the computed  $SI_{O-P}$  for all the strides of healthy subject 2.*

Subject 3					
trial	RIGHT STRIDE				mean
1	0,97	0,95	0,92		0,95
2	0,97	0,97	0,99		0,98
3	0,94	0,96	0,97		0,96
4	0,98	0,97	0,97		0,97
trial	LEFT STRIDE				mean
1	0,96	0,98			0,97
2	0,93	0,92	0,97		0,94
3	0,99	0,98			0,98
4	0,99	0,97	0,96	0,95	0,97

Table 5.5 Summary of the computed  $SI_{O-P}$  for all the strides of healthy subject 3.

Subject 4						
trial	RIGHT STRIDE					mean
1	0,93	0,99	0,99	0,99	0,90	0,96
2	0,89	0,98	0,99	0,84		0,93
3	0,97	0,98	0,96			0,97
4	0,90	0,97	0,96			0,94
trial	LEFT STRIDE					mean
1	0,98	0,94	0,93	0,960158		0,95
2	0,97	0,98	0,98			0,98
3	0,93	0,85	0,96			0,92
4	0,99	0,97	0,96	0,95		0,97

Table 5.6 Summary of the computed  $SI_{O-P}$  for all the strides of healthy subject 4.

Subject 5				
trial	RIGHT STRIDE			mean
1	0,89	0,98	0,90	0,92
2	0,95	0,99	0,99	0,98
3	0,87	0,97		0,92
4	0,84	0,84	0,91	0,87
trial	LEFT STRIDE			mean
1	0,94	1,00		0,97
2	0,90	0,91		0,90
3	0,93	0,96		0,95
4	0,87	0,82		0,84

Table 5.7 Summary of the computed  $SI_{O-P}$  for all the strides of healthy subject 5.

<b>Slo-P Vertical symmetry index</b>						
<b>healthy</b>	<b>symmetry index right foot strike</b>				<b>mean value</b>	<b>STD</b>
<b>age: 27-30</b>	trial 1	trial 2	trial 3	trial 4	<b>right</b>	
1	0,97	0,95	0,93	0,97	0,96	0,02
2	0,95	0,92	0,98	0,85	0,93	0,06
3	0,95	0,98	0,96	0,97	0,96	0,01
4	0,96	0,93	0,97	0,94	0,95	0,02
5	0,92	0,98	0,92	0,87	0,92	0,05
<b>healthy</b>	<b>symmetry index left foot strike</b>				<b>mean value</b>	<b>STD</b>
<b>age: 27-30</b>	trial 1	trial 2	trial 3	trial 4	<b>left</b>	
1	0,94	0,96	0,94	0,94	0,95	0,01
2	0,91	0,97	0,94	0,90	0,93	0,03
3	0,97	0,94	0,98	0,94	0,96	0,02
4	0,95	0,98	0,92	0,97	0,95	0,03
5	0,97	0,90	0,95	0,84	0,91	0,06
<b>mean_tot</b>					<b>0,94</b>	<b>0,02</b>

Table 5.8 Summary of the computed  $SI_{O-P}$  for all the trials of all the 5 healthy subjects

*Computed  $SI_{Y-M}$  index*

The computed value of the  $SI_{Y-M}$  index for the available strides of all the 5 healthy subjects are reported in Tables 5.9-5.13. It is possible to see that each stride of a subject has a little different level of symmetry index value from the others. This result is in good agreement with that obtained with the application of the index  $SI_{O-P}$ .

Subject 1					
trial	RIGHT STRIDE				mean
1	0,85	0,77	0,88		0,83
2	0,79	0,76	0,70	0,87	0,78
3	0,79	0,77	0,70		0,75
4	0,75	0,86	0,78	0,86	0,81
trial	LEFT STRIDE				mean
1	0,77	0,81	0,77		0,78
2	0,85	0,71	0,82	0,83	0,80
3	0,77	0,72			0,75
4	0,80	0,69	0,89	0,74	0,78

*Table 5.9 Summary of the computed  $SI_{Y-M}$  for all the strides of healthy subject 1.*

Subject 2				
trial	RIGHT STRIDE			mean
1	0,82	0,87	0,69	0,79
2	0,79	0,76	0,66	0,74
3	0,84	0,89	0,80	0,84
4	0,71	0,71	0,62	0,68
trial	LEFT STRIDE			mean
1	0,77	0,68		0,72
2	0,82	0,75		0,79
3	0,83	0,71		0,77
4	0,80	0,65	0,72	0,72

*Table 5.10 Summary of the computed  $SI_{Y-M}$  for all the strides of healthy subject 2.*

Subject 3						
trial	RIGHT STRIDE					mean
1	0,81	0,79	0,69			0,76
2	0,80	0,81	0,88			0,83
3	0,75	0,78	0,78			0,77
4	0,84	0,82	0,83			0,83
trial	LEFT STRIDE					mean
1	0,81	0,84				0,82
2	0,73	0,72	0,82			0,76
3	0,87	0,81				0,84
4	0,84	0,79	0,82	0,78		0,79

Table 5.11 Summary of the computed  $SI_{Y-M}$  for all the strides of healthy subject 3.

Subject 4						
trial	RIGHT STRIDE					mean
1	0,72	0,89	0,86	0,86	0,67	0,80
2	0,69	0,83	0,86	0,64		0,76
3	0,80	0,83	0,80			0,81
4	0,70	0,80	0,79			0,76
trial	LEFT STRIDE					mean
1	0,85	0,79	0,75	0,78		0,79
2	0,81	0,83	0,81			0,82
3	0,75	0,67	0,81			0,74
4	0,84	0,79	0,82	0,78		0,81

Table 5.12 Summary of the computed  $SI_{Y-M}$  for all the strides of healthy subject 4.

Subject 5				
trial	RIGHT STRIDE			mean
1	0,67	0,81	0,68	0,72
2	0,76	0,86	0,84	0,82
3	0,66	0,81		0,73
4	0,64	0,66	0,69	0,66
trial	LEFT STRIDE			mean
1	0,73	0,94		0,84
2	0,68	0,71		0,70
3	0,74	0,78		0,76
4	0,68	0,62		0,65

Table 5.13 Summary of the computed  $SI_{Y-M}$  for all the strides of healthy subject 5.

As expected, also for this index no relevant differences can be observed when considering the right and left strides for the healthy subjects.

The mean values of the  $SI_{Y-M}$  index for the trials are reported in Table 5.14 and it is of 0.77 ( $\pm 0.02$ ). This value is in good agreement with the results presented by Minetti et al. (2011) who reported a mean value of about 0.80 for healthy subjects walking at a low speed.

<b><math>SI_{Y-M}</math> Vertical symmetry index</b>						
<b>healthy</b>	<b>symmetry index right foot strike</b>				<b>mean value</b>	<b>STD</b>
<b>age: 27-30</b>	trial 1	trial 2	trial 3	trial 4	<b>right</b>	
1	0,83	0,78	0,75	0,81	0,80	0,04
2	0,79	0,74	0,84	0,68	0,76	0,07
3	0,76	0,83	0,77	0,83	0,80	0,04
4	0,80	0,76	0,81	0,76	0,78	0,03
5	0,72	0,82	0,73	0,66	0,73	0,07
<b>healthy</b>	<b>symmetry index left foot strike</b>				<b>mean value</b>	<b>STD</b>
<b>age: 27-30</b>	trial 1	trial 2	trial 3	trial 4	<b>left</b>	
1	0,78	0,80	0,75	0,78	0,78	0,02
2	0,72	0,79	0,77	0,72	0,75	0,03
3	0,82	0,76	0,84	0,79	0,80	0,04
4	0,79	0,82	0,74	0,81	0,79	0,03
5	0,84	0,70	0,76	0,65	0,74	0,08
<b>mean_tot</b>					<b>0,77</b>	<b>0,02</b>

Table 5.14 Summary of the computed  $SI_{Y-M}$  for all the trials of all the 5 healthy subjects

### 5.2.3 Symmetry indexes of pathological subjects

These data refer to tests carried out on 14 pathological subjects affected by hemiparesis that were divided in two groups with reference to their age.

- Group 1: age  $\geq 65$  years (8 subjects: reference number 2, 3, 5, 7, 10, 12, 14 and 15);
- Group 2: age in the range 40 to 64 years (6 subjects: reference number 1, 4, 6, 8, 16 and 17).

Since no relevant differences were observed between males and females, all of subjects independently from their gender are considered in the analysis.

The pathological subject carried out a variable number of strides per trial ranging from 3 to 5.

The diagrams of the vertical trajectory of the BCoM, for each pathological subject, computed as the average of all strides considering separately the contralateral strides and the homolateral ones are reported in figures 5.7 and 5.8 for group 2 and in figures 5.9 and 5.10 for group 1.

From these figures it is possible to observe that the vertical BCoM trajectories are different from each subject with reference both to the shape of the signal and the peak values.

It is also possible to see that for both groups the diagrams of the homolateral side reported a flat first peak and a specular situation is proposed in the diagrams of the contralateral side. This shape highlights the asymmetric gait of hemiparetic subjects in particular due to their physical limitations to lift the pelvis during the single support phase of gait cycle of the hemiparetic side.

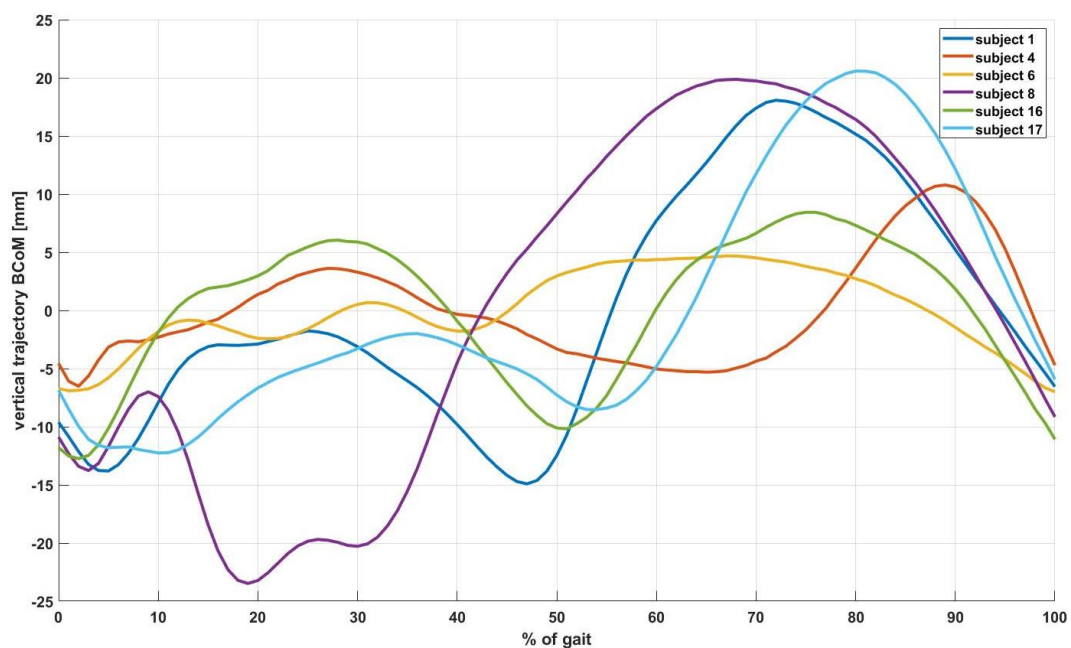


Figure 5.7 Vertical displacement of the BCoM trajectory (mm) normalized on the stride of the homolateral side of the pathological subject of Group 2 (age range 40 to 64 years)

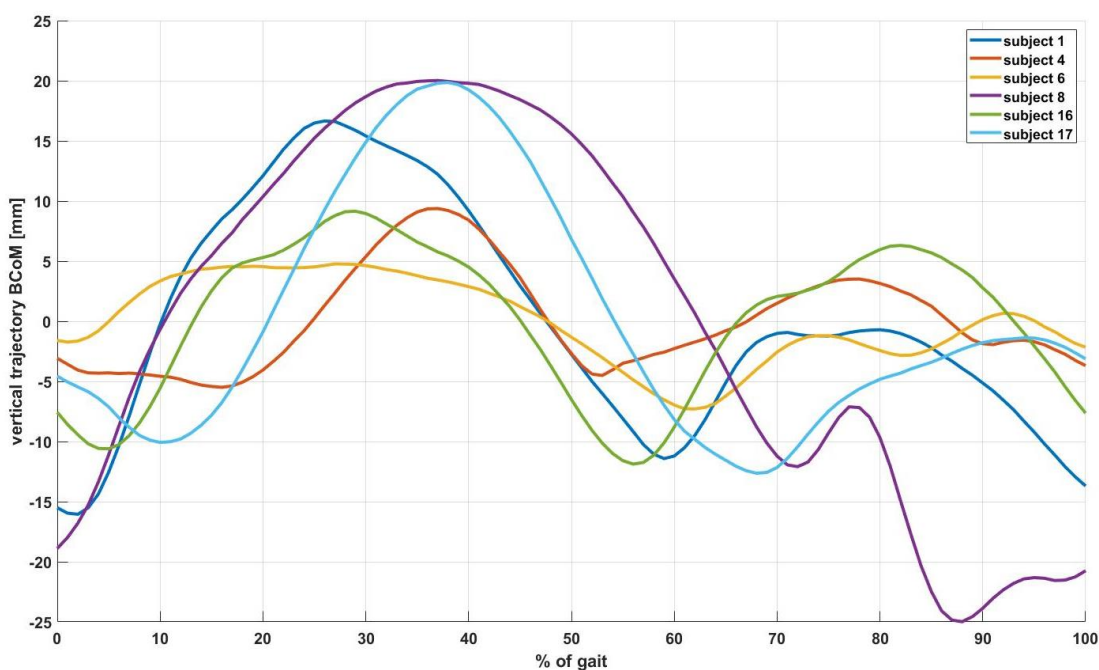


Figure 5.8 Vertical displacement of the BCoM trajectory (mm) normalized on the stride of the contralateral side of the pathological subject of Group 2 (age range 40 to 64 years)

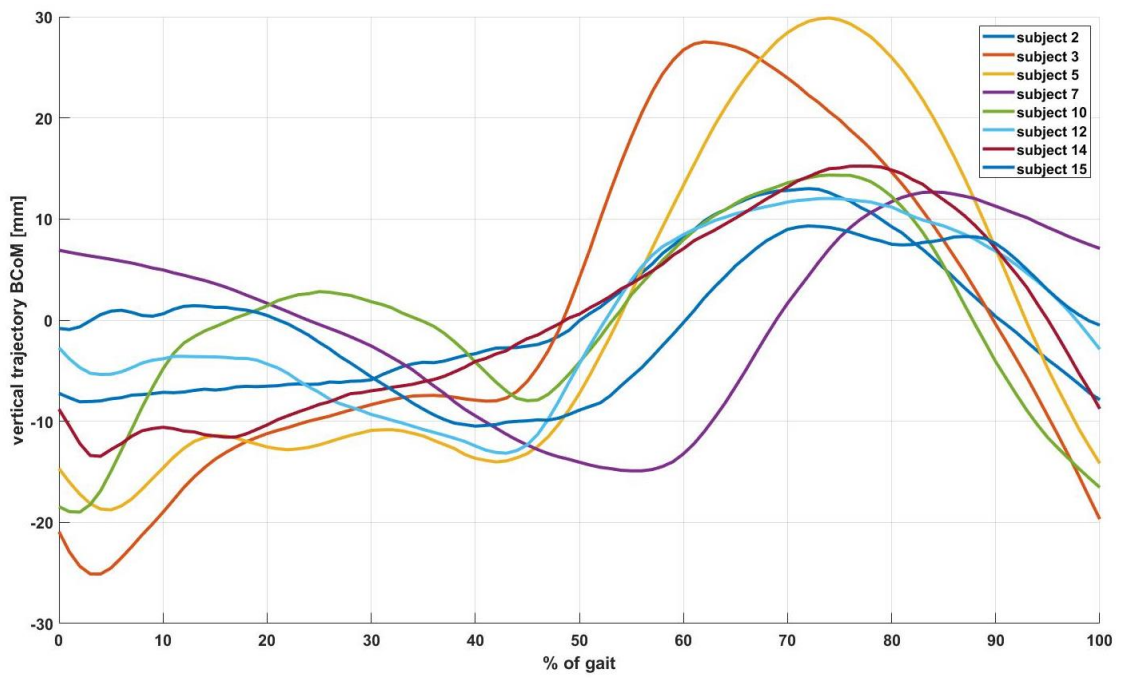


Figure 5.9 Vertical displacement of the BCoM trajectory (mm) normalized on the stride of the homolateral side of the pathological subject of Group 1 (age  $\geq 65$  years)

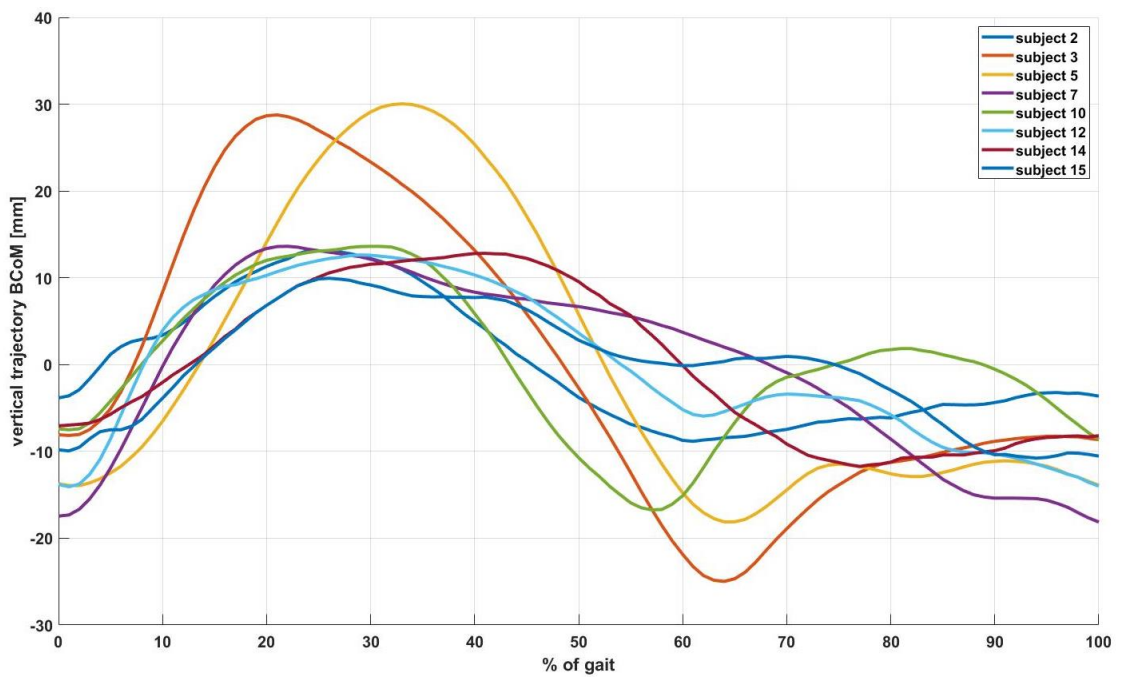


Figure 5.10 Vertical displacement of the BCoM trajectory (mm) normalized on the stride of the contralateral side of the pathological subject of Group 1 (age  $\geq 65$  years)

#### *Computed $SI_{O-P}$ index*

The computed value of the  $SI_{O-P}$  index for all the 8 pathological subjects with an age  $\geq 65$  years (Group 1) are reported in Table 5.15 and those with an age ranging from 40 years to 64 years (Group 2) are reported in Table 5.16.

It is possible to see that there is a clear difference from the mean value of the  $SI_{O-P}$  index computed using the data of Group 1 subjects and the mean value of the  $SI_{O-P}$  index computed using the data of Group 2. The Group 1  $SI_{O-P}$  mean value is 0.22 ( $\pm 0.02$ ) while the Group 2  $SI_{O-P}$  index is 0.43 ( $\pm 0.02$ ). The Group 2 mean value of the  $SI_{O-P}$  index is strongly affected by the subject 8, who is an outlier since it has very low values of the  $SI_{O-P}$  index. From the analysis of the vertical trajectory of BCoM of subject 8, it is clear that this patient's gait cycle was completely deformed (see Figures 5.4-5.5). Without considering the data of this patient, the mean value of the  $SI_{O-P}$  index for Group 2 rises to 0.51 ( $\pm 0.02$ ). It can also be observed that the values of the  $SI_{O-P}$  index for the subject of Group 1 presents a smaller dispersion than the younger subjects.

Comparing these values with the mean values of the  $SI_{O-P}$  index for the healthy patients the differences are:

- Group 1 the mean value is 76% less than the healthy subject index.
- Group 2 the mean value is 54% less than the healthy subject index.

<b>SI<sub>O-P</sub> Vertical symmetry index</b>						
<b>Pathological</b>	<b>symmetry index homolateral foot strike</b>				<b>mean value</b>	<b>STD</b>
<b>&gt; 65</b>	<b>trial 1</b>	<b>trial 2</b>	<b>trial 3</b>	<b>trial 4</b>	<b>homo</b>	
2	0,16	0,21	0,20	0,24	0,20	0,03
3	0,09	0,22	0,13	0,07	0,13	0,06
5	0,22	0,22	0,24	0,16	0,21	0,03
7	0,23	0,18	0,25	0,17	0,21	0,04
10	0,57	0,55	0,59	0,45	0,54	0,06
12	0,16	0,11	0,16	0,15	0,15	0,02
14	0,21	0,10	0,14	0,21	0,17	0,05
15	0,21	0,27	0,25	0,32	0,26	0,04
<b>Pathological</b>	<b>symmetry index contralateral foot strike</b>				<b>mean value</b>	<b>STD</b>
<b>&gt; 65</b>	<b>trial 1</b>	<b>trial 2</b>	<b>trial 3</b>	<b>trial 4</b>	<b>contra</b>	
2	0,17	0,15	0,16	0,18	0,17	0,01
3	0,09	0,19	0,10	0,09	0,12	0,05
5	0,22	0,24	0,23	0,15	0,21	0,04
7	0,23	0,15	0,17	0,17	0,18	0,03
10	0,59	0,56	0,55	0,37	0,52	0,10
12	0,15	0,13	0,15	0,17	0,15	0,02
14	0,26	0,13	0,08	0,21	0,17	0,08
15	0,20	0,23	0,27	0,23	0,23	0,03
<b>mean_tot</b>					<b>0,22</b>	<b>0,02</b>

Table 5.15 Summary of the computed SI<sub>O-P</sub> for all the trials of the 8 pathological subjects with an age  $\geq 65$  (Group 1)

<b>SI<sub>O-P</sub> Vertical symmetry index</b>						
<b>Pathological</b>	<b>symmetry index homolateral foot strike</b>				<b>mean value</b>	<b>STD</b>
<b>from 40 to 65</b>	<b>trial 1</b>	<b>trial 2</b>	<b>trial 3</b>	<b>trial 4</b>	<b>homo</b>	
1	0,46	0,36	0,36	0,43	0,40	0,05
4	0,53	0,61	0,58	0,50	0,56	0,05
6	0,18	0,21	0,18	0,26	0,21	0,04
8	0,03	0,04	0,03	0,02	0,03	0,01
16	0,90	0,89	0,89	0,86	0,88	0,02
17	0,51	0,41	0,48	0,48	0,47	0,04
<b>Pathological</b>	<b>symmetry index contralateral foot strike</b>				<b>mean value</b>	<b>STD</b>
<b>from 40 to 65</b>	<b>trial 1</b>	<b>trial 2</b>	<b>trial 3</b>	<b>trial 4</b>	<b>contra</b>	
1	0,62	0,43	0,43	0,45	0,48	0,09
4	0,49	0,57	0,57	0,51	0,54	0,04
6	0,19	0,16	0,16	0,20	0,18	0,02
8	0,03	0,04	0,03	0,02	0,03	0,01
16	0,86	0,90	0,92	0,93	0,90	0,03
17	0,48	0,38	0,51	0,52	0,47	0,07
<b>mean_tot</b>					<b>0,43</b>	<b>0,02</b>

Table 5.16 Summary of the computed SI<sub>O-P</sub> for all the trials of the 8 pathological subjects with an age ranging from 40 to 65 years old (Group 2)

*Computed SI<sub>Y-M</sub> index*

The computed value of the SI<sub>Y-M</sub> index for all the 8 pathological subjects with an age  $\geq 65$  years (Group 1) are reported in Table 5.17 and those with an age ranging from 40 years to 64 years (Group 2) are reported in Table 5.18.

It is possible to see that there is a clear difference from the mean value of the SI<sub>Y-M</sub> index computed using the data of Group 1 subjects and the mean value of the SI<sub>Y-M</sub> index computed using the data of Group 2.

The Group 1 SI<sub>Y-M</sub> mean value is 0.35 ( $\pm 0.01$ ) while the Group 2 SI<sub>Y-M</sub> index is 0.45 ( $\pm 0.01$ ). The Group 2 mean value of the SI<sub>Y-M</sub> index is, as in the previous case, affected by data of subject 8, but less than in the case of the SI<sub>O-P</sub>. Without considering the values of this patient the mean value of the SI<sub>Y-M</sub> for Group 2 rises to 0.49 ( $\pm 0.02$ ). In this case, also, the values of the index for the subjects of Group 1 presents a smaller dispersion than that of the younger subjects.

Comparing these values with the mean values of the SI<sub>Y-M</sub> index for the healthy patients the differences are:

- Group 1 the mean values are 54% less than the healthy subject.
- Group 2 the mean values are 41% less than the healthy subject.

<b>Si<sub>y-M</sub> Vertical symmetry index</b>						
<b>Pathological</b>	<b>symmetry index homolateral foot strike</b>				<b>mean value</b>	<b>STD</b>
<b>&gt; 65</b>	<b>trial 1</b>	<b>trial 2</b>	<b>trial 3</b>	<b>trial 4</b>	<b>homo</b>	
2	0,32	0,35	0,36	0,38	0,35	0,03
3	0,26	0,37	0,30	0,23	0,29	0,06
5	0,36	0,37	0,37	0,32	0,36	0,02
7	0,36	0,32	0,36	0,32	0,34	0,02
10	0,52	0,49	0,55	0,47	0,51	0,04
12	0,32	0,28	0,32	0,32	0,31	0,02
14	0,32	0,25	0,28	0,34	0,30	0,04
15	0,36	0,40	0,39	0,42	0,39	0,02
<b>Pathological</b>	<b>symmetry index contralateral foot strike</b>				<b>mean value</b>	<b>STD</b>
<b>&gt; 65</b>	<b>trial 1</b>	<b>trial 2</b>	<b>trial 3</b>	<b>trial 4</b>	<b>contra</b>	
2	0,35	0,32	0,33	0,33	0,33	0,01
3	0,25	0,35	0,27	0,25	0,28	0,05
5	0,36	0,37	0,36	0,31	0,35	0,03
7	0,37	0,31	0,32	0,32	0,33	0,02
10	0,52	0,51	0,50	0,43	0,49	0,04
12	0,30	0,28	0,30	0,31	0,30	0,01
14	0,36	0,27	0,26	0,35	0,31	0,05
15	0,35	0,37	0,40	0,39	0,38	0,02
<b>mean_tot</b>					<b>0,35</b>	<b>0,01</b>

Table 5.17 Summary of the computed SI<sub>Y-M</sub> for all the trials of the 8 pathological subjects with an age  $\geq 65$  (Group 1)

<b>SI<sub>Y-M</sub> Vertical symmetry index</b>						
<b>Pathological</b>	<b>symmetry index homolateral foot strike</b>				<b>mean value</b>	<b>STD</b>
<b>from 40 to 65</b>	<b>trial 1</b>	<b>trial 2</b>	<b>trial 3</b>	<b>trial 4</b>	<b>homo</b>	
1	0,47	0,41	0,41	0,45	0,44	0,03
4	0,49	0,53	0,50	0,47	0,50	0,03
6	0,35	0,36	0,34	0,39	0,36	0,02
8	0,19	0,23	0,21	0,17	0,20	0,03
16	0,72	0,71	0,71	0,67	0,70	0,02
17	0,49	0,42	0,47	0,47	0,46	0,03
<b>Pathological</b>	<b>symmetry index contralateral foot strike</b>				<b>mean value</b>	<b>STD</b>
<b>from 40 to 65</b>	<b>trial 1</b>	<b>trial 2</b>	<b>trial 3</b>	<b>trial 4</b>	<b>contra</b>	
1	0,54	0,45	0,44	0,45	0,47	0,05
4	0,47	0,50	0,50	0,48	0,49	0,02
6	0,35	0,33	0,32	0,35	0,34	0,02
8	0,20	0,23	0,20	0,19	0,21	0,02
16	0,69	0,73	0,72	0,75	0,72	0,03
17	0,48	0,42	0,48	0,48	0,47	0,03
<b>mean_tot</b>					<b>0,45</b>	<b>0,01</b>

Table 5.18 Summary of the computed SI<sub>Y-M</sub> for all the trials of the 8 pathological subjects with an age ranging from 40 to 65 years old (Group 2)

#### 5.2.4 Comparison of the results obtained with the SI<sub>O-P</sub> index and SI<sub>Y-M</sub> index

The comparison of the results obtained with the computation of the two indexes, using the available gait data, shows that both of them provide a good indication of the gait symmetry or asymmetry, but with some differences in the obtained values. Both indexes highlight a difference between the computed values for the healthy and the pathological subjects.

For healthy subjects the values (SI<sub>O-P</sub>: 0.94 ±0.02 and SI<sub>Y-M</sub>: 0.77 ±0.02) are close to 1, that means gait symmetry, as expected. The result obtained with the application of the SI<sub>Y-M</sub> seems to indicate a certain degree of asymmetry of the healthy gaits, that is not confirmed by the observational analyses of video recording. This result can be explained with the fact that this index is less sensitive than the SI<sub>O-P</sub> when managing values that are close to the extreme values of their range (that is to say: close to 1 for symmetry or close to 0 for total asymmetry).

For the pathological subjects the computed values are, for both indexes, much lower than 1, this indicates that the studied hemiparetic subjects have a walking alteration, as expected by the analysis of the gait trajectory, that affect the gait symmetry.

It was also possible to see that younger pathological subjects ( $SI_{O-P}$  index mean value =  $0.43 \pm 0.02$ ;  $SI_{Y-M}$  index mean value =  $0.45 \pm 0.01$ ) have usually higher values than the older subjects ( $SI_{O-P}$  index mean value =  $0.22 \pm 0.02$ ;  $SI_{Y-M}$  index mean value =  $0.35 \pm 0.01$ ). It is therefore possible to conclude that age is an important factor and it should be considered in the clinical observation of the gait symmetry. This factor has been highlighted by both the studied indexes.

From this comparison, it is possible to conclude that  $SI_{O-P}$  index amplifies the extreme values i.e. if a gait is symmetrical the index values is closer to 1 than the  $SI_{Y-M}$  index, while if the gait is asymmetrical the  $SI_{O-P}$  index is closer to zero than the  $SI_{Y-M}$  index. This behavior depends on the fact that the  $SI_{O-P}$  index uses the sum of a square value of the harmonic coefficients and this amplifies the ability of the index to detect the symmetry or the anomalies of the gait. This behavior should suggest that the  $SI_{O-P}$  index should be more efficient in the clinical analysis than the  $SI_{Y-M}$  index for the analysis of pathological subjects with important anomalies of the gait.

## 6. Conclusions and future developments

Human gait is a complex cyclic spatio-temporally movement that requires the movement of the body joints in coordinate sequence. Several researches dealt with the objective assessment and biomechanical description of human gait characteristics, such as symmetry, variability and smoothness and different methods and approaches for the investigation of gait symmetry have been proposed.

Despite the several symmetry indexes have been used in physiological analysis of gait, some challenges are still open for the identification of robust and suitable methodology in pathological patterns. Recent analysis suggested the application of frequency analysis to biological signals to evaluate characteristics and components that cannot be detected in time domain.

This thesis focuses on the characterization of the human gait examining the Body Centre of Mass (BCoM) trajectory using the spectral analysis of the Fourier series.

In this work, the vertical displacement of the BCoM trajectory has been analyzed.

Two symmetry indexes, proposed in literature, based on combinations of the Fourier series coefficients, developed respectively for the assessment of the gait symmetry of amputee and non-amputee subjects (Ochoa-Diaz & Padilha, 2020) and the gait symmetry of healthy subjects walking and running at different speeds (Minetti et al. 2011), have been studied to verify their feasibility when applied to hemiparetic gait and compared with the values obtained by a control group of healthy subjects.

The analysis of the hemiparetic gait symmetry is difficult since each patient affected by hemiparesis, to face his condition, develops personal and different compensation actions and this fact make a possible generalization with a simple index quite challenging.

The computation of the indexes has been carried out based on the experimental data of the BCoM trajectory acquired in a previous study. These data refer to two groups: healthy young subjects (5 subject considered as the control group) and 14 pathological patients with different ages. The pathological subjects were than divided in two sub-groups: over 65 years old and between 40 to 64 years old.

In healthy subjects both indexes ( $SI_{O-P}$ :  $0.94 \pm 0.02$  and  $SI_{Y-M}$ :  $0.77 \pm 0.02$ ) provide values close to 1, that represent a symmetrical gait.

The results obtained for healthy subjects are also in good agreement with the results obtained by the authors that proposed the indexes, when applied to healthy gait.

When considering all the pathological subjects, the  $SI_{O-P}$  index indicates a mean value of  $0.31 \pm 0.23$ , while the  $SI_{Y-M}$  index provides a mean value of  $0.39 \pm 0.13$ . These values are much lower than those of healthy subjects and show that hemiparetic subjects have a walking alteration, as expected.

It was also possible to see that younger pathological subjects have usually higher values, even if lower than the healthy ones, ( $SI_{O-P}$  index mean value =  $0.43 \pm 0.02$ ;  $SI_{Y-M}$  index mean value =  $0.45 \pm 0.01$ ) for both symmetry indexes than the old subjects ( $SI_{O-P}$  index mean value =  $0.22 \pm 0.02$ ;  $SI_{Y-M}$  index mean value =  $0.35 \pm 0.01$ ). From the presented results it is possible to conclude that age is an important factor, and it should be considered in the clinical observation of the gait symmetry.

In conclusion, these indexes have shown to be feasible to detect hemiparetic gait asymmetry and could be adopted in clinic analysis, could be a good parameter to check an improvement of a pathological subject before and after a rehabilitation treatment.

Further development of the proposed methodology could be considered an extended populations of subject (healthy and pathological) or applied to a different pathological condition and the obtained results can be compared, considering the pathology and how it affects the gait. The same procedure of spectral analysis might be carried out considering different types of biomechanical signals for example the acceleration.

In a future work, it may be advisable to use more efficient methods to carry out the numerical integration for this specific application as explain in chapter 3. And also another interesting improvements of this thesis could be done also considering the symmetry indexes in the mediolateral and in the progression directions of the BCoM trajectory.

## Bibliography

- Alexander RM. (2003). *Principles of Animal Locomotion*. Princeton, Princeton University Press.
- Bellanca J.L., Lowry K.A., Vanswearingen J. M., Brach J. S. & Redfern M. S. (2013). Harmonic ratios: A quantification of step-to-step symmetry, *Journal of Biomechanics* 46, pp. 828–831. doi: 10.1016/j.jbiomech.2012.12.008.
- Block J.A. & Shakoov N. (2010). Lower limb osteoarthritis: biomechanical alterations and implications for therapy, *Curr. Opin. Rheumatol.* 22.
- Butkov E. (1968). *Mathematical Physics*, Addison-Wesley, Reading (MA).
- Cappozzo A., Catalani F., Della Croce U. & Leardini A. (1995). Position and orientation in space of bones during movement: anatomical frame definition and determination, *Clinical Biomechanics*, 10 (4), pp. 171–178, doi: 10.1016/0268-0033(95)91394-T.
- Cappozzo A., Della Croce U., Leardini A. & Chiari L. (2005). Human movement analysis using stereophotogrammetry. Part 1: theoretical backgrounds. *Gait & Posture* 21, pp. 186–196.
- Carpentier J., Benallegue M. & Laumond J-P. (2017). On the Centre of Mass Motion in Human Walking, *Int. Journal of Automation and Computing*, 14(5), doi:10.1007/s11633-017-1088-5.
- Cavagna G. (2017). *Physiological Aspects of Legged Terrestrial Locomotion: The Motor and the Machine*. Cham, Springer Int Publisher AG.
- Cestari Soto M. (2017). Variable-stiffness joints with embedded force sensors for high performance wearable gait exoskeletons, PhD Thesis, Universidad Politecnica de Madrid, Madrid.
- Davis R. B. & Ounpuu S. (1992). Kinetics of normal gait. in Perry J. (1992) *Gait Analysis: Normal and Pathological Functions*. Thorofare, NJ, pp. 120-133.
- Enoka, R. M. (1996). Eccentric contractions require unique activation strategies by the nervous system. *Journal of Applied Physiology*, 81(6), pp. 2339–2346.
- Esser P., Dawes H., Collett J. & Howells K. (2013). Insights into gait disorders: Walking variability using phase plot analysis, Parkinson’s disease,” *Gait Posture*, 38(4), pp. 648–652, doi: 10.1016/j.gaitpost.2013.02.016
- Ferrari A., Reverberi S. & Benedetti M.G. (2013). L’arto inferiore nella paralisi cerebrale infantile. *Semeiotica e chirurgia funzionale*, Springer-Verlag, doi: 10.1007/978-88-470-2814-2.
- Frigo C., Rabuffetti M., Kerrigan D.C., Deming L.C. & Pedotti A. (1998). Functionally oriented and clinically feasible quantitative gait analysis method. *Med. Biol. EngComput*, 36,

pp. 179-185.

Fröberg C. E. (1985). *Numerical mathematics: theory and computer applications*, Addison-Wesley Longman (US)

Gage H. (1964). *Accelerographic analysis of human gait*. The American Society of Mechanical Engineers, 1–12 64-WA/HUF-8.

Gage JR. (1991). *Gait Analysis in Cerebral Palsy*, MacKeith Press., New York (USA).

Goswami A. (2003). Kinematic quantification of gait symmetry based on bilateral cyclograms, *Proc XIXth Congr. Int. Soc. Biomech.*

Gutierrez-Farewik E.M., Bartonek A. & Saraste H. (2006). Comparison and evaluation of two common methods to measure center of mass displacement in three dimensions during gait, *Human Movement Science*, 25, pp. 238–256, doi:10.1016/j.humov.2005.11.001.

Herzog W., Nigg B.M., Read L.J. & Olsson E. (1989). Asymmetries in ground reaction force patterns in normal human gait, *Med. Sci. Sport Exerc.*, 21, pp. 110–114.

Hoerzer S., Federolf P.A., Maurer C., Baltich J. & Nigg B.M. (2015) Footwear decreases gait asymmetry during running, *PLoS One* 10, e0138631, doi: 10.1371/journal.pone.0138631.

Leardini A., Sawacha Z., Paolini G., Ingrosso S., Nativio R. & Benedetti M.G. (2007). A new anatomically based protocol for gait analysis in children, *Gait Posture*. 26(4), pp. 560-571.

Lee J.B., Sutter K.J., Askew C.D. & Burkett B.J. (2010). Identifying symmetry in running gait using a single inertial sensor. *Journal of Science and Medicine in Sport*, 13, pp. 559–563, doi: 10.1016/j.jsams.2009.08.004.

Lieber R.L. (2002). *Skeletal Muscle Structure, Function, and Plasticity: The Physiological Basis of Rehabilitation*, Lippincott Williams & Wilkins, Baltimore (USA).

McLester S. & Pierre P. (2008). *Applied Biomechanics. Concepts and Connections*, Thomson Wadsworth, Belmont (USA).

McMahon TA. (1974). *Muscles, Reflexes, and Locomotion*. Princeton, NJ: Princeton University Press.

Menz H.B., Lord S.R. & Fitzpatrick R.C. (2003a). Acceleration patterns of the head and pelvis when walking are associated with risk of falling in community dwelling older people. *The Journals of Gerontology. Series A, Biological Sciences and Medical Sciences* 58, M446–M452.

Menz H.B., Lord S.R. & Fitzpatrick R.C. (2003b). Acceleration patterns of the head and pelvis when walking on level and irregular surfaces. *Gait and Posture* 18, pp. 35–46.

Minetti A.E., Cisotti C. & Mian O.S. (2011). The mathematical description of the body centre

of mass 3D path in human and animal locomotion, *Journal of Biomechanics* 44 (8), pp. 1471–1477, doi: 10.1016/j.jbiomech.2011.03.014.

Ochoa-Diaz C. & Padilha A. L. Bó (2020). Symmetry Analysis of Amputee Gait Based on Body Center of Mass Trajectory and Discrete Fourier Transform, *Sensors*, 2020, 20, doi:10.3390/s20082392.

Panero E., Digo E., Dimanico U., Artusi A.C., Zibetti M. & Gastaldi L. (2021). Effect of Deep Brain Stimulation Frequency on Gait Symmetry, Smoothness and Variability using IMU, 2021 IEEE International Symposium on Medical Measurements and Applications, doi:10.1109/MeMeA52024.2021.9478602.

Pasciuto I., Bergamini E., Iosa M., Vannozzi G. & Cappozzo A. (2017). Overcoming the limitations of the Harmonic Ratio for the reliable assessment of gait symmetry, *Journal of Biomechanics* 53, pp. 84-89, doi: 10.1016/j.jbiomech.2017.01.005.

Perry J. (1992). *Gait Analysis: Normal and Pathological Functions*. Thorofare, New York (USA).

Perry J. & Burnfield J. (2010) *Gait Analysis. Normal and Pathological Function*, SLACK Incorporated (USA).

Ploof G., Alqahtani B., Alghamdi F., Flynn G. & Xia Yan C. (2017) Center of mass estimation using motion capture system, 2017 IEEE 15th Intl Conf on Dependable, Autonomic and Secure Computing, 15th Intl Conf on Pervasive Intelligence and Computing, 3rd Intl Conf on Big Data Intelligence and Computing and Cyber Science and Technology Congress.

Rabuffetti M. & Crenna P. (2004). A modular protocol for the analysis of movement in children, *Gait Posture* 20, pp. 577-578.

Robinson, R. O., Herzog, W. & Nigg, B. M. (1987). Use of force platform variables to quantify the effects of chiropractic manipulation on gait symmetry. *J. Manipulative Physiol. Ther.* 10, pp. 172–176.

Sabatini A.M., Ligorio G. & Mannini A. (2015). Fourier-based integration of quasi-periodic gait accelerations for drift-free displacement estimation using inertial sensors, *BioMed Eng OnLine* 14, doi:10.1186/s12938-015-0103-8.

Sadeghi H., Allard P., Prince F. & Labelle H. (2000). Symmetry and limb dominance in able-bodied gait: a review, *Gait Posture* 12, pp. 34–45, doi:10.1016/S0966-6362(00)00070-9.

Sant'Anna A., Salarian A. & Wickstrom N. (2011). A New Measure of Movement Symmetry in Early Parkinson's Disease Patients Using Symbolic Processing of Inertial Sensor Data, *IEEE Transaction on Biomedical Engineering*, 58(7), pp. 2127-2135.

Saunders J.B.D., Inman V. & Eberhart H. (1953). The major determinants in normal and

pathological gait. *J. Bone Jt. Surg. Am.* (1953) 35-A:543–58.

Simonetti A., Bergamini E., Vannozzi G., Bascou J. & Pillet H. (2021). Estimation of 3D Body Center of Mass Acceleration and Instantaneous Velocity from a Wearable Inertial Sensor Network in Transfemoral Amputee Gait: A Case Study, *Sensors*, 21(9), pp. 3129; doi: 10.3390/s21093129.

Smidt G. L., Aurora J.S. & Johnston R.C. (1971). Accelerographic Analysis of several types of walking, *American Journal of Physical Medicine*, 50 (6).

Stauber W. T. (1989). Eccentric action of muscles: Physiology, injury, and adaptation. *Exercise and Sports Science Reviews*, 17, pp. 157–186.

Yack H.J. & Berger R.C. (1993). Dynamic stability in the elderly: identifying a possible measure. *Journal of Gerontology* 48, M225–M230.

Tabor P., Iwanska D., Grabowska O., Karczewska-Lindinger M., Popieluch A. & Mastalerz A. (2021). Evaluation of selected indices of gait asymmetry for the assessment of running asymmetry, *Gait and Posture*, 86, pp. 1-6

Tesio L. & Rota V. (2019). The motion of Body Center of Mass during walking: a review oriented to clinical approach, *Frontiers in Neurology*, September 2019; doi:10.3389/fneur.2019.00999.

Tesio L., Rota V., Chessa C. & Perucca L. (2010). The 3D path of body centre of mass during adult human walking on force treadmill, *Journal of Biomechanics*, 43, pp. 938-944, doi:10.1016/j.jbiomech.2009.10.049.

Vaughn C.L., Davis B.L. & O'Connor J.C. (1992). *Dynamics of Human Gait*, Kiboho Publishers, Cape Town (SA).

Viteckovaa S., Kutileka P., Svoboda Z., Krupickaa R., Kauler J. & Szaboa Z., (2018). Gait symmetry measures: A review of current and prospective methods, *Biomedical Signal Processing and Control*, 42, pp. 89-100, doi: 10.1016/j.bspc.2018.01.013.

Wafai L., Zayegh A., Woulfe J., Aziz S.M. & Begg R. (2015). Identification of foot pathologies based on plantar pressure asymmetry, *Sensors*, 15, pp. 20392–20408, doi: 10.3390/s150820392.

Willems P.A., Schepens B., Detrembleur C. (2012). Deambulazione normale, *Medicina Riabilitativa*, 19 (2), doi: 10.1016/S1283-078X(12)62015-X.

Zifchock R.A., Davis I., Higginson J. & Royer T. (2008). The symmetry angle: a novel, robust method of quantifying asymmetry, *Gait Posture*, 27, pp. 622–627, doi:10.1016/j.gaitpost.2007.08.006.

Zuk M. & Trzeciak M. (2017). Anatomical protocol for gait analysis: joint kinematics measurement and its repeatability, *Journal of Theoretical and Applied Mechanics*, 55(1), pp. 369–376, doi: 10.15632/jtam-pl.55.1.369

Zverev Y. (2015). Spatial asymmetry of post-stroke hemiparetic gait: assessment and recommendations for physical rehabilitation, *Tanzan. J. Health Res.*, 17

## **Websites**

<http://www.idmil.org> (last access 13th February 2022)

<http://www.idmil.org/mocap/Plug-in-Gait+Marker+Placement.pdf> (last access 13th February 2022)

<https://gpemmocap.wordpress.com/tag/vicon/> (last access 13th February 2022)

<https://www.gpem.net/software-motion-analysis> (last access 13th February 2022)

<https://docs.vicon.com/display/Nexus25/Plug-in+Gait+kinematic+and+kinetic+calculations>

<https://www.ouh.nhs.uk/gait-lab/research/oxford-foot-model.aspx> (last access 13th February 2022)

<http://www.dimnp.unipi.it/gabiccini-m/RAR/LabBioIng.pdf> (last access 13th February 2022)

<http://www.dimnp.unipi.it/gabiccini-m/RAR/LabBioIng.pdf> (last access 13th February 2022)

<https://docs.vicon.com> (last access 13th February 2022)

Annex 1:

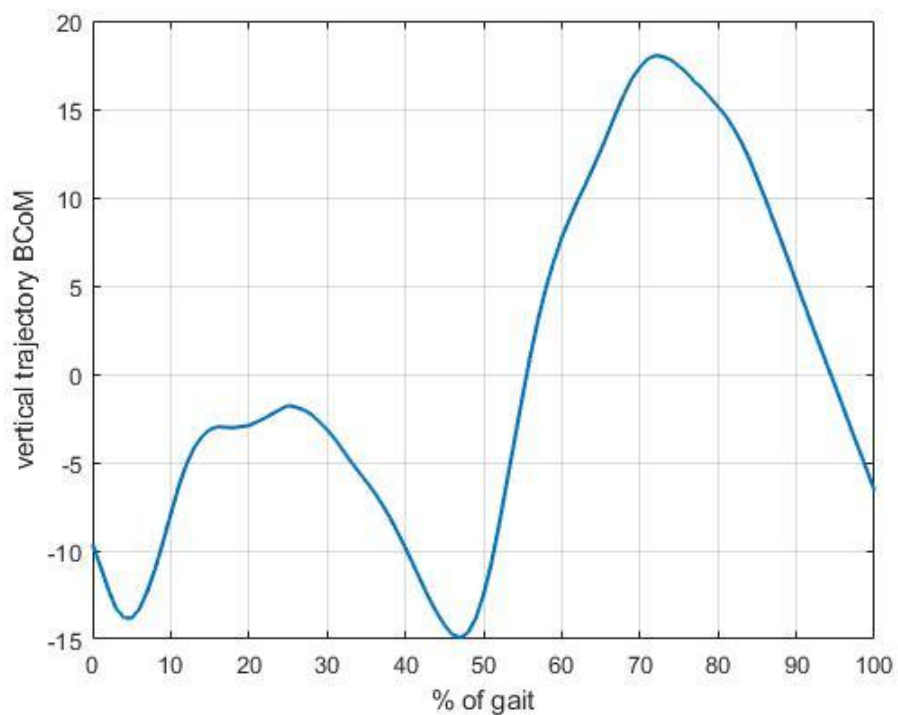


Figure A1-1 Vertical displacement of the BCoM trajectory (mm) normalized on the gait of homolateral side for pathological subject 1.

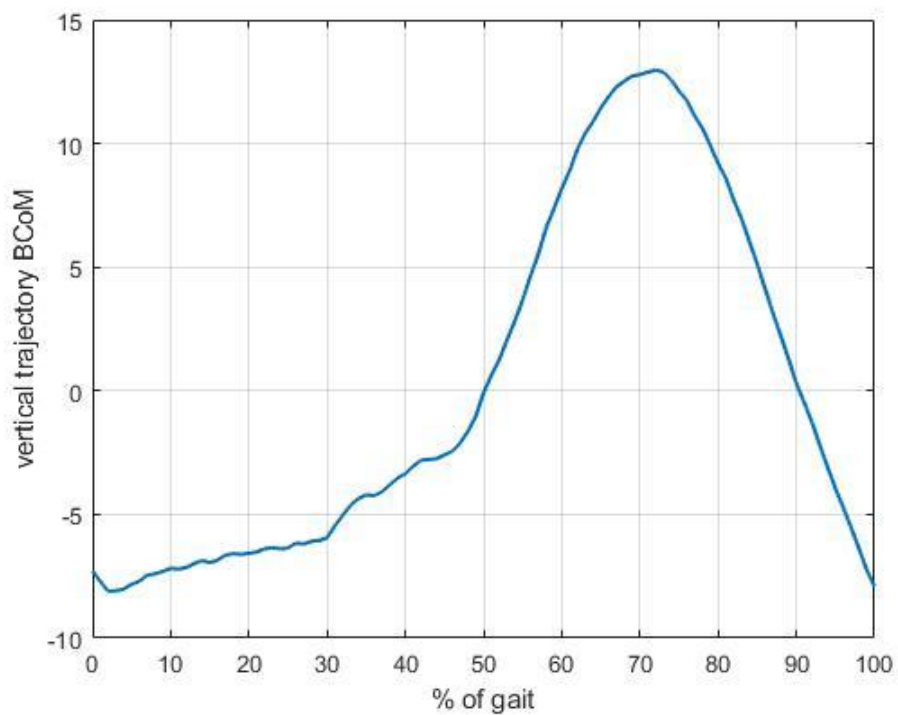


Figure A1-2 Vertical displacement of the BCoM trajectory (mm) normalized on the gait of homolateral side for pathological subject 2.

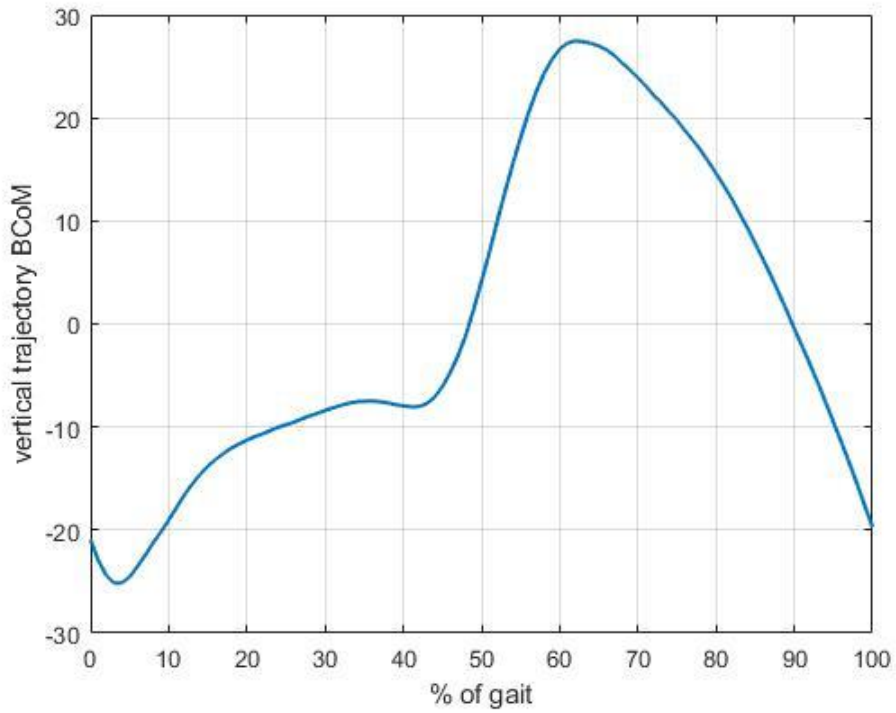


Figure A1-3 Vertical displacement of the BCoM trajectory (mm) normalized on the gait of homolateral side for pathological subject 3.

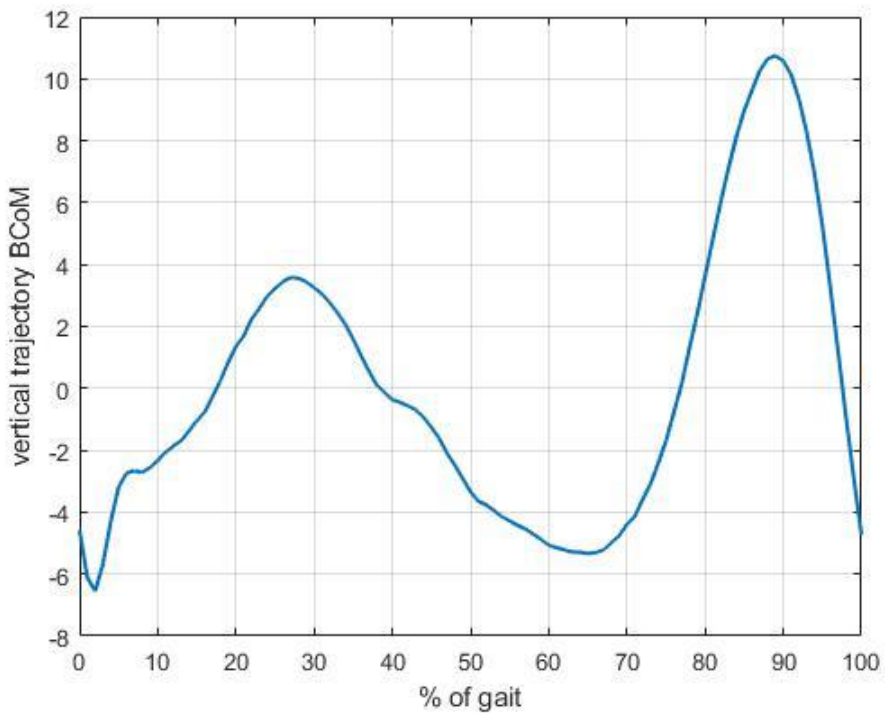
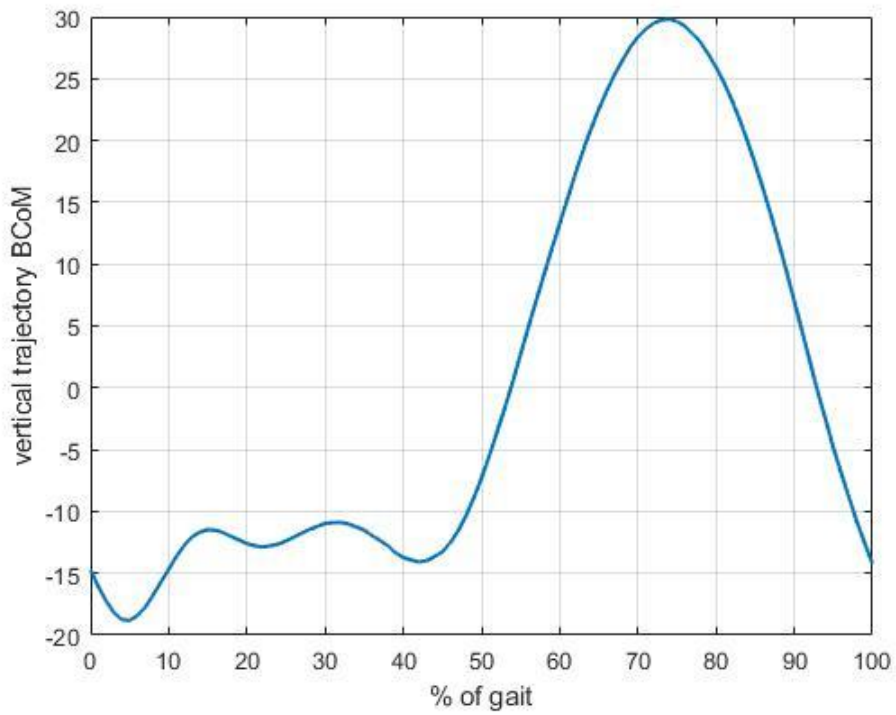
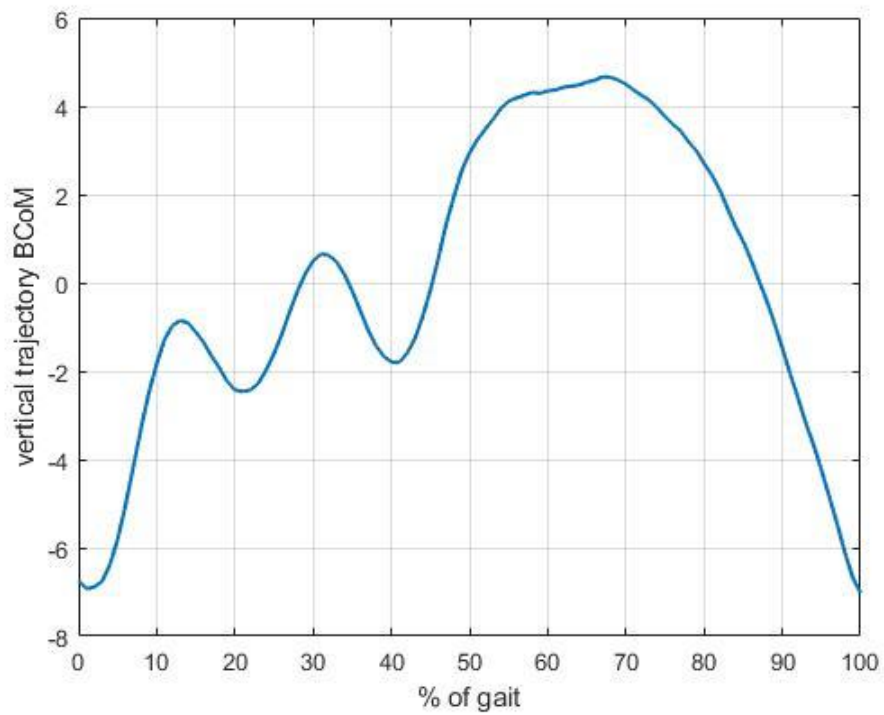


Figure A1-4 Vertical displacement of the BCoM trajectory (mm) normalized on the gait of homolateral side for pathological subject 4.



*Figure A1-5 Vertical displacement of the BCoM trajectory (mm) normalized on the gait of homolateral side for pathological subject 5.*



*Figure A1-6 Vertical displacement of the BCoM trajectory (mm) normalized on the gait of homolateral side for pathological subject 6.*

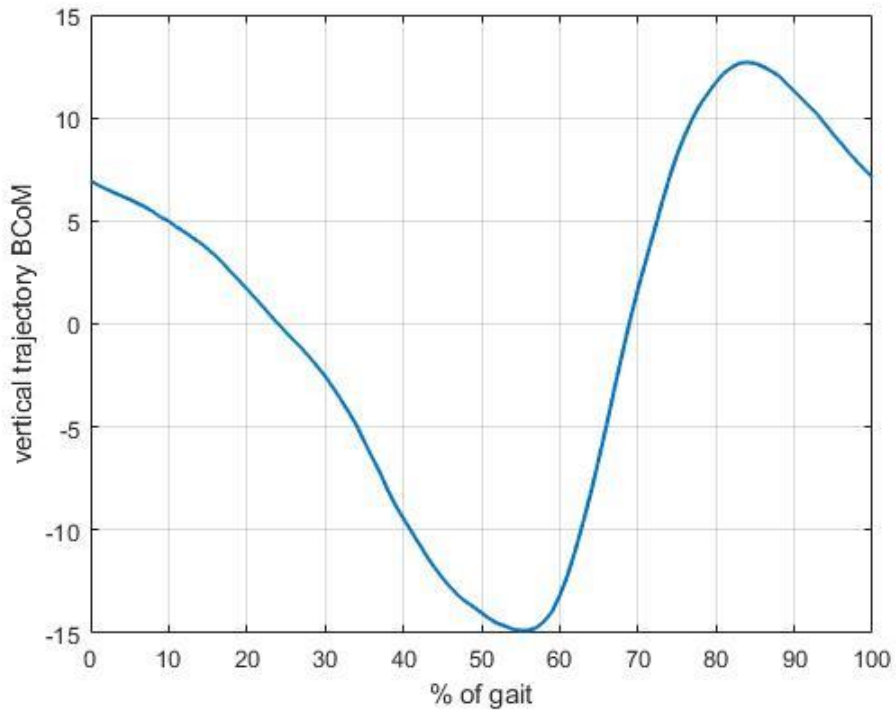


*Figure A1-7 Vertical displacement of the BCoM trajectory (mm) normalized on the gait of homolateral side for pathological subject 7.*

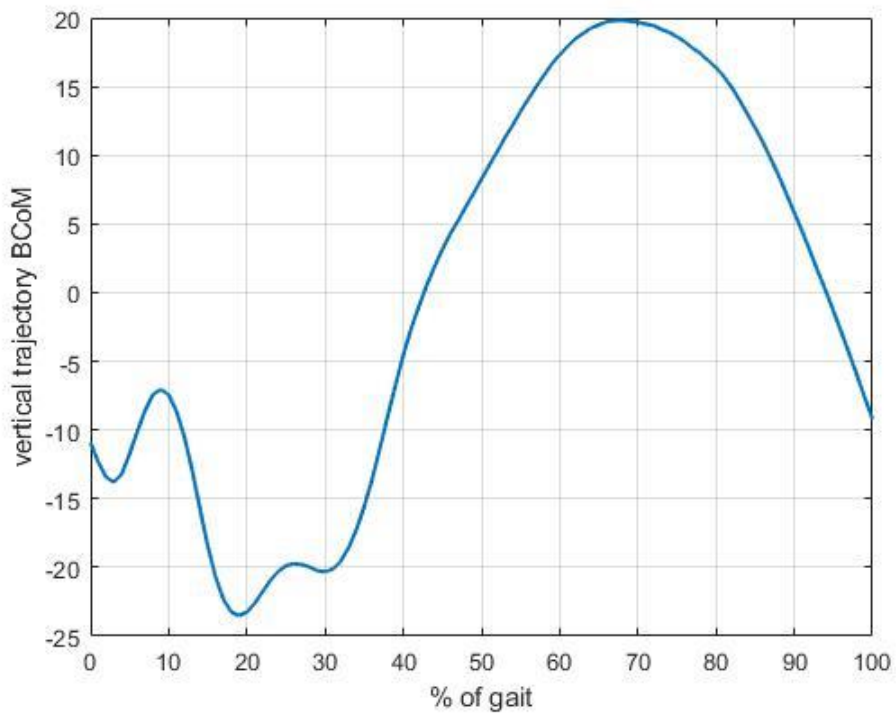


*Figure A1-8 Vertical displacement of the BCoM trajectory (mm) normalized on the gait of homolateral side for pathological subject 8.*

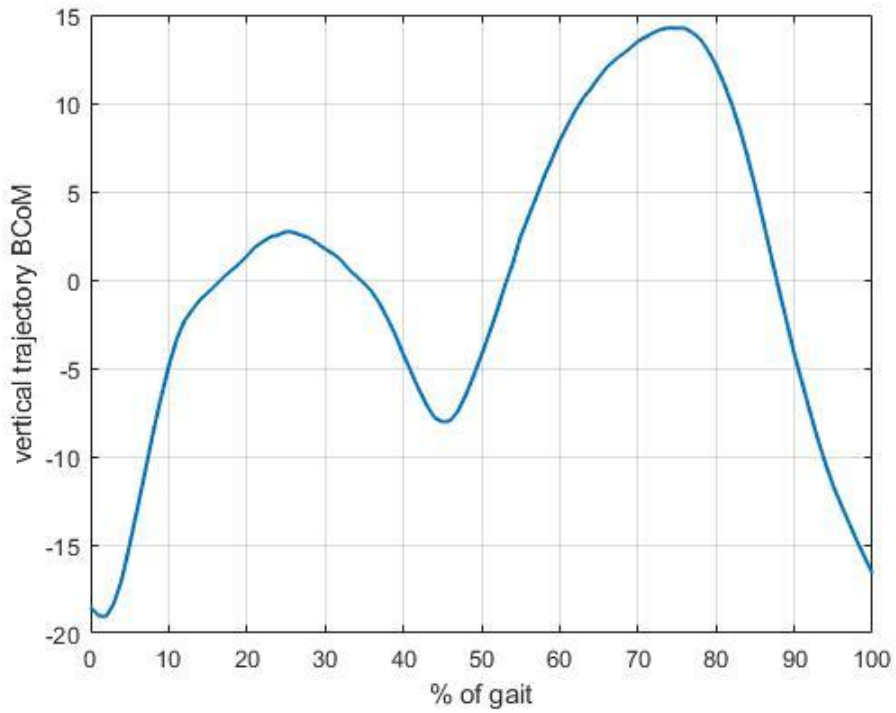


*Figure A1-9 Vertical displacement of the BCoM trajectory (mm) normalized on the gait of homolateral side for pathological subject 10.*

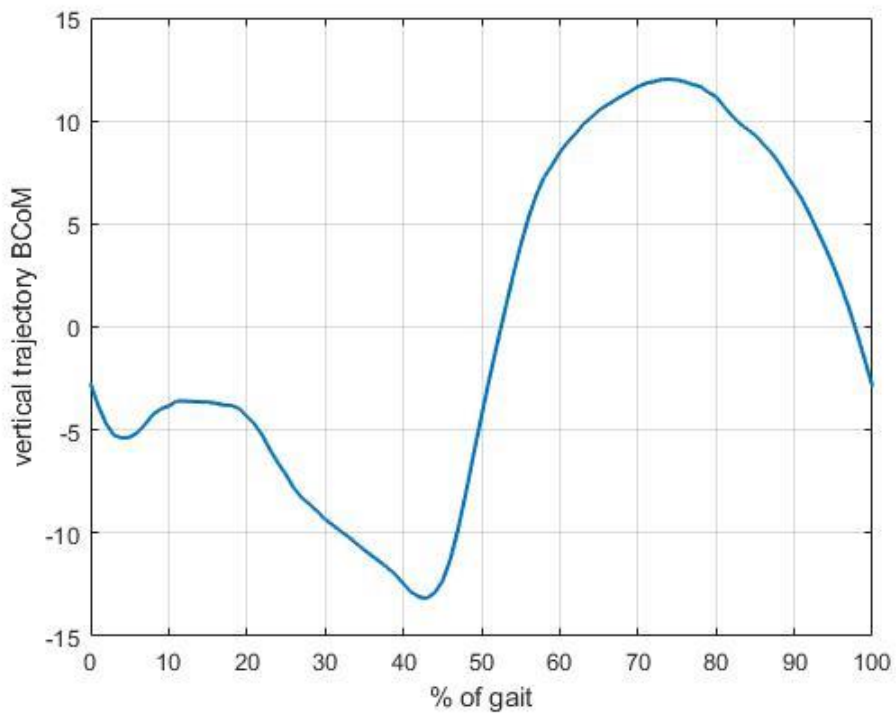


*Figure A1-10 Vertical displacement of the BCoM trajectory (mm) normalized on the gait of homolateral side for pathological subject 12.*

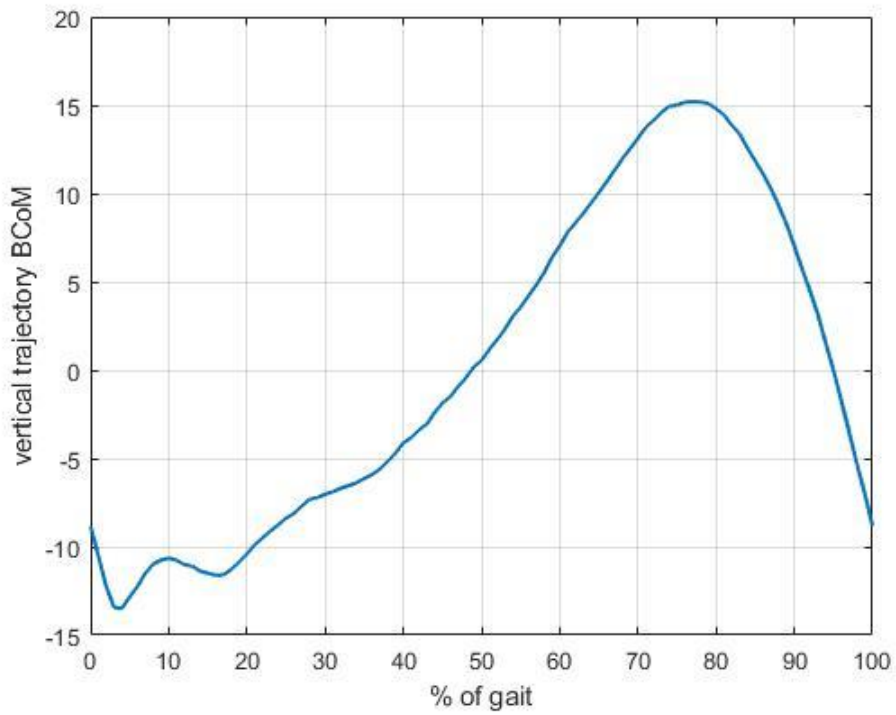


*Figure A1-11 Vertical displacement of the BCoM trajectory (mm) normalized on the gait of homolateral side for pathological subject 14.*

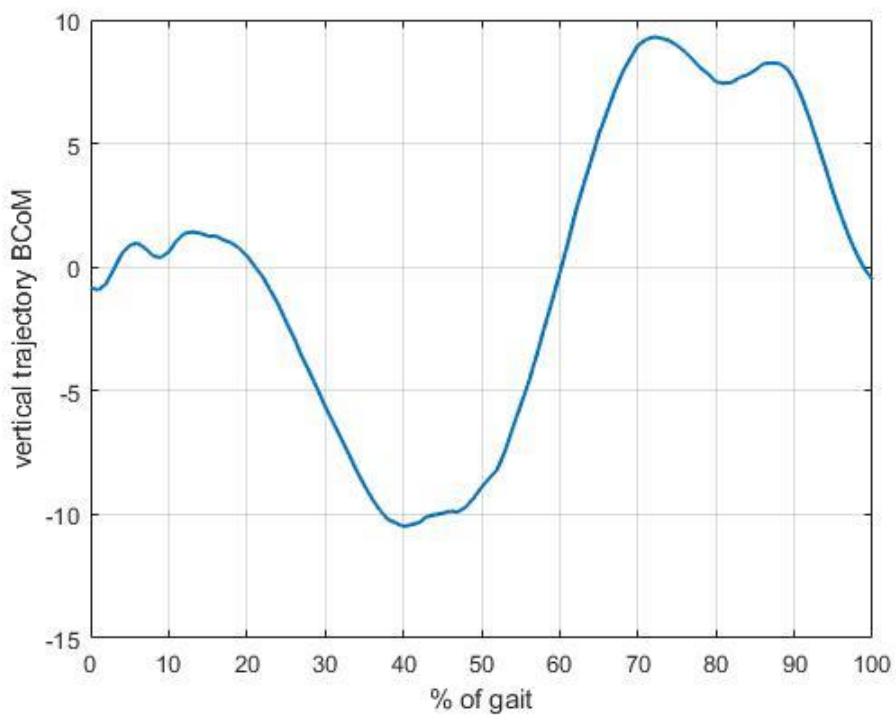


*Figure A1-12 Vertical displacement of the BCoM trajectory (mm) normalized on the gait of homolateral side for pathological subject 15.*

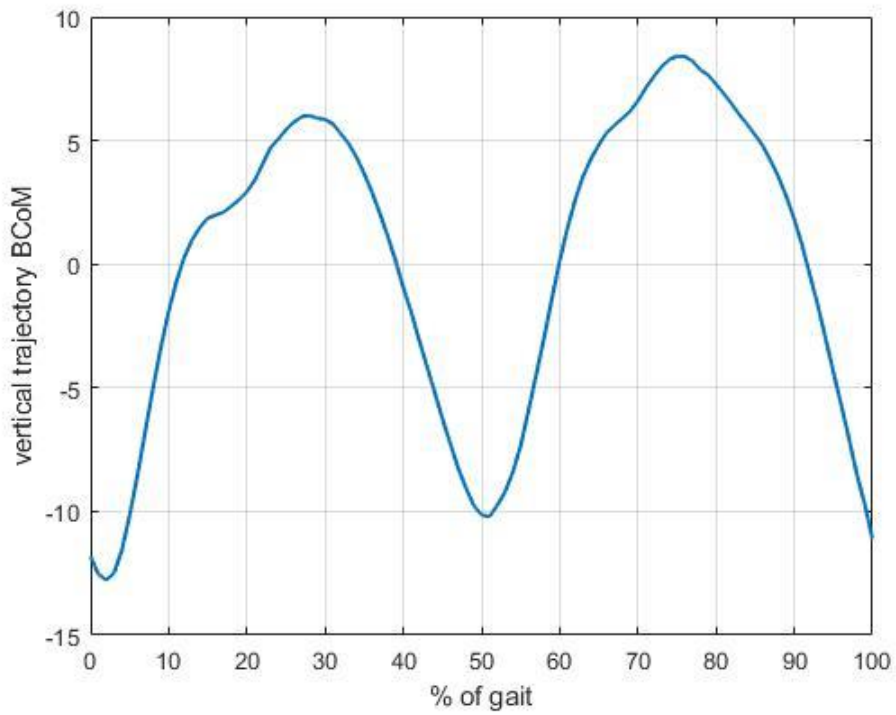


*Figure A1-13 Vertical displacement of the BCoM trajectory (mm) normalized on the gait of homolateral side for pathological subject 16.*

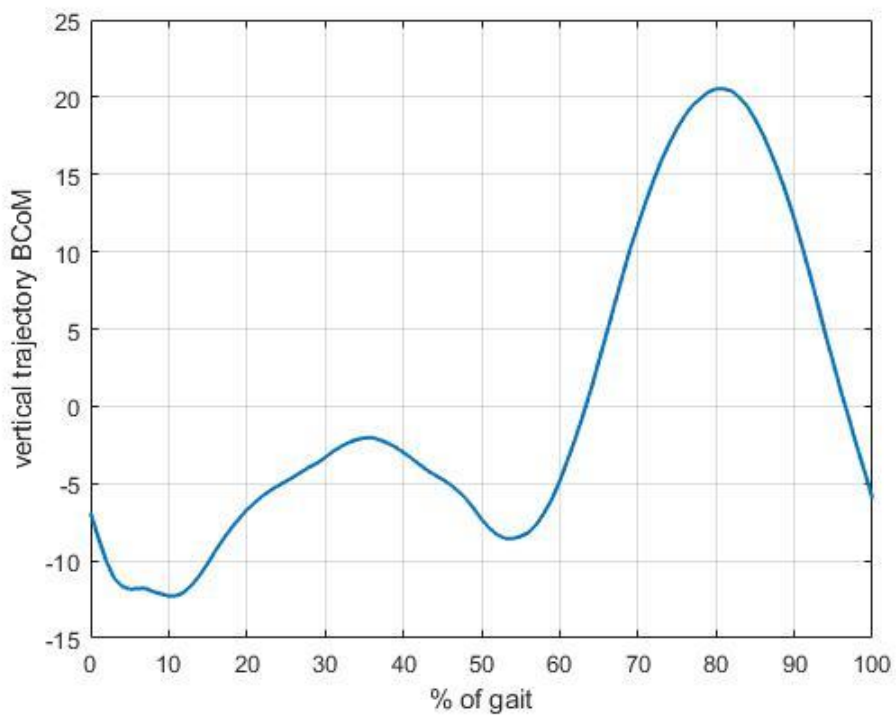


*Figure A1-14 Vertical displacement of the BCoM trajectory (mm) normalized on the gait of homolateral side for pathological subject 17.*

## *Ringraziamenti*

*Desidero ringraziare i miei relatori che mi hanno seguito con costanza e che mi hanno dato la possibilità approfondire un ramo dell'ingegneria meccanica che da sempre mi ha incuriosito e appassionato.*

*Inoltre, desidero ringraziare le persone care che in questi anni mi sono state vicine e grazie alle quali sono arrivata a concludere questo percorso che è stato sicuramente ricco di gioie ma anche di molti momenti di difficoltà:*

*I miei genitori, che ogni giorno instancabilmente non hanno mai smesso di credere in me anche quando io stessa perdevo le speranze, che con amore e affetto hanno sostenuto ogni mio passo per farmi raggiungere questo importante obiettivo;*

*Mio marito Gianluca, che più di tutti ha saputo starmi accanto con tenerezza, e senza farmi mai mancare un sorriso a fine giornata;*

*Lorenzo e Cristina, due solide presenze, poco invadenti ma sempre presenti, una certezza sulla quale poter contare;*

*I miei cari compagni di viaggio del Poli: Elena, Marta, Flaminia, Gabriele e Stefano, i regali più belli di questo percorso, amici veri con i quali ho potuto condividere tanto e che hanno, ciascuno con le sue qualità, arricchito le mie giornate;*

*Francesca, una presenza insostituibile che giorno dopo giorno mi ha insegnato a guardare con fiducia le difficoltà e a renderle qualcosa di bello;*

*Enrico e Benedetta, amici storici, che mi hanno sempre supportato e che con semplicità mi sono stati accanto, e infine, mio zio Piero, che ha il dono di rendere semplici anche gli argomenti più complessi.*